Probe Report

Title: Discovery of Potent and Highly Selective Inhibitors of GSK3b

Authors: W. Frank An, Andrew R. Germain, Joshua A. Bishop, Partha P. Nag, Shailesh Metkar, Joshua Ketterman, Michelle Walk, Michel Weiwer, Xiulin Liu, Debasis Patnaik, Yan-Ling Zhang, Jennifer Gale, Wendy Zhao, Taner Kaya, Doug Barker, Florence F. Wagner, Ed B. Holson, Sivaraman Dandapani, Jose Perez, Benito Munoz, Michelle Palmer, Jen Q. Pan, Stephen J. Haggarty, Stuart L. Schreiber

Abstract:

The serine/threonine kinase glycogen synthase kinase-3 beta (GSK3b) is a known master regulator for several cellular pathways that include insulin signaling and glycogen synthesis, neurotrophic factor signaling, Wnt signaling, neurotransmitter signaling and microtubule dynamics. Consequently, this enzyme has been implicated in multiple human disorders including Alzheimer's disease, bipolar disorder, noninsulin-dependent diabetes mellitus, cardiac hypertrophy, and cancer. Precisely how GSK3b maintains its pathway specificity efficiently at the crossroads of many cellular processes is still unclear. Many inhibitors of GSK3b exist, however these compounds have been found lacking in selectivity, with CHIR 99021 considered most potent and selective. The goal for this project is to identify potent and highly selective small molecule probes to investigate GSK3b biology in cellular and ultimately in whole animal models. A library of over three hundred twenty thousand compounds was screened against human GSK3b. Among the inhibitors identified, CID 5706819 showed decent potency and excellent selectivity inhibiting only five out of over three hundred kinases at 10 µM by over fifty percent. Subsequent chemical modifications of CID 5706819, guided by a co-crystal structure with GSK3b, and a battery of biochemical and cell-based assays led to CID 56840716/ML320 that inhibits GSK3b at IC_{50} between 10-30 nM. ML320 has a superior kinome-wide selectivity profile compared to CHIR99021. Further, ML320 demonstrates excellent cellular activity in inhibiting GSK3b-mediated Tau phosphorylation in SH-SY5Y neuroblastoma cells (IC_{50} of 1 µM), and in relieving negative regulation by GSK3b on cellular beta-catenin degradation and TCF/LEF promoter activities with EC_{50} of 5 µM in both assays. At the same time, no cellular toxicity by ML320 was observed in SH-SY5Y cells at the highest testing concentration of 30 µM. Taken together, ML320 is a potent and highly selective small molecular probe against GSK3b, allowing better investigation and interpretation of GSK3b cellular functions than the existing prior art. ML320 scaffold also holds the promise to deliver additional compounds with further

improved biochemical, cellular, and pharmacokinetic properties suitable for investigating *in vivo* roles of GSK3b in pertinent animal physiology and pathology.

Probe Structure & Characteristics:
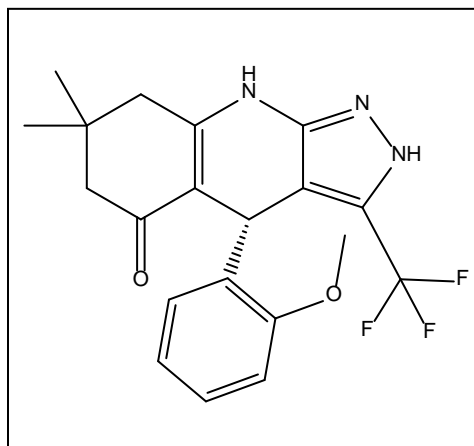
ML320

CID/ML	Target Name	IC$_{50}$ (nM) [SID, AID]	Anti-target Name	IC$_{50}$ (µM) [SID, AID]	Fold Selective	Phospho-Tau ELISA in SHSY5Y Cells (IC$_{50}$, µM) [SID, AID]
CID 56840716/ ML320	GSK3b	24 [SID 13497044, AID 623998]	CDK5	8.9 [SID 13497044, AID 623999]	380	1.03 [SID 134970446, AID 624057]

Recommendations for scientific use of the probe:

There exists significant evidence for a critical role for GSK3 signaling in the regulation of neurogenesis, neurodevelopment, and in neuroplasticity. GSK3 function is modulated by both mood stabilizers that treat bipolar disorder patients and antipsychotics for treating schizophrenia. Aberrant GSK3 signaling has further been implicated in the etiology of neuropsychiatric disorders which demonstrates a role for the inhibition of GSK3 by the schizophrenia-associated gene DISC1 (1). Accordingly, the identification of small-molecule probes that inhibit GSK3 signaling will be valuable tool compounds for probing the role of Wnt/GSK3 signaling in the pathophysiology of bipolar disorder and other neuropsychiatric disorders and eventually as candidate therapeutics for modulating human neurogenesis. A summary of potential experimental uses of the molecular probe we have defined include:

- At a basic research level, since the Wnt/GSK3 signaling has been shown to play an important role in regulating mammalian neurogenesis and neurodevelopment (2,3) we anticipate that a GSK3 probe will provide a critically needed, precise tool to probe the GSK/Wnt molecular pathways both in *in vitro* studies with human and rodent neural progenitors, and also, after further optimization, as probes of these pathways *in vivo*.

- Aberrant Tau phosphorylation, including at GSK3 sites, has been implicated in the pathophysiology of a number of human neurodegenerative disorders, including Alzheimer's disease and the primary tauopathies (e.g. progressive supranuclear palsy and other frontotemporal dementias). (4,5) Decreasing Tau phosphorylation with a selective GSK3 inhibitor will provide insight into the underlying disease mechanisms and may provide a method of reversing disease symptoms.

- For efforts using patient-specific stem cell models, we anticipate being able to systematically assess whether there are differences in the response of induced pluripotent stem cells-neural progenitor cells (iPSC-NPCs) from patients with neuropsychiatric disorders to GSK3 modulators including a panel of iPSC models that we and others are developing from patients with bipolar disorder, schizophrenia, and Fragile X syndrome (6)—disorders in which there exists evidence for dysregulation of GSK3 signaling that may be causally involved in the underlying pathophysiology.

- In the specific context of on-going studies on the role of DISC1/GSK3 signaling in the pathophysiology of neuropsychiatric disorders (1), it will now be feasible to investigate whether selective GSK3 inhibition can rescue deficits caused by genetic variation in human/mouse DISC1, including in assays of *in vivo* neurogenesis in embryonic and adult mice.

- Most broadly, through the reversal or compensation of deficits, the modulation of post-natal and adult neurogenesis has been proposed as a potential therapeutic avenue for multiple neuropsychiatric and neurodegenerative disorders including bipolar disorder, major depression, traumatic brain injury, Alzheimer's disease, Parkinson's disease, and Huntington's disease.

1   Introduction

Scientific Rationale

The serine/threonine kinase glycogen synthase kinase-3 beta (GSK3b) is a known master regulator for several cellular pathways that include insulin signaling and glycogen synthesis, neurotrophic factor signaling, Wnt signaling, neurotransmitter signaling and microtubule dynamics (7,8,9). Consequently, this enzyme has a critical role in metabolism, transcription, development, cell survival, and neuronal functions and has been implicated in multiple human

disorders including Alzheimer's disease, bipolar disorder, noninsulin-dependent diabetes mellitus, cardiac hypertrophy, and cancer (10,11,12,13,14). Precisely how GSK3b maintains its pathway specificity efficiently at the crossroads of many cellular processes is still unclear. In this light, the long-term goal of our program is to develop highly selective, potent, and brain penetrant inhibitors of GSK3b with best-in-class selectivity and efficacy toward modulating GSK3b signaling. Of particular interest is the ability to develop GSK3b inhibitors that regulate Wnt-signaling as a proxy for the pathways involved in neuroplasticity that we hypothesize are critical for regulating mood in bipolar disorder and potentially other psychotic disorders. Thus, highly selective small molecule modulators are needed to help elucidate GSK3b function and regulation in central nervous system disorders. Currently, no such small molecule exists with the correct combination of selectivity and pharmacokinetic properties to accurately perturb the role of GSK3b in established rodent models of memory and mood.

The objective of the experiments in this probe report is to identify small molecule inhibitors of GSK3b signaling that show improved potency, selectivity and physiological stability over the current prior art modulators. The final probe will have demonstrated potency (<1 µM), kinase selectivity (>10-fold IC_{50}), inhibition of Tau phosphorylation (IC_{50}<10 µM) and activation of Wnt signaling (EC_{50} <10 µM) with an end-point goal of translating cellular data to *in vivo* models. These results will uncover the absolute relevance of GSK3b signaling in CNS disorders.

In the most extensive analysis of GSK3 inhibitors reported to date, four of the most promising GSK3 inhibitors were tested head to head against a panel of 30 kinases (15). Based on this study, the compound CHIR 99021 was found to be most potent and selective with an IC_{50} against GSK3b of 40 nM and an IC_{50} against CDK2 of 1.4 µM without inhibiting any of the other kinases at 1 µM. Further discussion of the prior art and a comparison to the probe compound to the prior art can be found in Section 4.1.

2   Materials and Methods

See subsections for a detailed description of the materials and methods used for each assay. A summary listing of completed assays and corresponding PubChem AID numbers is provided in **Appendix A** (Table A1). Refer to **Appendix B** for the detailed assay protocols.

2.1   Assays

2.1.1. Primary HTS (AID 2097)

The GSK3b primary screen was conducted in assay ready 1536 plates (Aurora 29847) that contain 2.5 nL/well of 10 mM compound. Human GSK3b as a GST fusion expressed in baculoviral system was purchased from BPS Bioscience (San Diego, CA). The GSK3b peptide substrate was from American Peptide (Sunnyvale, CA; Cat 311153). 1 µL /well of CABPE (22.5 nM GSK3b, 8 µM peptide in AB buffer (12.5 mM DTT, 0.25 mg/mL BSA, 0.5unit/mL Heparin)), 0.5 µL /well of 125 µM of ATP, and 1 µL /well of positive control 50 µM of GW8510 (positive control) or AB (DMSO only neutral control) in respective wells according to plate design using

BioRAPTR (Beckman, Brea, CA). Reactions were incubated at room temperature for 60 minutes. 2.5 µL /well of ADP-Glo (Promega, V9103) was added with BioRAPTR, and incubated at room temperature for 40 minutes followed by addition of 5 µL /well of ADP-Glo detection reagent (Promega, V9103) with Combi nL (Thermo, Waltham, MA) and incubation at room temperature for 30 minutes. The plates were read on a ViewLux (PerkinElmer, Waltham, MA) for luminescence. Data were scaled using the positive and neutral controls and fitted for IC_{50} as described in AID 2097.

2.1.2. Confirmatory assay (AID 434954)

The confirmatory assay was a retest of active compounds in primary HTS above and along with some of their negative analogues. The assay was performed the same as the primary screen except the compounds were tested in doses.

2.1.3. Counter screen of ADP-Glo reagents (AID 434947)

The ADP-Glo reagent counter screen is to identify false positives due to inhibition of the ADP-Glo detection system. 2.5 µL of 5 µM of ADP were incubated directly with compounds in doses at room temperature for 60 minutes. 2.5 µL /well of ADP-Glo (Promega, V9103) was added with BioRAPTR, and incubated at room temperature for 40 minutes followed by addition of 5 µL /well of ADP-Glo Detection (Promega, V9103) with Combi nL (Thermo, Waltham, MA) and incubation at room temperature for 30 minutes. The plates were read on a ViewLux (PerkinElmer, Waltham, MA) for luminescence. Data were scaled using the positive and neutral controls and fitted for IC50 as described in AID 434947.

2.1.4 Tau phosphorylation assay (AID 624057)

SH-SY5Y cells were maintained in DMEM supplemented with 10% heat-inactivated FBS and 1% penicillin-streptomycin (Invitrogen) unless otherwise stated. ELIZA kits for phospho-Tau (Ser199) and total Tau detection were purchased from Invitrogen (KHB0041, and KHB7041 respectively). Briefly, SH-SY5Y cells were seeded at 50,000 cells/200 µL / well in 96 well plates and after overnight incubation, treated with various doses of chemical compounds at 0.2 µL /well. The next day cells were washed with PBS twice before being lysed in 100 µL Lysis buffer/well. 50 µL of cell lysate of each sample was transferred to an ELISA vial coated with the capture antibody, and the mixture was incubated at room temperature for 2 hours, before the supernatant was aspirated, and each vial washed four times. 100 µL of detection antibody was then added to each well, incubated for 1 hour, and then washed four times. The amount of phospho-Tau and total Tau was measured by adding 100 µL of anti-rabbit IgG Horseradish peroxidase working solution to each well, and absorbance of each well at 450 nM was read on EnVision (PerkinElmer, Waltham, MA). Data were scaled using the positive and neutral controls and fitted for IC50. The detailed protocol is included in Appendix B.

2.1.5 Single Point Inhibitory Analysis of Selected Compounds (Carna Biosciences) (AID 624076)

Briefly, a selection of compounds was screened against a panel of kinases at a single concentration of 10 µM. The kinases were selected from all families of the kinome and in all represented 60% of the entire kinome for a total of 311 kinases screened. This was completed utilizing one of two assays depending on the kinase being examined

IMAP Assay. A solution of 4X inhibitor, 4X substrate/ATP/Metal solution and 2X kinase solution was prepared with assay buffer (20 mM HEPES, 0.01% Tween-20, 2mM DTT, pH 7.4) and mixed/incubated in 384 well black plates for 1 hour at room temperature. A solution of IMAP binding reagent (IMAP Screening Express kit; Molecular Devices) was added to each well and incubated for 30 minutes. Level of kinase activity was then evaluated by fluorescence polarization at 485 nM (exc) and 530 nM (emm) of each well.

Off-Chip Mobility Shift Assay (MSA). A solution of 4X inhibitor, 4X substrate/ATP-Metal solution and 2X Kinase solution was prepared with assay buffer (20 mM HEPES, 0.01% Triton X-100, 2mM DTT, pH 7.5) and mixed/incubated in 384 well plates for 1 or 5 hours depending on the kinase, at room temperature. A solution of termination buffer (QuickScout Screening assist MSA; Carna Biosciences) was added to each well. The entire reaction mixture was then applied to a LabChip3000 system (Caliper Life Science) and the product and substrate peptide peaks were separated and quantified. Evaluation of kinase activity was then determined based on ratio of calculated peak heights of product (P) and substrate (S) peptides (P/(P+S)).

2.1.6 Dose Response IC50 Determination of Selected Compounds Against Selected Kinases (Carna Biosciences)

Briefly, a selection of compounds was screened against a selected panel of kinases based on single point inhibitory ability to determine absolute inhibitory activity, leading to selectivity measurements. The assay utilized was identical to that of the single point inhibitory activity determination (MSA) but run in dose response. A solution of 4X inhibitor, 4X substrate/ATP Metal solution and 2X Kinase solution was prepared with assay buffer (20mM HEPES, 0.01% Triton X-100, 2mM DTT, pH 7.5) and mixed/incubated in 384 well plates for 1 or 5 hours depending on the kinase, at room temperature. A solution of termination buffer (QuickScout Screening assist MSA; Carna Biosciences) was added to each well. The entire reaction mixture was then applied to a LabChip3000 system (Caliper Life Science) and the product and substrate peptide peaks were separated and quantified. Evaluation of kinase activity was then determined based on ratio of calculated peak heights of product (P) and substrate (S) peptides (P/(P+S)).

2.1.7 Total Tau assay (AID 624057)

SH-SY5Y cells were maintained in DMEM supplemented with 10% heat-inactivated FBS and 1% penicillin-streptomycin (Invitrogen) unless otherwise stated. ELISA kits for total Tau detection were purchased from Invitrogen (KHB7041). SH-SY5Y cells were seeded at 50,000

cells/200 µL / well in 96 well plates and after overnight incubation, treated with various doses of chemical compounds at 0.2 µL /well. The next day cells were washed with PBS twice before being lysed in 100 µL Lysis buffer/well. 50 µL of cell lysate of each sample was transferred to an ELIZA vial coated with the capture antibody, and the mixture was incubated at room temperature for 2 hours, before the supernatant aspirated, and each vial washed four times. 100 µL of detection antibody was then added to each well, incubated for 1 hour, and washed four times. The amount of total Tau was measured by adding 100 µL of anti-rabbit IgG Horseradish peroxidase working solution to each well, and absorbance of each well at 450 nM was read on EnVision (PerkinElmer, Waltham, MA). Deviation from neutral controls was calculated and indicated toxicity in these neuroblastoma cells. Detailed protocol is included in Appendix B.

2.1.8 beta-Catenin Nuclear Localization Assay (AID 624086)

U2-OS cells stably expressing two complimentary β-Galactosidase fragments (one part on β-Catenin and the other constitutively expressed in the cell nucleus) were maintained in DMEM F12 supplemented with 10% FBS.   When β-Catenin translocates to the nucleus, the complimentary fragments form a complete β-Galactosidase, the amount of which is then quantified by β-galactosidase activity (DiscoveRx). Cells were seeded in a 384-well CulturPlate (Perkin Elmer, Boston, MA) with 10,000 per well in 20 µL DMEM F12 containing 10% FCS, 100 U/ml penicillin and 100 µg/mL streptomycin. After overnight incubation at 37°C, cells were stimulated with 100 nL chemical compound / well and then returned to the incubator for 6 h. Cells were disrupted using 12 µL substrate-containing lysis buffer from the PathHunter Detection Kit in the formulation specified by the supplier (DiscoveRx). Plates were incubated in the dark for 1 h at room temperature before measurement of β-galactosidase activity (luminescence) on an EnVision plate reader (PerkinElmer, Waltham, MA). Detailed protocol is included in Appendix B.

2.1.9 TCF/LEF reporter assay (AID 624088)

HEK293-pBARL cells were derived from HEK293 cells and they stably expressed a firefly-luciferase reporter gene driven by a promoter containing 12 copies of TCF/LEF binding sequences. These cells were maintained in DMEM and supplemented with 10% FBS and 1% penicillin-streptomycin (Invitrogen). Reporter gene assays were conducted in anti-biotic free media. TCF/LEF reporter gene activity was assayed as described previously (Pan et al, 2011, Neuropsychopharmacology). These cells also contained a renilla-luciferase reporter gene driven by the ubiquitous EF1α promoter as a control. HEK293-pBarl reporter cell lines were seeded into 384-well culture plates (Corning) at 6000 cells/well. 24 hours after plating, cells were treated overnight with relevant compounds and assayed using DualGlo assay kit (Promega). Luminescent intensities were read by EnVision (PerkinElmer, Waltham, MA). Firefly luciferase intensity is normalized by renilla luciferase intensity. The detailed protocol is included in Appendix B.

2.1.10 Secondary Surface Plasmon Resonance Affinity Determination (AID 624091)

Briefly, approximately 20,000 Response Units (RU) of anti GST-antibody (GE Healthcare Life Sciences) were immobilized on Flow Cell (FC) 1 and FC2 of a new, freshly conditioned CM5 SensorChip (GE Healthcare Life Sciences) in a Biacore T100 instrument utilizing the immobilization wizard of the T100 software package. Approximately 1,200 RU of recombinant GST (GE Healthcare Life Sciences) was then captured on FC1 utilizing the capture wizard protocol of the T100 software package. FC1 is used as a reference subtraction point for this and all SPR assays. Approximately 2,500 RU of recombinant GST-GSK3β was then captured on FC2 utilizing the capture wizard protocol of the T100 software package. FC2 is used as the active flow cell for this and all SPR assays. The analyte plate is generated in dose response fashion in TBS buffer containing a final concentration of 2% DMSO, with a final analyte concentration of 10 µM to 10 nM with a 2X dilution factor. A zero value is determined by running injections of buffer containing only 2% DMSO and no analyte. All injections are run in duplicate and are reference subtracted from FC1. A method consisting of a 60 second contact time and 60 second wash time with a flow rate of 30 µL /min was developed. The internal standard curve for DMSO values was generated with seven injections of DMSO consisting of 1, 1.25, 1.5, 2, 2.25, 2.5 and 3% DMSO in TBS running buffer. Analysis of compounds was done using the 1:1 binding model and affinity measurements in the Biacore T100 evaluation software package.

2.2 Probe Chemical Characterization

After preparation as described in Section 2.3, the probe (ML320) was analyzed by UPLC, ^{1}H and ^{13}C NMR spectroscopy, and high-resolution mass spectrometry. The data obtained from NMR and mass spectroscopy were consistent with the structure of the probe, and UPLC indicated an isolated purity of >95%. Characterization data (^{1}H, ^{13}C, ^{19}F NMR spectra and LC chromatogram) of the probe are provided in **Appendix E.**

The solubility of the probe (ML320) was experimentally determined to be 85 uM in phosphate buffered saline (PBS, pH 7.4, 23°C) solution. Plasma protein binding (PPB) was determined to be 93% bound in human plasma. The probe is stable in human plasma, with approximately 97% remaining after a 5-hour incubation period. The compound was found to be stable in glutathione (GSH) with 99% remaining after 48 hours.

The stability of the probe (ML320) in PBS (0.1% DMSO) was measured over 48 hours. We noticed that the concentration of the probe steadily increased over 48 hours to about 200% (data not shown). We believe that the gradual increase in concentration is the direct result of more compound dissolving in PBS over time. In other words, when we performed the PBS stability assay under the recommended conditions, we measured the kinetic solubility of the probe in PBS and not its stability. Thus, we decided to determine the total amount of the probe present in the well after the probe was treated with PBS alone for a given length of time. We added acetonitrile at various time points to wells containing the probe in PBS and measured the total amount of the probe. This result is shown in **Figure 1**. From these results, the probe seems to be stable in PBS since more than 95% is still present after 48 hours of incubation.

Figure 1. Stability Data for the Probe (ML320) in PBS Buffer (pH 7.4, 23°C) followed by addition of acetonitrile after 48 Hours
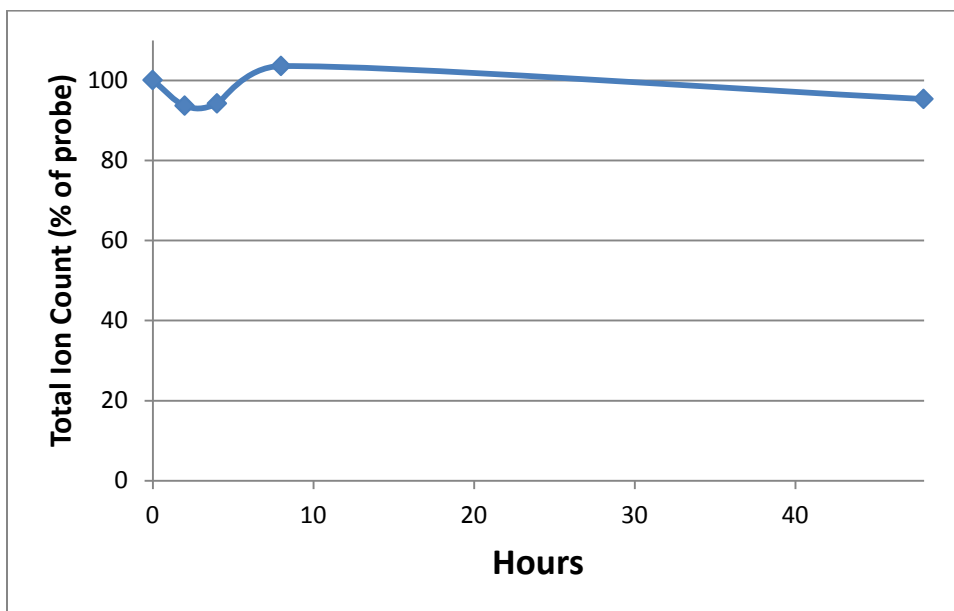
Table 1. Summary of Known Probe Properties in PubChem

IUPAC Chemical Name	(*R*)-4-(2-methoxyphenyl)-7,7-dimethyl-3-(trifluoromethyl)-6,7,8,9-tetrahydro-2*H*-pyrazolo[3,4-b]quinolin-5(4*H*)-one
PubChem CID	56840716
Molecular Weight	391.38691 [g/mol]
Molecular Formula	$C_{20}H_{20}F_3N_3O_2$
H-Bond Donor	2
H-Bond Acceptor	7
Rotatable Bond Count	2
Exact Mass	391.150762
Topological Polar Surface Area	62.7

2.3   Probe Preparation

The probe (ML320) was synthesized from 5,5-dimethylcyclohexane-1,3-dione, 2-methoxybenzaldehyde and 3-(trifluoromethyl)-1*H*-pyrazol-5-amine in one step (see **Scheme 1**). Heating of 5,5-dimethylcyclohexane-1,3-dione, 2-methoxybenzaldehyde and 3-(trifluoromethyl)-1*H*-pyrazol-5-amine in ethanol at 150°C in the microwave for 15 minutes provided the racemic probe 4-(2-methoxyphenyl)-7,7-dimethyl-3-(trifluoromethyl)-6,7,8,9-tetrahydro-2H-pyrazolo[3,4-b]quinolin-5(4*H*)-one in 40% yield. The enantiomers were then separated by chiral chromatography to yield the probe (*R*)-4-(2-methoxyphenyl)-7,7-dimethyl-3-(trifluoromethyl)-6,7,8,9-tetrahydro-2*H*-pyrazolo[3,4-b]quinolin-5(4*H*)-one.
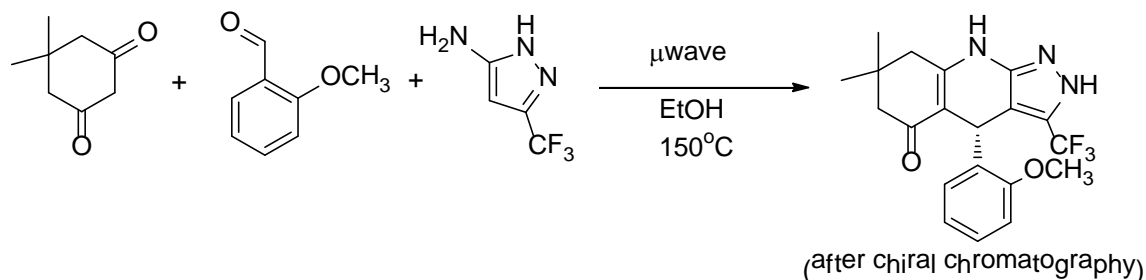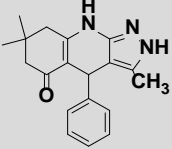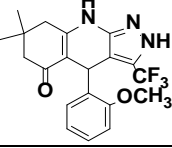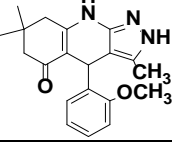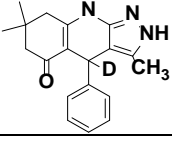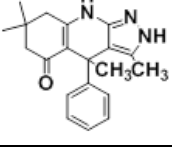
Scheme 1.   Synthesis of the Probe (ML320)

Experimental procedures for the synthesis of the probe (ML320) are provided in **Appendix C**.

2.4 Additional Analytical Analysis

The probe (ML320) was found to be 93% and 91% bound to human and mouse plasma respectively and stable in human and mouse plasma with 97% and 99% remaining after 5 hours. The hit compound, racemic probe and seven analogs were subjected to mouse microsomes for stability analysis (**Table 2**). The racemic probe was found to be unstable to mouse microsomes with <1% remaining after 1 hour. All other analogs that were unsubstituted at the benzylic position had <7% remaining after 1 hour, indicating that the primary metabolic liability is the benzylic position. Substitution at the benzylic position with a methyl group (Table 2, Entry 9) resulted in 32% compound remaining after 1 hour. Future analogs synthesized will be focused on compounds with substitution at the benzylic position to yield increased potency while maintaining this metabolic stability gain. Experimental procedures for the analytical assays are provided in **Appendix D**.

Table 2: Microsomal Stability of Select Compounds

No.	CID SID Broad ID	Structure	% Remaining after 1h Mouse Microsomes	GSK3β ADPGlo 10µM ATP IC_{50} (µM)
1	5706819 135378298 A81474003 (HTS Hit)		6.0	0.31
2	56589437 134959049 A89407846		0.3	0.13
3	5928898 135378292 A93281121		3.0	0.12
4	56589399 134216531 A25071499		6.8	0.62
9	56846669 135378259 A18945128		32	0.31

All values are the average of at least two replicates

3   Results

Table 3. Probe attributes:

Biological Characteristics	Probe Attributes
Target Activity: GSK3b	IC_{50} < 0.1 µM in primary assay
Selectivity: Anti-Target : CDK-5	> 10X selective for GSK3b over 200 other kinases including CDK5
Biological Mode of Action	Cell –based activity: Inhibits GSK3-mediated Tau phosphorylation at EC_{50} < 10 µM
MOA	Refractory to 100 µM ATP with an IC_{50} of < 250 nM
Cellular Toxicity	Non-toxic to cells at $\geq$ 20 µM
Functional Groups to be avoided	1. Chemically reactive groups 2. Metabolically labile compounds 3. pH sensitive or hydrolytically unstable compounds
Chemical Solubility Criteria	Soluble in assay buffer
Preferred but not necessary attributes	
Activates Wnt signaling pathway	EC_{50} < 10 µM
Stabilizes beta-catenin	EC_{50} < 10 µM

3.1   Summary of Screening Results

Figure 2 displays the critical path for probe development.

A high-throughput screen of approximately 320,000 compounds was completed against human GSK3b (AID 2097) in 1536-well plate format. The screen featured an average Z' > 0.8. Approximately 1,000 compounds showed more than 25% inhibition were selected as actives.

These actives, along with approximately 1,000 of their negative analogues in the library, were cherry-picked and their potencies (IC_{50}) against GSK3b assessed in a set number of dilutions in a confirmatory retest assay (AID 434954). In parallel, a counter screen to rule out false positives due to inhibition of detection reagents was also completed (AID 434947). Compounds with promising potency (IC_{50} < 1 µM against GSK3b at this stage) but not inhibiting detection reagents were further evaluated for structural features that are likely to render novelty, selectivity, and tractability.

The goal for this project was to obtain highly selective and potent, GSK3b inhibitors. Given that a great deal of work has been done on the GSK3b target, we focused on structural series that

do not possess scaffolds common to known kinase inhibitors. The selection of the dihydropyridine scaffold (Section 2.3, Scheme 1) as an initial probe starting point was based on results from ADP-Glo experiments (*vide infra*, Section 3.3, Table 5, Entry 1) that indicated a potency against GSK3b in the sub-micromolar range. This initial filter allowed for the selection of a limited number of scaffolds from the original library of more than 300,000 small molecules screened. Based on a search of PubChem, this scaffold had been analyzed in a large selection of assays (>600) but was confirmed as active in only one assay other than the assays described in this report, which did not pertain to kinase inhibition. Secondly, as illustrated above in Section 2.3, Scheme 1, the synthesis of this scaffold lent itself to rapid introduction of chemical diversity. This high synthetic tractability made for an attractive target from a chemistry vantage point. Last was our internally determined selectivity profile. In collaboration with Carna Biosciences, an initial selectivity analysis was done to determine the percent of the kinome inhibited by our initial HTS hit (CID 5706819). The selectivity assay described in Appendix B examined the inhibitory ability of the dihydropyridine scaffold against 311 kinases (representing 60% of the existing kinome) at a held concentration of 10 µM. Captured in **Table 3** below are the results of the only kinases inhibited greater than 50% by treatment with the dihydropyridine scaffold at 10 µM.

Table 4. Percent Inhibition of Selected Kinases by HTS Hit (CID 5706819) at 10 µM.

Kinase	% Inhibition at 10 µM compound
GSK3a	100
GSK3b	100
CK1d	94.4
CK1a	57.3
CK1e	50.0

As mentioned previously, the state of the art for GSK3b inhibition is CHIR99021. When this compound was compared for selectivity with the same criteria as the HTS hit, CHIR99021 inhibited 20 kinases greater than 50% at 10 µM (see Section 3.6 for comparison between CHIR99021 and CID 5706819). This initial selectivity analysis, combined with the ease of synthesis and excellent potency led to the conclusion that the dihydropyridine scaffold would be an excellent choice for further analysis as a probe candidate.

Surface Plasmon Resonance Examination

A direct binding assay was then utilized as a secondary analysis of compound activity. Surface Plasmon Resonance (SPR), was employed to examine a small collection of dihydropyridine derivatives synthesized as part of this probe report. Upon examination using this assay, it was discovered that substitution of the aryl ring at the 2-position led to increases in affinity of these molecules for GSK3b. The HTS hit (CID 5706819) has an experimentally determined K_D of 130

nM, the best compound to come out of the SPR analysis (CID 5928898, **Table 5, Entry 14**) has an experimentally determined K_D of 60 nM. A greater than 2-fold increase in affinity was achieved by a methoxy substitution at the 2-position of the aryl ring.

Separation of Enantiomers

Examination of the structure of CID 5928898 illustrates that a racemic mixture is present leading to the hypothesis that one enantiomer may be more active than the other. To test this hypothesis, separation of the two enantiomers was completed to arrive at a single compound. Illustrated in **Table 13, Entry 2** is CID 5524264, the R-enantiomer of CID 5928898. This enantiomer was examined *via* SPR affinity measurements and was shown to have a K_D of 24 nM, more than twice the affinity of the racemic mixture tested previously. Further testing of this enantiomer for activity against the list of kinases previously determined (**Table 4**), illustrated that CID 5524264 was selective for GSK3a/b and did not inhibit any of the CK1 family as seen when examining the racemic mixture. The absolute stereochemistry of the active enantiomer was determined through co-crystallization of CID 5524264 with GSK3b (see **Figure 4**).

The crystal structure also confirmed that the compound binds in the ATP binding site however it binds to different residues than other known GSK3b inhibitors, lending a potential explanation for the superior selectivity displayed by this series.

From these initial results, it was determined that the dihydropyridine scaffold could lead to a suitable probe that met all predisposed criteria (**Table 3**). At this point, medicinal chemistry, biochemical and cell biology efforts were initiated to pursue this scaffold.

55 compounds were synthesized (**Table 5-13**). The compounds were designed to explore SAR at different chemical moieties of the dihydropyridine scaffold, enhance desired properties and decrease liabilities, including potency, selectivity, solubility, and in some instances, microsomal stability. Racemic mixtures of certain analogs were separated and activities of enantiomers were measured (**Table 13**). A detailed discussion of SAR is provided in Section 3.4 and Section 4.

Biochemical characterization of these synthesized compounds were assayed against GSK3b (AID 623998) and CDK5/p25 (AID 623999), with CDK5/p25 serving as a counter target of GSK3b selectivity. Additional biochemical characterization for potency and selectivity were also performed at Carna Biosciences (AID 624076 and 624091). We also conducted a battery of cell-based assays to assess the cellular activity of a subset of these compounds. These cell-based assays include phosphorylation of Tau in SH-SY5Y human pathophysiology cells (AID 624057), beta-catenin nuclear translocation (AID 624086), and the TCF/LEF reporter assay that monitors the Wnt signaling pathway in HEK293 cells (AID 624088). The effects of these compounds on survival of SH-SY5Y pathophysiology cells were also monitored (AID 624057). Detailed discussions of cellular activities are provided in Section 3.5. The probe compound (ML320) consistently demonstrates 10-20 nM potency against GSK3b, 150-380 fold selectivity relative to CDK5/p25 (Section 3.4 Table 13, and Section 3.6), superior kinome selective profile

as compared to CHIR99021 (Section 3.6), and potent cellular activity (Section 3.4 Table 13 and Section 3.5).

![BROAD INSTITUTE]

Figure 2.   Critical Path for Probe Development
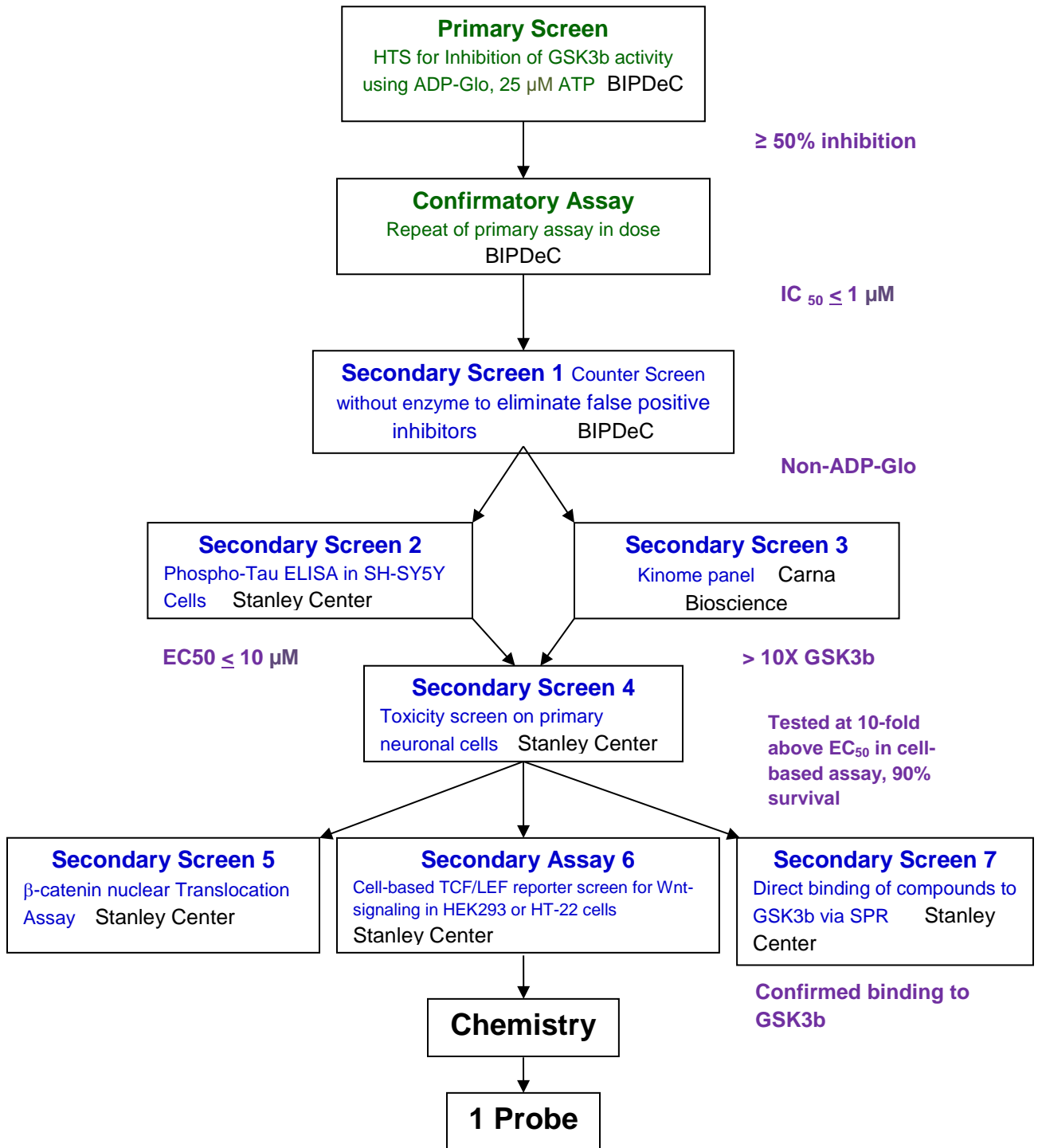
3.2 Dose Response Curves for Probe

Figure 3. Dose-dependent Activity of the Probe (ML320) in Target (GSK3b, left) and Anti-Target (CDK5, right). Representative curves with duplicated data (circles and triangles) are shown.
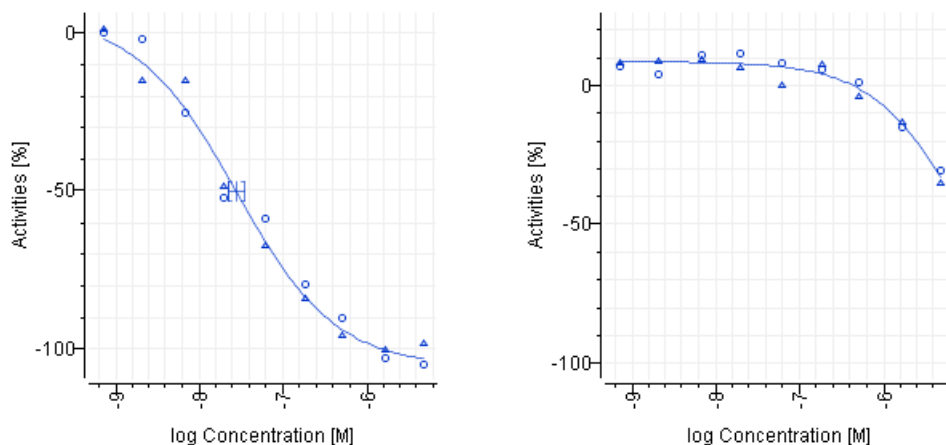
3.3 Scaffold/Moiety Chemical Liabilities

A search of PubChem for the hit compound from the primary screen (CID 5706819, **Table 5, Entry 1**) revealed that it had been tested in 652 bioassays and was confirmed as active only in one assay other than the assays described in this report. The assay was a screen for inhibitors of hydroxysteroid (17-beta) dehydrogenase 4 (HSD17B4) with a potency of 25.1 µM. Based on this information the compound does not seem to be a promiscuous inhibitor, also the scaffold does not contain any obvious chemical liabilities.

3.4 SAR Analysis

Screening results are described in **Tables 5-13**. In **Table 5**, results for the HTS hit (**Table 5, Entry 1**) and its enantiomers are shown. The (*S*)-enantiomer (**Table 5, Entry 2**) was found to be the active enantiomer, though the relative dispositions of the groups around the chiral carbon are the same as CID 5524264 (see **Section 3.1**), the *R/S* designation is reversed due to a switch in the priority of the groups, as it was approximately 25-times more potent than the l-enantiomer (**Table 5, Entry 3**) in the primary assay. Aromatization of the hit compound (**Table 5, Entry 4**) resulted in a complete loss of GSK3 activity indicating that the oxidation state of the hit compound was vital for activity.

Figure 4. a) Ribbon diagram depicting GSK3b and CID 5524264 in the ATP binding pocket b) Surface representation showing the binding site, binding orientation and absolute configuration of CID 5524264
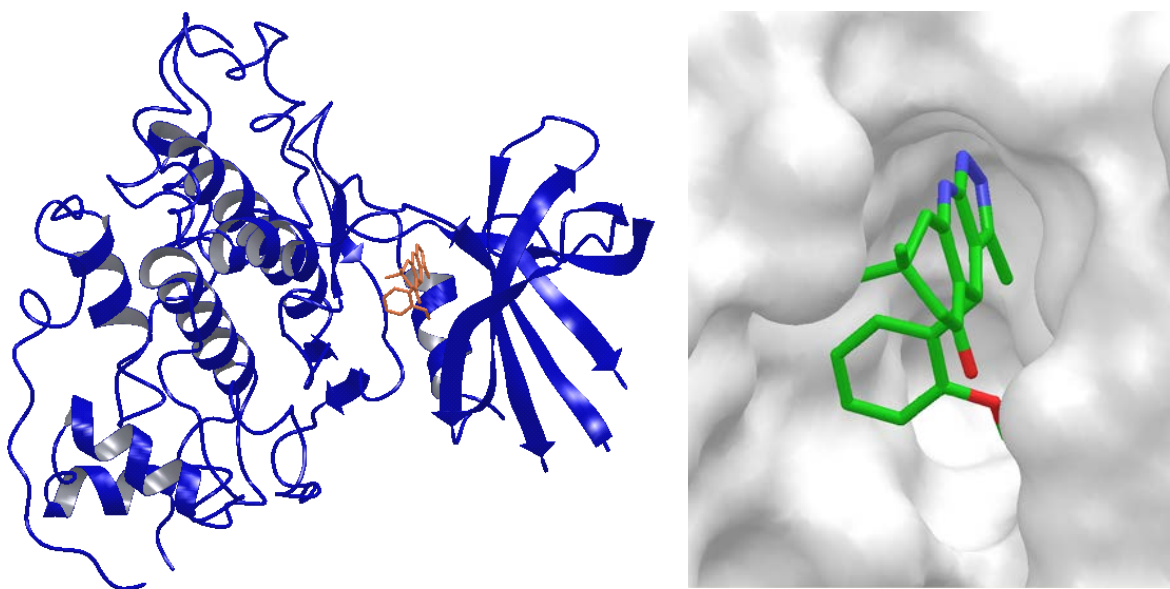
Table 6 describes the effect of replacing the phenyl group with alkyl substituents. Attempted replacement of the phenyl with a hydrogen resulted in the formation of an aromatized product (**Table 6, Entry 2**), which lost GSK3 inhibitory activity. The methyl replacement (**Table 6, Entry 3**) displayed similar activity in the primary assay, along with an increase in solubility, however no cellular activity. Substitution with either cyclopropyl (**Table 6, Entry 4**) or cyclohexyl (**Table 6, Entry 5**) resulted in a significant drop in activity.

Table 7 illustrates the effects of various substitutions on the phenyl ring. The nature of the substituent had little effect on the potency of the compound, fluoro, chloro, trifluormethyl, methyl, methoxy, and cyano all resulted in compounds with similar potency. The position of the substituent however, had a more profound impact on the activity. Substitution at the *ortho*-position resulted in the most potent compounds though, in general, the lowest selectivity versus CDK5. Compounds substituted at the *meta*-position were slightly less potent, but displayed higher selectivity over CDK5. Compounds which were substituted at the *para*-position resulted in a significant drop in GSK3 activity which can be predicted based on the binding observed in the crystal structure (**Figure 4**). The crystal structure shows that while there are pockets for substituents at the 2- and 3-position, the binding at the 4-position of the phenyl ring is too tight to tolerate groups larger than hydrogen. Compounds that were particularly interesting due to their activity in the primary assay and cell assays were the 2-fluoro compound (**Table 7, Entry**

2), 2-trifluoromethyl (**Table 7, Entry 8**), 2-methoxy (**Table 7, Entry 14**), 2-methylthio (**Table 7, Entry 21**), 3-trifluoromethyl (**Table 7, Entry 9**) and 3-cyano (**Table 7, Entry 18**).

The results from replacement of the phenyl group with heteroaromatics are shown in **Table 8**. Replacement of the phenyl group with thiophenes (**Table 8, Entries 2-4**) resulted in a drop in potency against GSK3 and no increase in cell activity. Imidazole replacement (**Table 8, Entry 5**) also led to a drop in potency against GSK3. Replacement with a 3-pyridyl group (**Table 8, Entry 7**) resulted in a compound that was equipotent with the hit compound and increased solubility, however had no appreciable cell activity. Other pyridyl replacements (**Table 8, Entries 6, 8, and 9**) resulted in a drop in potency compared to the hit compound.

Having investigated a range of common replacements and substitutions for the phenyl group, the 2-methoxy phenyl was chosen for its potency, selectivity and physical properties to use as the base compound for further SAR studies. The results of SAR studies on the A-ring are summarized in **Table 9**. Movement of the geminal dimethyl group to the α-position of the carbonyl (**Table 9, Entry 2**), resulted in a compound that had a drop in potency in the primary assay and a loss of activity in the cell assays. Removal of the geminal dimethyl group (**Table 9, Entry 3**) resulted in a loss of activity. Replacement of the six-membered ring with a five member ring provided the aromatized compound (**Table 9, Entry 4**), which had no activity against GSK3. Removal of the A-ring (**Table 9, Entry 5**) resulted in a significant drop in activity. Replacement of the germinal dimethyl with a cyclohexyl group (**Table 9, Entry 6**) provided a compound that was similarly potent to the lead compound (**Table 9, Entry 1**), however lost activity in the cell assays.

Table 10 contains data for which the pyrazole has been replaced or substituted at the methyl group. Removal of the methyl group from the pyrazole (**Table 10, Entry 2**) results in a compound that has comparable potency to the lead compound (**Table 10, Entry 1**) indicating that the methyl group is not vital for activity. Replacement of the methyl with larger alkyl groups, such as ethyl (**Table 10, Entry 3**), *iso*-propyl (**Table 10, Entry 4**), and *tert*-butyl (**Table 10, Entry 5**) display a trend of lowering the activity as the group increases in size. This can be explained by the crystal structure as there is a small pocket at this position that can be exploited for substitution allowing the increase in size to ethyl, however further increases result in negative interactions. The phenyl replacement (**Table 10, Entry 6**) results in a drop in potency and loses activity in the cell assays. The trifluoromethyl-containing pyrazole (**Table 10, Entry 7**), while similarly potent to the lead compound in the primary assay shows a significant improvement in the cell assays, presumably due to increase permeability. Replacement of the pyrazole with other aromatics, such as, an oxazole (**Table 10, Entry 8**) or phenyl (**Table 10, Entry 9**) provides compounds with limited activity.

As described in **Section 2.4**, the microsomal stability of this series is poor. Primarily the benzylic position appears to be prone to oxidation. As mentioned previously, the aromatized analog of the hit compound (**Table 5, Entry 4**) is inactive. Since our primary mode of metabolism presumably results in aromatized products we were interested in synthesizing compounds to block this site of metabolism. **Table 11** contains the data for compounds substituted at the
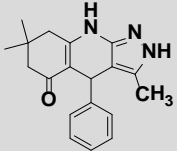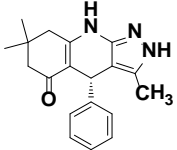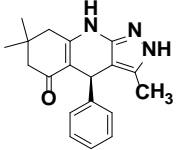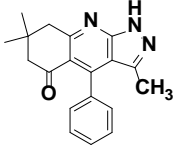
benzylic position. To test whether P450 mediated hydroxylation of the benzylic position was key to the poor metabolic stability profile of the series a compound in which the hydrogen at the benzylic position was replaced with a deuterium was synthesized in an effort to potentially take advantage of a secondary isotope effect and provide an analog with improved metabolic stability (**Table 11, Entry 2**). The deuterium replacement provides a compound that had similar activity to the hit compound, however as shown in **Table 2**, there was no improvement in microsomal stability. The crystal structure indicated that substitution at the benzylic position with a methyl group (**Table 8, Entry 3**) may be tolerated and this compound as shown in **Table 2**, displayed improved microsomal stability (6% to 32%) and also did not result in a loss in potency against GSK3, however this compound displayed no activity in the cell assays. Future efforts will be directed towards compounds that have a methyl at the benzylic position with improved cell activity.

Based on the results from substitution of the phenyl displayed in **Table 7** and pyrazole substitution shown in **Table 10**, several hybrid compounds were synthesized, those results are shown in **Table 12**. Replacement of the methyl on the pyrazole of the hit compound (**Table 5, Entry 1**) with a trifluoromethyl (**Table 12, Entry 2**) results in an increase in potency in the primary assay and activity in the cell assays indicating that the trifluoromethyl is beneficial for cell permeability. Mono- or di-substitution of the phenyl with fluoro and trifluoromethyl groups (**Table 12, Entries 3-5**), lead to compounds that while potent in the primary assay, lose activity in the cell-based assays.

The results from **Table 5** indicated that only one enantiomer in the racemic mixtures of the compounds was responsible for the activity observed which was then explained by the binding of the active enantiomer in the crystal structure, therefore separation of the enantiomers of several compounds was carried out and the data displayed in **Table 13**. As observed previously, the enantiomer where the phenyl was down (**Table 13, Entries 2, 5, and 8**) was the enantiomer responsible for the activity in all cases. Based on this data, I-4-(2-methoxyphenyl)-7,7-dimethyl-3-(trifluoromethyl)-6,7,8,9-tetrahydro-2*H*-pyrazolo[3,4-b]quinolin-5(4*H*)-one (**Table 13, Entry 8**) was chosen as the probe due to its excellent potency and selectivity.

![Broad Institute logo]
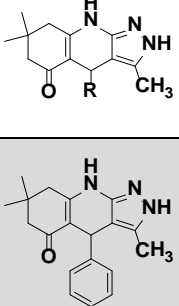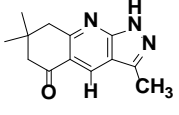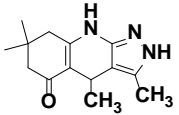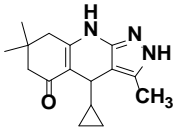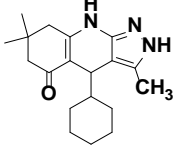
Table 5: Analysis of the HTS Hit Compound

No.	CID SID Broad ID	Structure	GSK3b ADPGlo IC$_{50}$ (µM)	CDK5 ADPGlo IC$_{50}$ (µM)	p-Tau Inhibition ELISA IC$_{50}$ (µM)	beta-Catenin translocation EC$_{50}$ (µM)	TCF/LEF EC$_{50}$ (µM)	Solubility (µM)	Protein Binding % bound	Plasma Stability % remaining
1	5706819 135378298 A81474003 (HTS Hit)		0.31	51.4	NT	inactive	inactive	15.2	H:88.2 M:83.7	H:105.5 M:96.9
2	5523858 135378275 K53064963		0.47	28.5	NT	NT	31	>100	H:86.1 M:83.1	H:97.2 M:96.1
3	5523859 135378277 K48477130		12.2	inactive	NT	NT	inactive	>100	H:86.1 M:83.1	H:97.2 M:96.1
4	56846674 135378250 K81801433		65.5	41.4	NT	NT	inactive	29.1	H:97.5 M:95.9	H:113.4 M:99.8
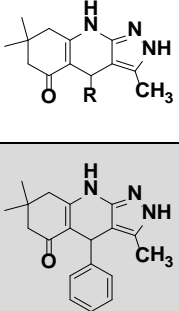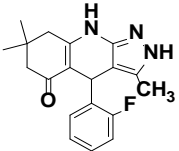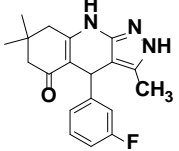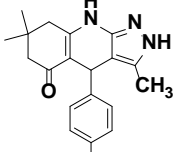
All compounds tested were synthesized; All values are the average of at least three replicates; NT = not tested; ATP concentration = K$_M$[a]
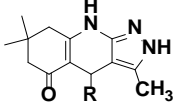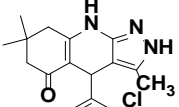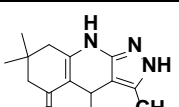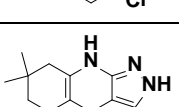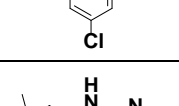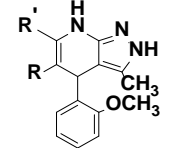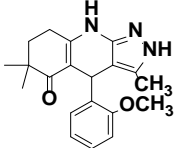
Table 6: SAR of Alkyl Replacements of Phenyl Group
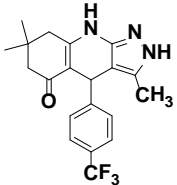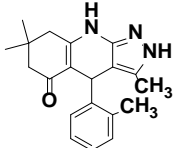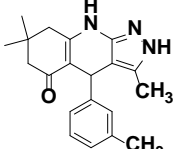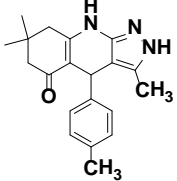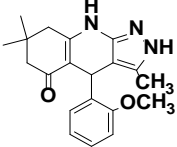
No.	CID SID Broad ID	Structure	GSK3b ADPGlo IC$_{50}$ (µM)	CDK5 ADPGlo IC$_{50}$ (µM)	p-Tau Inhibition ELISA IC$_{50}$ (µM)	beta-Catenin translocation EC$_{50}$ (µM)	TCF/LEF EC$_{50}$ (µM)	Solubility (µM)	Protein Binding % bound	Plasma Stability % remaining
1	5706819 135378298 A81474003 (HTS Hit)		0.31	51.4	NT	inactive	inactive	15.2	H:88.2 M:83.7	H:105.5 M:96.9
2	21600856 134216530 K57760477		82.2	inactive	NT	inactive	inactive	>100	H:74.9 M:84.3	H:96.4 M:86.5
3	56589407 134216535 A68720648		0.53	27.8	NT	>100	inactive	>100	H:66.3 M:57.6	H:152 M:132
4	56589416 134216529 A39560430		3.05	67.0	NT	inactive	inactive	60	H:77 M:78.1	H:87.4 M:101
5	56589404 134216533 A00865489		56.1	inactive	NT	inactive	inactive	1.1	H:93.7 M:95.2	H:92.5 M:106
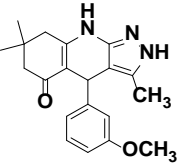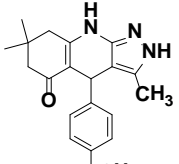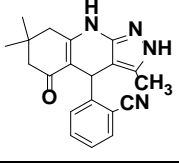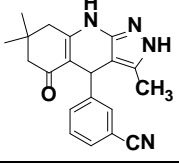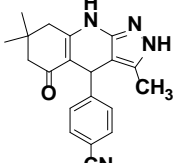
All compounds tested were synthesized; All values are the average of at least three replicates; NT = not tested; ATP concentration = K$_M$[a]
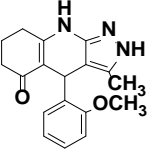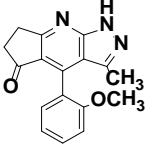
Table 7: SAR of Mono-Substitution on the Phenyl Group

No.	CID SID Broad ID	Structure	GSK3b ADPGlo IC$_{50}$ (µM)	CDK5 ADPGlo IC$_{50}$ (µM)	p-Tau Inhibition ELISA IC$_{50}$ (µM)	beta-Catenin translocation EC$_{50}$ (µM)	TCF/LEF EC$_{50}$ (µM)	Solubility (µM)	Protein Binding % bound	Plasma Stability % remaining
1	5706819 135378298 A81474003 (HTS Hit)		0.31	51.4	NT	inactive	inactive	15.2	H:88.2 M:83.7	H:105.5 M:96.9
2	5830978 135378268 A79621161		0.13	12.0	NT	NT	12.7	7	H:90.1 M:83.0	H:101.8 M:85.0
3	56846672 135378290 A72805722		0.54	31.0	NT	NT	inactive	2.8	H:91.3 M:84.6	H:99.8 M:89.8
4	5771498 134959047 A84174319		2.96	77.0	NT	NT	inactive	3.2	H:91.9 M:88.2	H:96.1 M:89.3

No.	CID SID Broad ID	Structure	GSK3b ADPGlo IC$_{50}$ (µM)	CDK5 ADPGlo IC$_{50}$ (µM)	p-Tau Inhibition ELISA IC$_{50}$ (µM)	beta-Catenin translocation EC$_{50}$ (µM)	TCF/LEF EC$_{50}$ (µM)	Solubility (µM)	Protein Binding % bound	Plasma Stability % remaining
5	56589396 134216542 A69205554		0.30	5.10	4.49	41.1	24.0	44.9	H:94.9 M:94.4	H:83.5 M:84.2
6	5841835 135378254 A87060530		0.92	21.3	NT	NT	31.3	5.9	H:96.2 M:95.0	H:108.5 M:87.3
7	6030657 135378291 A55919723		4.44	Inactive	NT	NT	inactive	8.6	H:92.1 M:96.6	H:83.2 M:96.2
8	56589435 134216517 A06244137		0.04	0.84	4.24	12.0	9.59	63.9	H:90.3 M:94.7	H:89.3 M:96.9
9	56589400 134216536 A65149943		0.20	10.9	4.68	11.2	7.67	10.4	H:96.4 M:97.1	H:81.6 M:97.1
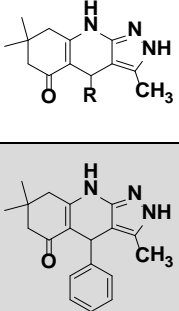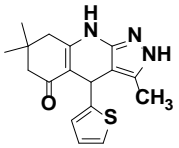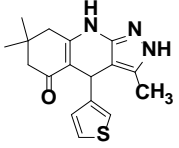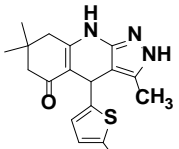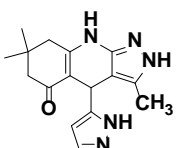
No.	CID SID Broad ID	Structure	GSK3b ADPGlo IC$_{50}$ (µM)	CDK5 ADPGlo IC$_{50}$ (µM)	p-Tau Inhibition ELISA IC$_{50}$ (µM)	beta-Catenin translocation EC$_{50}$ (µM)	TCF/LEF EC$_{50}$ (µM)	Solubility (µM)	Protein Binding % bound	Plasma Stability % remaining
10	56589424 134216539 A72352862		9.29	Inactive	NT	inactive	inactive	0.1	H:97.1 M:93.0	H:91.2 M:73.0
11	56589427 134216540 A77897948		0.46	16.5	NT	>100	inactive	53.9	H:92.9 M:93.8	H:79.1 M:66.6
12	56589421 134216527 A82372682		0.61	39.7	NT	77.6	inactive	5.7	H:91 M:90.6	H:93.4 M:103
13	5742470 135378257 A22268946		2.16	Inactive	NT	NT	inactive	12.3	H:90.4 M:83.9	H:95.1 M:96.5
14	5928898 135378292 A93281121		0.12	6.00	9.15	NT	17.85	>100	H:78.4 M:77.1	H:95.9 M:87.2
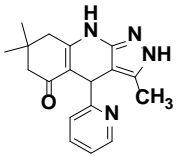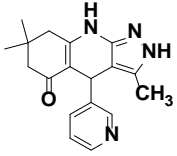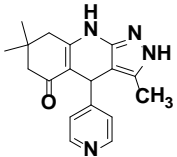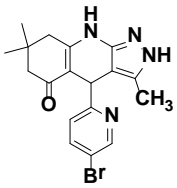
No.	CID SID Broad ID	Structure	GSK3b ADPGlo IC$_{50}$ (µM)	CDK5 ADPGlo IC$_{50}$ (µM)	p-Tau Inhibition ELISA IC$_{50}$ (µM)	beta-Catenin translocation EC$_{50}$ (µM)	TCF/LEF EC$_{50}$ (µM)	Solubility (µM)	Protein Binding % bound	Plasma Stability % remaining
15	6260725 134959046 A51039558		1.17	45.7	NT	NT	inactive	>100	H:81.0 M:81.2	H:99.2 M:95.1
16	5742535 134959045 A12008354		14.7	Inactive	NT	NT	inactive	18.8	H:84.6 M:79.1	H:95.8 M:92.2
17	56846661 135378253 A46809983		0.13	4.04	NT	NT	23.4	87.0	H:82.9 M:72.5	H:97.8 M:98.6
18	56846667 135378252 A68017047		0.05	6.81	2.50	12.0	5.16	49.3	H:83.9 M:82.6	H:96.4 M:99.9
19	56846675 135378280 A68415921		10.4	Inactive	NT	NT	inactive	41.4	H:79.8 M:86.0	H:98.2 M:98.5

All compounds tested were synthesized; All values are the average of at least three replicates; NT = not tested; ATP concentration = K$_M$[a]
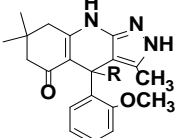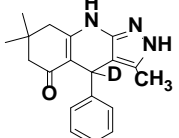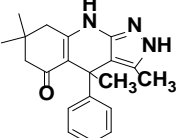
Table 8: SAR of Heteroaromatic Replacements of Phenyl Group
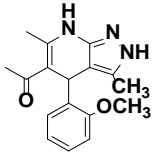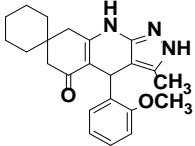
No.	CID SID Broad ID	Structure	GSK3b ADPGlo IC$_{50}$ (µM)	CDK5 ADPGlo IC$_{50}$ (µM)	p-Tau Inhibition ELISA IC$_{50}$ (µM)	beta-Catenin translocation EC$_{50}$ (µM)	TCF/LEF EC$_{50}$ (µM)	Solubility (µM)	Protein Binding % bound	Plasma Stability % remaining
1	5706819 135378298 A81474003 (HTS Hit)		0.31	51.4	NT	inactive	inactive	15.2	H:88.2 M:83.7	H:105.5 M:96.9
2	5908141 24817562 A81368340		0.63	32.3	NT	NT	inactive	6.0	H:79.6 M:78.9	H:99.4 M:95.0
3	6012776 135378295 A94249096		1.37	41.7	NT	NT	inactive	21.6	H:92.1 M:79.5	H:98.9 M:96.2
4	56846658 135378294 A52310989		1.14	73.4	NT	NT	inactive	0.4	H:70.8 M:85.7	H:86.5 M:96.8
5	56846666 135378304 A21447687		1.88	42.4	NT	inactive	inactive	>100	H:62.5 M:49.2	H:96.9 M:96.4

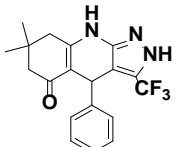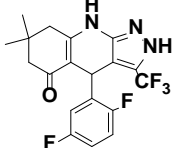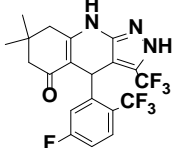| No.	CID SID Broad ID	Structure	GSK3b ADPGlo IC$_{50}$ (µM)	CDK5 ADPGlo IC$_{50}$ (µM)	p-Tau Inhibition ELISA IC$_{50}$ (µM)	beta-Catenin translocation EC$_{50}$ (µM)	TCF/LEF EC$_{50}$ (µM)	Solubility (µM)	Protein Binding % bound	Plasma Stability % remaining
6	5779597 135378260 A34667232		1.02	59.2	NT	NT	inactive	>100	H:74.9 M:43.8	H:97.7 M:99.5
7	5928899 134959044 A13580936		0.41	37.5	NT	NT	inactive	>100	H:59.2 M:52.8	H:97.2 M:97.6
8	5776323 135378265 A27573812		6.92	Inactive	NT	NT	inactive	>100	H:74.6 M:53.8	H:99.7 M:98.2
9	56846664 135378285 A92494754		4.99	Inactive	NT	NT	inactive	16.1	H:81.5 M:87.2	H:97.0 M:96.4

All compounds tested were synthesized; All values are the average of at least three replicates; NT = not tested; ATP concentration = K$_M$[a]
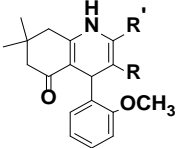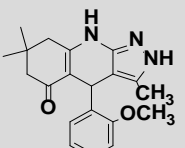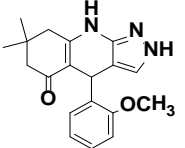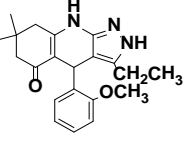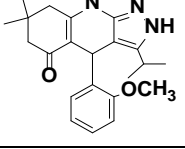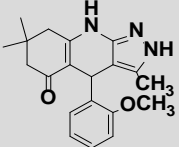
Table 9: SAR of the A ring
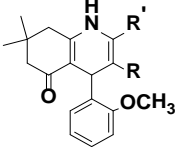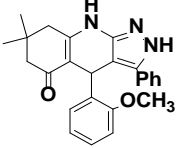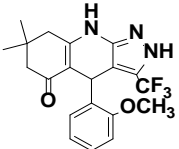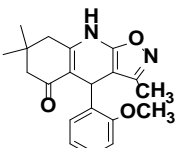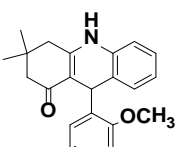
No.	CID SID Broad ID	Structure	GSK3b ADPGlo IC$_{50}$ (µM)	CDK5 ADPGlo IC$_{50}$ (µM)	p-Tau Inhibition ELISA IC$_{50}$ (µM)	beta-Catenin translocation EC$_{50}$ (µM)	TCF/LEF EC$_{50}$ (µM)	Solubility (µM)	Protein Binding % bound	Plasma Stability % remaining
1	5928898 135378292 A93281121		0.12	6.00	9.15	NT	17.85	>100	H:78.4 M:77.1	H:95.9 M:87.2
2	56589417 134216543 A17304198		0.52	10.1	NT	inactive	inactive	18.7	H:76.8 M:87.4	H:67.7 M:72
3	56589434 134216519 A58222361		3.42	15.1	NT	inactive	inactive	>100	H:71.4 M:69.1	H:116 M:99.1
4	56589433 134216541 K14309116		61.8	34.6	NT	inactive	inactive	>100	H:78.7 M:81.6	H:86.7 M:71.8

No.	CID SID Broad ID	Structure	GSK3b ADPGlo IC$_{50}$ (µM)	CDK5 ADPGlo IC$_{50}$ (µM)	p-Tau Inhibition ELISA IC$_{50}$ (µM)	beta-Catenin translocation EC$_{50}$ (µM)	TCF/LEF EC$_{50}$ (µM)	Solubility (µM)	Protein Binding % bound	Plasma Stability % remaining
5	56589422 134216532 A27740005		3.00	9.55	NT	inactive	inactive	82.5	H: 88.5 M: 81.5	H:127 M:125
6	56589428 134216522 A58173130		0.28	5.88	NT	inactive	>100	37.5	H:96.6 M:94.8	H:92.4 M:92.1

All compounds tested were synthesized; All values are the average of at least three replicates; NT = not tested; ATP concentration = K$_M$[a]
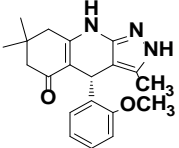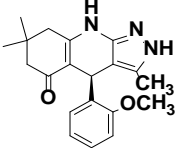
Table 10: SAR of the pyrazole

No.	CID SID Broad ID	Structure	GSK3b ADPGlo IC$_{50}$ (µM)	CDK5 ADPGlo IC$_{50}$ (µM)	p-Tau Inhibition ELISA IC$_{50}$ (µM)	beta-Catenin translocation EC$_{50}$ (µM)	TCF/LEF EC$_{50}$ (µM)	Solubility (µM)	Protein Binding % bound	Plasma Stability % remaining
1	5928898 135378292 A93281121		0.12	6.00	9.15	NT	17.85	>100	H:78.4 M:77.1	H:95.9 M:87.2
2	56589405 134216525 A20140771		0.12	5.82	NT	30.4	11.4	69.0	H:80.5 M:77.3	H:111 M:102
3	56589411 134216523 A83138212		0.08	2.22	NT	24.6	16.2	97.7	H:83.6 M:83.6	H:90.9 M:95.7
4	56589429 134216528 A38867463		0.42	4.84	NT	95.6	inactive	>100	H:90.1 M:91.6	H:96.5 M:95.4

No.	CID SID Broad ID	Structure	GSK3b ADPGlo IC$_{50}$ (µM)	CDK5 ADPGlo IC$_{50}$ (µM)	p-Tau Inhibition ELISA IC$_{50}$ (µM)	beta-Catenin translocation EC$_{50}$ (µM)	TCF/LEF EC$_{50}$ (µM)	Solubility (µM)	Protein Binding % bound	Plasma Stability % remaining
5	56589431 134216520 A50330863		0.83	inactive	NT	82.3	inactive	94.5	H: 93.2 M: 92	H:92.2 M:90.7
6	20911996 134216524 A76161480		1.55	52.6	NT	inactive	inactive	2.1	H:97.6 M:97.8	H:89.4 M:97.7
7	56589437 134959049 A89407846		0.13	21.0	1.76	8.07	5.82	83.0	H:95 M:94.7	H:98.9 M:98.7
8	17601325 134216518 A49475934		148	inactive	NT	inactive	inactive	66.8	H:84.7 M:77.5	H:68.4 M:56.3
9	56589432 134216521 A68123779		inactive	inactive	NT	inactive	inactive	53.4	H:94 M:98.6	H:93.1 M:103
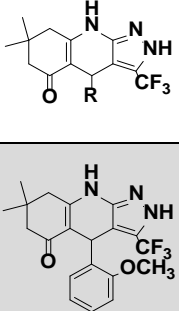
All compounds tested were synthesized; All values are the average of at least three replicates; NT = not tested; ATP concentration = K$_M$[a]

Table 11: SAR of the Benzylic Position

No.	CID SID Broad ID	Structure	GSK3b ADPGlo IC$_{50}$ (µM)	CDK5 ADPGlo IC$_{50}$ (µM)	p-Tau Inhibition ELISA IC$_{50}$ (µM)	beta-Catenin translocation EC$_{50}$ (µM)	TCF/LEF EC$_{50}$ (µM)	Solubility (µM)	Protein Binding % bound	Plasma Stability % remaining
1	5706819 135378298 A81474003 (HTS Hit)		0.31	51.4	NT	NT	inactive	15.2	H:88.2 M:83.7	H:105.5 M:96.9
2	56589399 134216531 A25071499		0.62	56.1	NT	67.3	42.4	0.9	H:85.3 M:83.2	H:96.2 M:98.6
3	56846669 135378259 A18945128		0.31	14.5	NT	inactive	inactive	>100	H:88.9 M:84.8	H:96.8 M:99.7

All compounds tested were synthesized; All values are the average of at least three replicates; NT = not tested; ATP concentration = K$_M$[a]
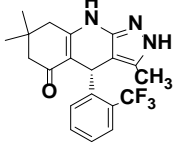
Table 12: SAR with the CF3-pyrazole
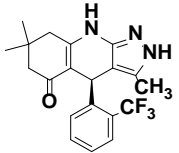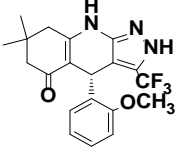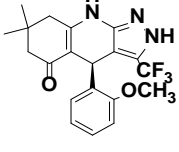
No.	CID SID Broad ID	Structure	GSK3b ADPGlo IC$_{50}$ (µM)	CDK5 ADPGlo IC$_{50}$ (µM)	p-Tau Inhibition ELISA IC$_{50}$ (µM)	beta-Catenin translocation EC$_{50}$ (µM)	TCF/LEF EC$_{50}$ (µM)	Solubility (µM)	Protein Binding % bound	Plasma Stability % remaining
1	56589437 134959049 A89407846		0.13	21.0	1.76	8.07	5.82	83.0	H:95 M:94.7	H:98.9 M:98.7
2	56846668 135378282 A69208616		0.04	22.2	0.51	5.59	8.88	1.2	H:97.1 M:96.6	H:96.4 M:99.9
3	56846660 135378283 A82169570		0.18	47.3	NT	NT	30.6	63.5	H:83.6 M:100	H:99.8 M:97.3
4	56846654 135378251 A64792829		0.45	47.4	NT	NT	inactive	53.9	H:95.8 M:94.4	H:86.5 M:99.3
5	56846680 135378276 A72180724		0.05	8.29	NT	NT	inactive	18.1	H:99.3 M:99.3	H:99.7 M:99.4

All compounds tested were synthesized; All values are the average of at least three replicates; NT = not tested; ATP concentration = $K_M{}^a$

Table 13: Potency of Enantiomers

No.	CID SID Broad ID	Structure	GSK3b ADPGlo IC$_{50}$ (µM)	CDK5 ADPGlo IC$_{50}$ (µM)	p-Tau Inhibition ELISA IC$_{50}$ (µM)	beta-Catenin translocation EC$_{50}$ (µM)	TCF/LEF EC$_{50}$ (µM)	Solubility (µM)	Protein Binding % bound	Plasma Stability % remaining
1	5928898 135378292 A93281121		0.12	6.00	9.15	NT	17.85	>100	H:78.4 M:77.1	H:95.9 M:87.2
2	5524264 135378281 K01093937		0.01	4.18	5.02	NT	inactive	>100	H:86.6 M:82.5	H:99.4 M:95.4
3	5524264 135378270 K31509421		7.37	157	NT	NT	inactive	>100	H:86.6 M:82.5	H:99.4 M:95.4
4	56589435 134216517 A06244137		0.04	0.84	4.24	12.0	9.59	63.9	H:90.3 M:94.7	H:89.3 M:96.9
5	56840724 134970447 K94990229		0.04	0.46	1.80	3.27	4.96	72.6	H:92.2 M:92.2	H:95.4 M:98.6

No.	CID SID Broad ID	Structure	GSK3b ADPGlo IC$_{50}$ (µM)	CDK5 ADPGlo IC$_{50}$ (µM)	p-Tau Inhibition ELISA IC$_{50}$ (µM)	beta-Catenin translocation EC$_{50}$ (µM)	TCF/LEF EC$_{50}$ (µM)	Solubility (µM)	Protein Binding % bound	Plasma Stability % remaining
6	56840711 134970448 K95932625		5.57	83.8	inactive	inactive	inactive	71.6	H:95.6 M:95.0	H:79.5 M:95.3
7	56589437 134959049 A89407846		0.13	21.0	1.76	8.07	5.82	83.0	H:95 M:94.7	H:98.9 M:98.7
8	56840716 134970446 K81491172		0.02	8.94	1.03	5.28	4.8	84.7	H:93.0 M:90.7	H:96.8 M:99.3
9	56840709 134970449 K10018594		1.59	inactive	inactive	>100	inactive	77.3	H:96.9 M:93.9	H:97.1 M:99.5

All compounds tested were synthesized; All values are the average of at least three replicates; NT = not tested; ATP concentration = K$_M$[a]

3.5   Cellular Activity

GSK3b is constitutively active and often serves as a negative regulator of cellular signaling. The inhibition of GSK3b removes this negative regulation resulting in the activation of various cellular pathways. Many proteins, including beta-catenin in the Wnt signaling pathway and Tau protein in the microtubule dynamics, are subject to GSK3b phosphorylation. Specifically, GSK3b directly phosphorylates Tau protein at Ser199 and modulates Tau's self-assembly. Hyperphosphorylation of Tau is implicated in the pathophysiology of Alzheimer's disorder. Beta-catenin is phosphorylated by GSK3b in the *N*-terminal region and this phosphorylation marks the protein for degradation. Accumulation of beta-catenin following GSK3b inhibition translocates to the nucleus and activates TCF/LEF promoter driven genes in the canonical Wnt pathway. We chose Tau and b-catenin as two independent substrates to evaluate GSK3b inhibition in three cellular assays:

1) Assess the amount of Tau-phosphorylation (Ser199) in SH-SY5Y cells upon GSK3b inhibition (AID 624057);

2) Evaluate the amount of beta-catenin nuclear accumulation following GSK3b inhibition in OS-O2 cells (AID 624086) and subsequent activation of TCF/LEF by increased nuclear beta-catenin in HEK293 cells (AID 624088).

After it was clear that the phenyl group was important for enzymatic inhibitory effects based on the HTS hit (**Table 5, Entry 1**), mono substitution on the phenyl group was explored, and some of the enzymatically active compounds were further evaluated in cellular assays (**Table 7**). Cloro-, methoxy, and trifluoromethyl substitution at 2-position of the phenyl group (**Table 7, Entry 5, 8, and 14**) generated compounds with < 1 µM IC_{50} in enzymatic assays, and were active in inhibiting Tau-phosphorylation (IC_{50} < 10 µM) by GSK3b. A 3-substitution with a trifluoromethyl group on the phenyl ring was also active phospho-Tau assay (**Table 7, Entry 9**). These compounds were similarly active in the beta-catenin nuclear translocation assay and TCF/LEF reporter assay with EC_{50} between 5 and 25 µM.

Interestingly, compounds replacing phenyl group with heteroaromatic rings reduced enzymatic potency, and lost cellular activity (**Table 8**). They were inactive in the TCF/LEF reporter assay, indicating the importance of the phenyl group in cell based assays. Similarly, changes on the A ring reduced enzymatic potency, and rendered the compounds inactive in cellular assays (**Table 9**), suggesting that cellular SAR at these two positions were sensitive to changes.

Based on the 2-methoxy on the phenyl ring (**Table 7, Entry 14**), substitutions on the pyrazole were explored (**Table 10**). Trifluoro substitution on the pyrazole (**Table 10, Entry 7**) had the best cellular activity within the series, with a submicromolar (0.48 µM) IC_{50} in p-Tau ELISA, and an EC_{50} in the TCF/LEF reporter assay of <10 µM. Benzylic position changes, however, made the compounds largely inactive in cellular assays (**Table 11**).

Based on the results of **Table 10**, the trifluoro substitution on the pyrazole was fixed and substitution on the phenyl ring was further evaluated in enzymatic and cellular assays (**Table**

12), and 2-methoxy on the phenyl ring is found to have the superior cellular activity profile (**Table 12**).

As expected, enzymatically active enantiomers were also found to be active in cells (**Table 10, Entries 2, 5, and 8**). While the Entries 2, 5, 6 (Table 10) have similar enzymatic activities, Entry 5 (Table 10) demonstrated reduced selectivity against CDK5. Finally, Entry 8 trifluoro substitutions on the pyrazol ring displayed superior GSK3b inhibition across three cellular assays. Therefore, I-4-(2-methoxyphenyl)-7,7-dimethyl-3-(trifluoromethyl)-6,7,8,9-tetrahydro-2*H*-pyrazolo[3,4-b]quinolin-5(4*H*)-one (**Table 10, Entry 8**) was chosen as the probe due to its excellent potency and selectivity.

3.6 Profiling Assays

Kinome Wide Selectivity. A key component to generating a useful probe for determining the role of GSK3b in CNS is solidifying selectivity of action. As mentioned in **Section 3.1**, the HTS hit (CID5706819) was very attractive from this line of investigation. Illustrated below in **Figure 5** are graphs that depict the percentage of the kinome that is inhibited by each compound investigated. As can be clearly seen, CHIR99021 is of very low selectivity in comparison to the dihydropyridines identified in this probe report. The HTS hit (CID5706819) shows excellent selectivity against this panel of 311 kinases, inhibiting only 5 kinases as described earlier. Two other compounds examined in this fashion (CID5524264 and ML320) showed similar impressive selectivity marks, inhibiting only 2.3 and 2.6% of the kinome respectively, with markedly improved potencies discussed in the next section.

Figure 5. Percent of Kinome Inhibited by CHIR99021 and Three New Compounds
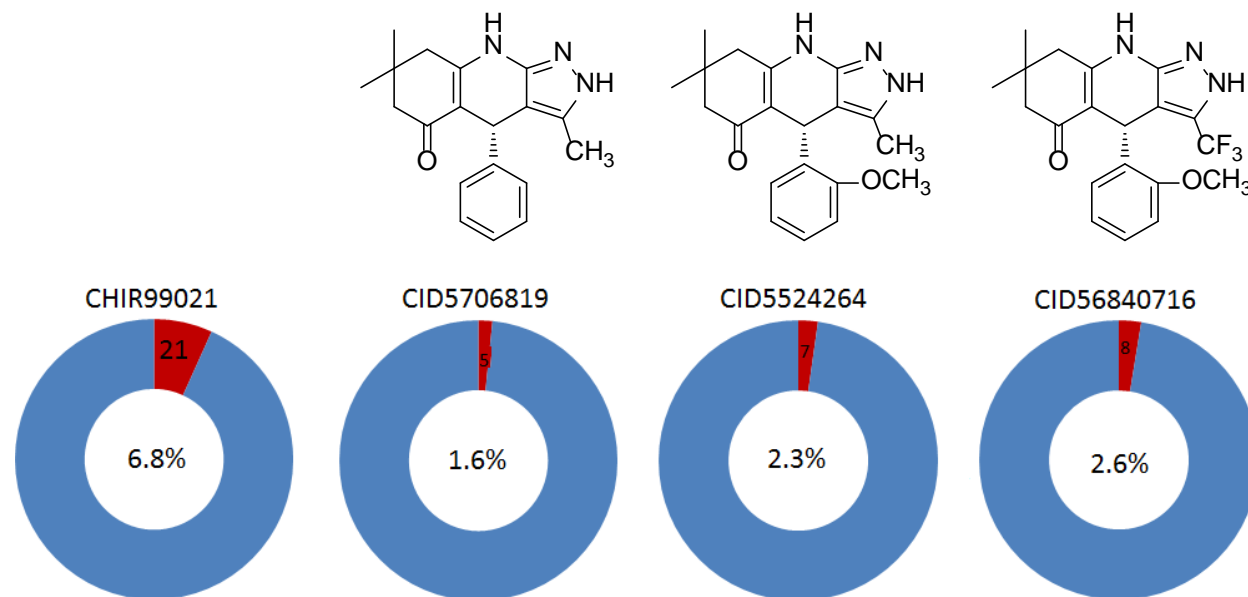
Absolute Selectivity Determination. A second delimiter utilized in arriving at the probe compound was the absolute selectivity in IC_{50} of each compound against the target kinase

(GSK3b) and the next closest anti-target. In the three cases above (CID 5706819, CID 5524564 and ML320) the choice of which compound to pursue became very clear when looking at these values. Illustrated below (**Table 14**) are the IC_{50} determinations for two of these compounds against selected kinases that were inhibited more than 50% at a concentration of 10 μM.

Table 14. Absolute Selectivity of Selected Compounds.

Kinase	CID5524264 IC_{50} μM	Selectivity Factor	Kinase	ML320 IC_{50} μM	Selectivity Factor
GSK3α	0.027	--	GSK3α	0.013	--
GSK3β	0.061	--	GSK3β	0.012	--
CDK2/CycA2	1.5	25	CDK2/CycA2	3.9	325
CDK2/CycE1	2.2	36	CDK2/CycE1	4.4	367
CDK5	1.4	23	CDK5	1.8	150

Utilizing an absolute measurement instead of a general selectivity profile allows for the conclusion that ML320 is much more selective than CID 5524264 (selectivity factor of 150 compared to 23 against CDK5 the kinase inhibited by the highest % at 10 μM). The selectivity factor in this case is determined by comparing the IC_{50} of the compound against GSK3b, to that against the other competing kinases. The matter of selectivity is discussed in more detail in the discussion section.

4   Discussion

Beginning from the hit from HTS (**Table 5, Entry 1**), we investigated the SAR of four regions of the molecule through the synthesis of 55 compounds (**Figure 6**), the benzylic position, the pyrazole moiety, the phenyl ring, and the diketone derived ring on the western portion of the molecule guided by crystal structure analysis (**see Figure 4**). Substitution at the benzylic position with a methyl group was tolerated. Oxidation of the central ring led to a loss in activity. The pyrazole moiety was required for activity, however modifications to the pyrazole were tolerated and substitution with a trifluoromethyl group was found to be optimal. Through SAR of the phenyl ring, it was found that substitution at the 2- or 3-position was optimal for activity. Substitution with heteroaromatics was tolerated, but led to a slight loss in activity. Compounds with substitution at the 4-position were found to display limited activity. Trifluoromethyl or methoxy substitution at the 2- or 3-position was found to be optimal for cell activity. The probe (ML320, **Table 13, Entry 8**) was identified as much more potent than the hit compound, especially in cellular assays in which the hit compound was inactive.

Figure 6.　　SAR Summary
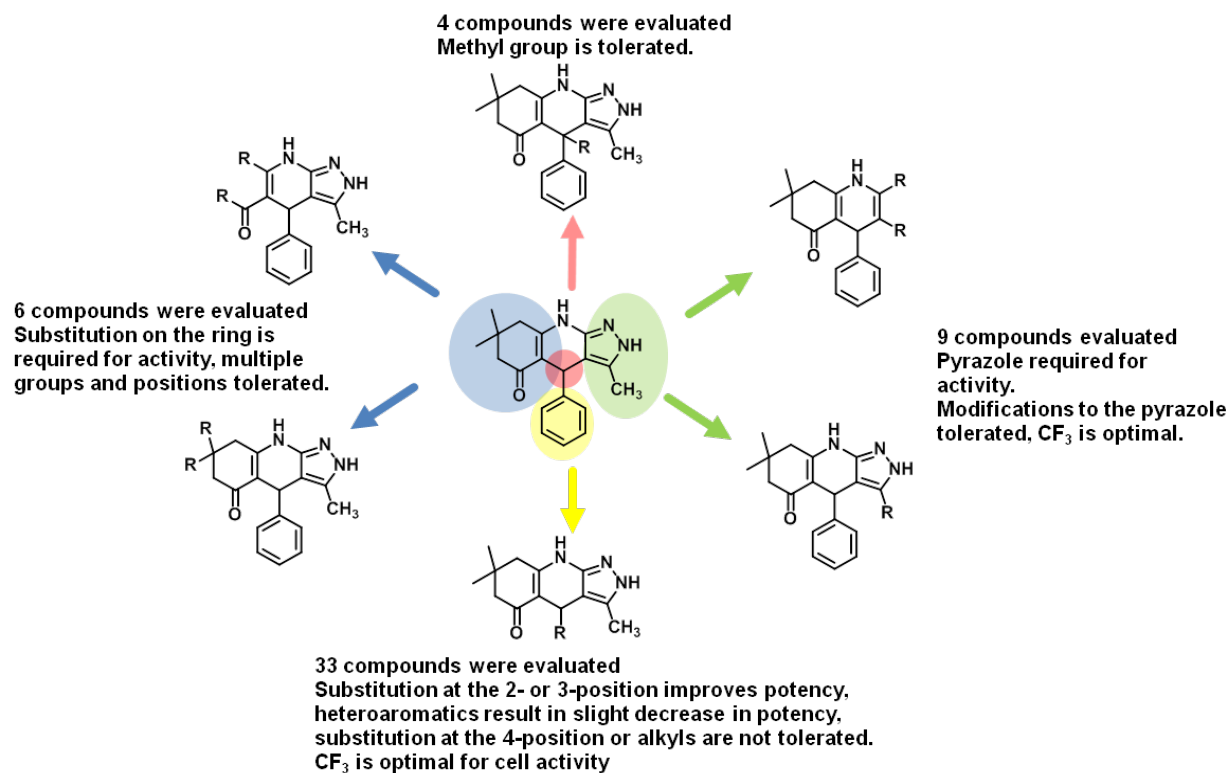
Overall, the data supports the identification of a potent (i.e., IC_{50} = 0.02 µM) probe (ML320) that inhibits GSK3 and is selective against 307 other kinases with greater than 150-fold selectivity (*vida infra*). The probe was found to be active in three different cell assays that display the compound's ability to inhibit GSK3 in different cellular contexts in which GSK3 is implicated.

4.1 Comparison to Existing Art and How the New Probe is an Improvement

After searching the literature, it is clear that there are other inhibitors of GSK3b, however the compounds which have been tested against other kinases have been found lacking in selectivity.(16-20) The kinases that the compounds most often inhibit are the cyclin-dependent kinases (CDKs), to which GSK3 is most closely related. As mentioned previously (Section 1), comparison of known GSK3 inhibitors determined CHIR 99021 (**1, Figure 7**) to be the state or the art. It displayed an IC_{50} of 40 nM against GSK3 and an IC_{50} of 1.4 µM against CDK2 without inhibiting any other kinases at 1 µM. AR A014418 (**2**) inhibited GSK3 with an IC_{50} of 140 nM, CDK2 with an IC_{50} of 6.9 µM and showed little effect on the other kinases at 10 µM. SB 216763 (**3**) and SB 415286 (**4**) were potent, but less selective with IC_{50} values of 100 and 200 nM respectively against GSK3, 0.6 and 0.8 µM against CDK2, and 0.8 and 0.9 µM against DRYK1a. Based on this information, the assay providers have run a screen of CHIR 99021 against >300 kinases confirming that the compound inhibits CDK2 along with many other kinases including CDK5, CDK9, LIMK1, CLK1, PLK1, ERK5 at greater than 50% at 10 µM. A

comparison of the activity and physical properties of ML320 and CHIR 990211 is shown in **Table 15** and a comparison of ML320 activity to the kinase profile of CHIR 990211 is shown in **Table 16**. As can been seen in the tables below, ML320 displays comparable potency to CHIR 99021 in all assays while displaying significantly greater selectivity against the kinome. Furthermore, based on the microsomal data in **Table 2**, there is promise for developing a GSK3 inhibitor of this class with microsomal stability and potency, allowing for *in vivo* studies that are not possible with CHIR 99021 due to its poor physical properties.

Figure 7. Known Inhibitors Against GSK3

CHIR 99021 1

AR A014418 2

SB216763 3

SB415286 4
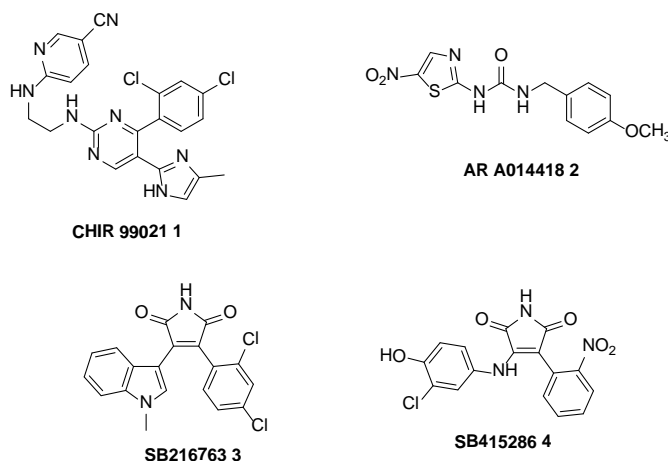
Table 15. Comparison of Activity and Physical Properties of CHIR99021 and ML320

Description	CHIR 99021	ML320
IC$_{50}$ ADP Glo GSK3b (µM)	0.008	0.02
TCF/LEF (µM)	6.0	4.8
beta-Catenin Translocation (µM)	10.0	5.28
p-Tau (µM)	0.44	1.03
cLogP	3.57	4.34
tPSA	115	67
Log BBB (calculated)	-0.38	0.33
Microsomal Stability	M: 4%	M: 0%

Table 16. Comparison of CHIR 99021 Kinase profile and ML320 (% Inhibition at 10 μM)

Kinase	CHIR 99021	ML320
GSK3a	99.9	99.9
GSK3b	99.9	99.9
BRAF	53.8	10.8
CDK2/CycA2	79.3	78.7
CDK2/CycE1	67.2	73.5
CDK4	65.3	19
CDK5	51.2	86.7
CDK9	88.1	20.5
CK1g1	85.8	0.5
CK1g3	70.5	3.2

Kinase	CHIR 99021	ML320
DYKR1B	70.5	52.5
Erk5	61.3	0.6
HIPK4	55.5	3.2
LIMK1	78.9	6.7
MAP2K6	65.3	0.1
MELK	53.5	4.5
MLK3	52.7	18.8
PKR	57.1	0.1
PLK1	59.2	21.3
RSK3	53.6	0.1

4.2   Mechanism of Action Studies

ML320 demonstrates inhibitory characteristics consistent with it being an ATP-competitive inhibitor. We measured its IC_{50}s against GSK3b at two different ATP concentrations. Compared with an IC_{50} of 24 nM at 7 μM ATP (AID 623998), the IC50 of ML320 at 100 μM of ATP increased to 143 nM (AID 624027), suggesting ATP-competitive inhibition.

Cellularly, inhibition of GSK3b by ML320 removes negative regulation of two important signaling pathways in microtubule dynamics and Wnt signaling. Beta-catenin in the Wnt pathway and Tau protein in the microtubule dynamics, are subject to GSK3b phosphorylation. GSK3b is constitutively active and often serves as a negative regulator of cellular signaling. Specifically, inhibition of GSK3b inhibits the phosphorylation of Tau protein, and the inhibition of beta-catenin phosphorylation prevents the b-catenin degradation, promotes its nuclear translocation and subsequently activates TCF/LEF reporter (AID 624057, AID 624086, AID 624088). As such, this probe would be an excellent tool to investigate Wnt pathway as well as probe for microtubule dynamics in cells and potentially in animals.

4.3 Planned Future Studies

Further medicinal chemistry efforts will be focused on improving the potency of compounds containing substitution at the benzylic position using the knowledge gained from the SAR of other parts of the molecule (**Figure 8**). As substitution with a trifluoromethyl group on the pyrazole (**Table 10, Entry 7**) resulted in a significant increase in potency, specifically in cellular assays, the corresponding compound with a methyl at the benzylic position will be synthesized and tested for activity. Also substitution of the phenyl ring of compounds substituted with a methyl at the benzylic position will be tested as that has been shown to increase potency from the HTS hit (**Table 7**). Lastly, we will further probe the benzylic position to understand the SAR at this position.

Figure 8. Future Medicinal Chemistry Plans
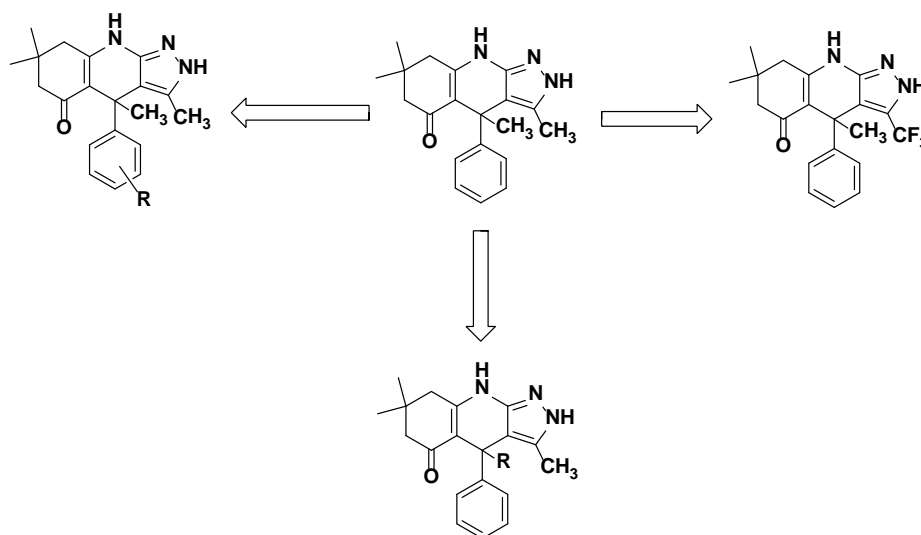
The probe will be used in further cellular assays, including as a tool to probe the GSK/Wnt molecular pathways *in vitro* through the use of human and rodent neural progenitor cells to determine their ability to promote neurogenesis. Through the use of induced pluripotent stem cells-neural progenitor cells (iPSC-NPCs) from patients with neuropsychiatric disorders, such as bipolar disorder and schizophrenia, we plan to determine whether there are differences in response to GSK3 modulators. This would allow us to determine the role of dysregulated GSK3 signaling in the underlying pathologies. With the probe in hand, it will also be possible to determine the effect of selective GSK3 inhibition on cells which have a genetic variation in DISC1 to help understand the role of DISC1/GSK3 signaling in the pathophysiology of neuropsychiatric disorders.

We hope that with further optimization of the probe, we will be able to also test these hypotheses *in vivo*, as well as test the effect of selective GSK3 inhibitors on mouse models for neuropsychiatric disorders, such as the amphetamine induced hyperactivity model (AIH) for mania and the forced swim test and learned helplessness tests for depression.

5   References

1) Mao Y, Ge X, Frank CL, Madison J, Koehler AN, Doud MK, Tassa C, Berry EM, Petryshen TL, Soda T, Biechele T, Moon RT, Haggarty SJ, TsaiLH. DISC1 regulates neural progenitor proliferation via modulation of GSK3β/β-catenin signaling. Cell. 2009 Mar;136(6):1017-1031. PubMed PMID: 19303846; PMCID: PMC2704382

2) Chen G, Rajkowska G, Du F, Seraji-Bozorgzad N, Manji HK. Enhancement of hippocampal neurogenesis by lithium. J Neurochem. 2000 Oct;75(4):1729-34. PubMed PMID: 10987856.

3) Wexler EM, Geschwind DH, Palmer TD. Lithium regulates adult hippocampal progenitor development through canonical Wnt pathway activation. Mol Psychiatry. 2008 Mar;13(3):285-92. PubMed PMID: 17968353.

4) Lee VM, Brunden KR, Hutton M, Trojanowski JQ. Developing therapeutic approaches to tau, selected kinases, and related neuronal protein targets. Cold Spring Harb Perspect Med. 2011 Sep;1(1):a006437. PubMed PMID: 22229117; PMCID: PMC3234455.

5) Hooper C, Killick R, Lovestone S. The GSK3 hypothesis of Alzheimer's disease. J Neurochem. 2008 Mar;104(6):1433-9. PubMed PMID: 18088381; PMCID: PMC3073119.

6) Sheridan SD, Theriault K, Zhao F, Reis S, Madison J, Loring J., Daheron L, Haggarty SJ. Epigenetic characterization of the FMR1 gene and aberrant neurodevelopment in human induced pluripotent stem cell models of Fragile X syndrome.PloS One, 2011;6(10):e26203. PubMed PMID: 22022567; PMCID: PMC3192166.

7) Forde, JE and Dale, TC. Glycogen synthase kinase 3: a key regulator of cellular fate. Cell Mol Life Sci, 2007 Aug;64(15):1930-44. PubMed PMID: 17530463.

8) Phiel CJ, Wilson CA, Lee VM-Y, Klein PS. GSK-3alpha regulates production of Alzheimer's disease amyloid-beta peptides. Nature, 2003 May;423(6938):435-9. PubMed PMID: 12761548.

9) Beaulieu JM, Gainetdinov RR, Caron MG. The Akt-GSK-3 signaling cascade in the actions of dopamine. Trends Pharmacol Sci, 2007 Apr;28(4):166-72. PubMed PMID: 17349698.

10) Gould TD, Picchini AM, Einat H, Husseini K. Targeting glycogen synthase kinase-3 in the CNS: implications for the development of new treatments for mood disorders. Curr Drug Targets, 2006 Nov;7(11):1399-409. PubMed PMID:17100580.

11) Matsuda T, Zhai P, Maejima Y, Hong C, Gao S, Tian B, Goto K, Takaqi H, Tamamori-Adachi M, Kitajima S, Sadoshima J. Distinct roles of GSK-3{alpha} and GSK-3{beta} phosphorylation in the heart under pressure overload. Proc Natl Acad Sci U S A, 2008 Dec;105(52):20900-5. PubMed PMID: 19106302; PMCID: PMC2634936

12) Biechele TL, Moon RT. Assaying beta-catenin/TCF transcription with beta-catenin/TCF transcription-based reporter constructs. Methods Mol Biol, 2008;468:99-110. PubMed PMID: 19099249.

13) Woodgett JR. Physiological roles of glycogen synthase kinase-3: potential as a therapeutic target for diabetes and other disorders. Curr Drug Targets Immune Endocr Metabol Disord, 2003 Dec;3(4):281-90. PubMed PMID: 14683459.

14) Manoukian AS, Woodgett JR. Role of glycogen synthase kinase-3 in cancer: regulation by Wnts and other signaling pathways. Adv Cancer Res, 2002;84:203-29. PubMed PMID: 11883528.

15) Bain J, McLauchlan H, Elliott M, Cohen P. The specificities of protein kinase inhibitors: an update. Biochem J, 2003;371:199-204. PubMed PMID: 12534346.

16) Leclerc S, Garnier M, Hoessel R, Marko D, Bibb JA, Snyder GL, Greengard P, Biernat J, Wu YZ, Mandelkow EM, Eisenbrand G, Meijer L. Indirubins inhibit glycogen synthase kinase-3 beta and CDK5/p25, two protein kinases involved in abnormal tau phosphorylation in Alzheimer's disease. A property common to most cyclin- dependent kinase inhibitors? J Biol Chem, 2001;276: 251-260. PubMed PMID: 11013232.

17) Meijer L, Skaltsounis AL, Magiatis P, Polychronopoulos P, Knockaert M, Leost M, Ryan XP, Vonica CA, Brivanlou A, Dajani R, Crovace C, Tarricone C, Musacchio A, Roe SM, Pearl L, Greengard P. GSK-3-selective inhibitors derived from Tyrian purple indirubins. Chem Biol, 2003;10: 1255-1266. PubMed PMID: 14700633.

18) Polychronopoulos P, Magiatis P, Skaltsounis AL, Myrianthopoulos V, Mikros E, Tarricone A, Musacchio A, Roe SM, Pearl L, Leost M, Greengard P, Meijer L. Structural basis for the synthesis of indirubins as potent and selective inhibitors of glycogen synthase kinase-3 and cyclin-dependent kinases. J Med Chem, 2004;47:935-946. PubMed PMID: 14761195.

19) Leost M, Schultz C, Link A, Wu YZ, Biernat J, Mandelkow EM, Bibb JA, Snyder GL, Greengard P, Zaharevitz DW, Gussio R, Senderowicz AM, Sausville EA, Kunick C, Meijer L. Paullones are potent inhibitors of glycogen synthase kinase-3beta and cyclin-dependent kinase 5/p25. Eur J Biochem, 2000;267:5983-5994. PubMed PMID: 10998059.

20) Chang YT, Gray NS, Rosania GR, Sutherlin DP, Kwon S, Norman TC, Sarohia R, Leost M, Meijer L, Schultz PG. Synthesis and application of functionally diverse 2,6,9-trisubstituted purine libraries as CDK inhibitors. Chem Biol, 1999;7:51-63. PubMed PMID: 10375538.

Appendix A: Assay Summary Table

Table A1. Summary of Completed Assays and AIDs

PubChem AID No.	Type	Target	Concentration Range (µM)	Samples Tested
2119	Summary	NA	NA	NA
2097	Primary	GSK3b	10	320K
434954	Confirmatory	GSK3b	0.013-30	2198
434947	Secondary	ADP-Glo reagents	0.013-30	2198
623998	Secondary	GSK3b	0.0008-50	90
623999	Secondary	CDK5/p25	0.0008-50	90
624027	Secondary	GSK3b	0.0008-50	20
624057	Secondary	GSK3b on Tau phosphorylation	0.005-35	33
624076	Secondary	GSK3b and other kinases	10	1
624091	Secondary	GSK3b and other kinases	0.0003-10	6
624057	Secondary	Toxicity on SH-SY5Y cells	0.005-35	33
624088	Secondary	Wnt signaling pathway	0.005-35	33
624086	Secondary	Wnt signaling pathway	0.005-35	33
SPR	Secondary	GSK3b	0.010-10	75

NA= not applicable

Appendix B: Detailed Assay Protocols

Primary HTS (AID 2097)

1. Dispense 1 µL/well of CABPE, 0.5 µL of ATP, and 1 µL of positive control GW8510 or AB in respective wells according to plate design to 1536-well assay ready plates (Aurora 29847) that contain 2.5 nL/well of 10 mM compound using BioRAPTR (Beckman) to start the reaction. Incubate at room temperature for 60 minutes.
2. Add 2.5 µL /well of ADP-Glo (Promega, V9103) with BioRAPTR, incubate at room temperature for 40 minutes
3. Add 5 µL /well of ADP-Glo (Promega, V9103) with Combi nL (Thermo), incubate at room temperature for 30 minutes
4. Read on ViewLux (PerkinElmer) for luminescence

Solutions:

AB:

25	mM	Tris7.5
10	mM	MgCl2

GW8510 (in AB, Sigma G7791)

50	µM	GW8510

CABPE (in AB):

12.5	mM	DTT (Sigma 43816)
0.25	mg/ml	BSA (Sigma A4503)
0.5	U/ml	Heparin (Baxter NDC 0641-2440-41)
8	µM	Peptide (American Peptide)
22.5	nM	GSK3beta (BPS Biosciences)

Peptide: Tyr-Arg-Arg-Ala-Ala-Val-Pro-Pro-Ser-Pro-Ser-Leu-Ser-Arg-His-Ser-Ser-Pro-His-Gln-Ser(PO3H2)-Glu-Asp-Glu-Glu-Glu

ATP (in AB, Promega V9103 component):

125	µM	ATP

Confirmatory assay (AID 434954)

1. Dispense 1 µL /well of CABPE, 0.5 µL of ATP, and 1 µL of positive control GW8510 or AB in respective wells according to plate design to 1536-well assay ready plates (Aurora 29847) that contain 2.5 nL/well of 10 mM compound using BioRAPTR (Beckman) to start the reaction. Incubate at room temperature for 60 minutes.
2. Add 2.5 µL /well of ADP-Glo (Promega, V9103) with BioRAPTR, incubate at room temperature for 40 minutes
3. Add 5 µL /well of ADP-Glo (Promega, V9103) with Combi nL (Thermo), incubate at room temperature for 30 minutes
4. Read on ViewLux (PerkinElmer) for luminescence

Solutions:

AB:

25	mM	Tris7.5
10	mM	MgCl2

GW8510 (in AB, Sigma G7791)

50	µM	GW8510

CABPE (in AB):

12.5	mM	DTT (Sigma 43816)
0.25	mg/ml	BSA (Sigma A4503)
0.5	U/ml	Heparin (Baxter NDC 0641-2440-41)
8	µM	Peptide (American Peptide)
22.5	nM	GSK3b (BPS Biosciences)

Peptide: Tyr-Arg-Arg-Ala-Ala-Val-Pro-Pro-Ser-Pro-Ser-Leu-Ser-Arg-His-Ser-Ser-Pro-His-Gln-Ser(PO3H2)-Glu-Asp-Glu-Glu-Glu

ATP (in AB, Promega V9103 component):

125	µM	ATP

Counter screen of ADP-Glo reagents (AID 434947)

1. Dispense 2.5 µL of 5 µM ADP or buffer AB into wells on 1536-well assay ready plates according to plate design (Aurora 29847) generated by acoustic transfer using Labcyte Echo that contain 7.5 nL/well of compound in doses.

2. Add 2.5 µL /well of ADP-Glo (Promega, V9103) with Combi nL (Thermo), incubate at room temperature for 40 minutes

3. Add 5 µL /well of ADP-Glo (Promega, V9103) with Combi nL (Thermo), incubate at room temperature for 35 minutes

4. Read on ViewLux (PerkinElmer) for luminescence

Solutions:

AB: 25 mM Tris/HCl pH7.5, 10 mM MgCl2

ADP: 5 µM ADP (in AB, Promega V9103 component)

Human Tau and phospho-Tau (Ser199) Cell-based Immunoassay (ELISA)

Outline:

A standard protocol using an immunoassay kit to quantify total Tau protein and phospho-Tau (Ser199) protein in SH-SY5Y human neuroblastoma cells.

Tissue Culture:

Media: DMEM 4.5g glucose, L-glut, - sodium pyruvate (Cellgro #10-017-CV) / 10% FBS (Invitrogen 10082) / 1% penicillin-streptomycin (Invitrogen 15140)

Plate Type: Costar 96 well black, TC treated culture plates (8795BC), can also use white or clear Eppendorf 96 well PCR plates, colorless (951020401)

Reagents:

1. **Human Tau (Total) ELISA Kit from Invitrogen (#KHB0041)**
   a. Human Tau (Total) Standard
   b. Standard Diluent Buffer
   c. Tau Antibody Coated Wells
   d. Human Tau (Total) Detection Antibody
   e. Anti-Rabbit IgG HRP
   f. Streptavidin-HRP Diluent
   g. Wash Buffer Concentrate
   h. Stabilized Chromogen
   i. Stop Solution
2. **Human pTau (Ser199) ELISA Kit from Invitrogen (#KHB7041)**
   a. Human pTau (Ser199) Standard
   b. Standard Diluent Buffer
   c. Tau Antibody Coated Wells
   d. Human pTau (Ser199) Detection Antibody
   e. Anti-Rabbit IgG HRP
   f. Streptavidin-HRP Diluent
   g. Wash Buffer Concentrate
   h. Stabilized Chromogen
   i. Stop Solution

Protocol:
1. Seed 50,000 cells in 200 μL per well in cell culture media (250,000 cells/ml)
2. Incubate cells overnight @ 37 °C
3. Induce cells with appropriate doses of GSK3 inhibitors
4. Incubate for approximately 24 hrs @ 37 °C
5. Harvest cell lysate:
   a. Wash cells once with cold PBS
   b. Add 100 μL cold lysis buffer and pipette up and down vigorously
   c. Transfer lysate to 96 well PCR plate

d. Centrifuge at 4,000rpm for 20 minutes at 4 degree C
6. Reagent Preparation:
   a. Reconstitute Human Tau (Total) Standard with 1300 µL Standard Diluent Buffer.
      i. Make serial dilutions of the standard according to the following table:

Standard:	Add	Into
2000 pg/ml		
1000 pg/ml	300 µL of 2000 pg/ml standard	300 µL Diluent Buffer
500 pg/ml	300 µL of 1000 pg/ml standard	300 µL Diluent Buffer
250 pg/ml	300 µL of 500 pg/ml standard	300 µL Diluent Buffer
125 pg/ml	300 µL of 250 pg/ml standard	300 µL Diluent Buffer
62.5 pg/ml	300 µL of 125 pg/ml standard	300 µL Diluent Buffer
32.1 pg/ml	300 µL of 62.5 pg/ml standard	300 µL Diluent Buffer
0 pg/ml	300 µL Diluent Buffer	Empty Tube

   b. Reconstitute Human pTau (Ser199) Standard with 1730 µL of Standard Diluent Buffer. Gently mix. Allow to rest for 10 minutes
      i. Make serial dilutions of the standard according to the following table:

Standard:	Add	Into
1000 pg/ml		
500 pg/ml	300 µL of 1000 pg/ml standard	300 µL Diluent Buffer
250 pg/ml	300 µL of 500 pg/ml standard	300 µL Diluent Buffer
125 pg/ml	300 µL of 250 pg/ml standard	300 µL Diluent Buffer
62.5 pg/ml	300 µL of 125 pg/ml standard	300 µL Diluent Buffer
31.2 pg/ml	300 µL of 62.5 pg/ml standard	300 µL Diluent Buffer
15.6 pg/ml	300 µL of 31.2 pg/ml standard	300 µL Diluent Buffer
0 pg/ml	300 µL Diluent Buffer	Empty Tube

   c. Dilute anti-rabbit IgG HRP for both Human Tau (Total) and Human pTau (Ser199) by allowing it to reach room temperature, then use the following table

# of 8 well Strips	Vol of anti-rabbit IgG HRP	Vol of HRP Diluent
2	20 µL	2 ml
4	40 µL	4 ml
6	60 µL	6 ml
8	80 µL	8 ml
10	100 µL	10 ml
12	120 µL	12 ml

    d. Dilute wash buffer from 25X concentrate:
        i. Amount of wash buffer = (x)*(8)*(400)*(4)*(3), where x = number of strips of ELISA plate
        ii. Dilute 24 volumes with deionizer water (ie 5ml concentrate into 120ml water)

7. Warm well strips and determine how many are needed, insert them into the frame
8. Load standards:
    a. Load 100 µL of standard diluent buffer into ZERO wells
    b. Load 100 µL of each standard concentrations (both total Tau and pTau) to wells in DUPLICATE
9. Load samples:
    a. To each well that will be analyzed for total Tau, add 85µl standard diluent buffer + 15 µL cell lysate
    b. To each well that will be analyzed for pTau (Ser199) add 50 µL standard diluent buffer + 50 µL cell lysate
    c. BE SURE TO NOTE WHICH WELLS/PLATES WILL BE ANALYZED for total Tau versus pTau.
    d. Tap gently on side of plate to mix
10. Leave duplicate wells empty for chromogen blank
11. Cover and incubate plate for 2 hours at room temperature
    a. NOTE: Maintain same order of addition for all reagents to ensure equal incubation times for all wells
12. Aspirate wells, do not scratch the inside wall of wells
13. Wash wells 4 times:
    a. Add 400 µL diluted wash buffer, leave for 30 seconds, aspirate all wells
    b. Alternatively, use automated plate washer and program in a 30 second hold between each cycle
14. Add 100 µL of detection antibody solution to each well EXCEPT chromogen blanks
    a. Add anti-total Tau to wells being analyzed for total Tau
    b. Add anti-pTau (Ser199) to wells being analyzed for pTau (Ser199)
    c. Tap gently on side of plate to mix
15. Cover and incubate plate for 1 hour at room temperature

16. Aspirate and wash wells 4 times as before
17. Add 100 µL of anti-rabbit IgG HRP working solution (prepared ahead) to each well EXCEPT chromogen blanks
18. Cover plate and incubate for 30 minutes at room temperature
19. Aspirate and wash wells 4 times as before
20. Add 100 µL of stabilized chromogen to each well, the liquid will turn blue
21. Incubate for 30 minutes at room temperature in the DARK, do not cover plate with foil
22. Add 100 µL of stop solution to each well, tap gently on side of plate to mix
23. Read the absorbance of each well at 450nm (within 2 hours of adding stop solution)

Carna Single Point Inhibition Determination

1. Preparation of test compound solution
   a. The test compound was dissolved in and diluted with dimethylsulfoxide (DMSO) to generate a 100X sample solution. This was then diluted to 4X sample solution in assay buffer to make the final test compound solution. Reference compounds for assay control were prepared similarly.
2. Assay reagents and procedures
   a. IMAP Assay
      i. The 5 µL of 4X compound solution, 5 µL of 4X substrate/ATP/Metal solution, and 10 µL of 2X kinase solution were prepared with assay buffer (20mM HEPES, 0.01% Tween-20, 2mM DTT, pH7.4) and mixed and incubated in a well of polystyrene 384 well black microplate for 1 hour at room temperature.
      ii. 60 µL of IMAP binding reagent (IMAP Screening Express kit; Molecular Devices) was added to the well, and incubated for 30 minutes.
      iii. The kinase reaction was evaluated by fluorescence polarization at 485 nM for excitation and 530nM for emission of the well.
   b. Off-chip Mobility Shift Assay (MSA)
      i. The 5 µL of 4X compound solution, 5 µL of 4X substrate/ATP/Metal solution, and 10 µL of 2X kinase solution were prepared with assay buffer (20 mM HEPES, 0.01% Triton X-100, 2mM DTT, pH 7.5) and mixed and incubated in a well of polypropylene 384 well microplate for 1 or 5 hours at room temperature depending on kinase being examined.
      ii. 60 µL of termination buffer (QuickScout Screening Assist MSA; Carna Biosciences) was added to the well
      iii. The reaction mixture was applied to LabChip3000 system (Caliper Life Science), and the product and substrate peptide peaks were separated and quantitated.
      iv. The kinase reaction was evaluated by the product ratio calculated from peak heights of product (P) and substrate (S) peptides (P/(P+S))

Carna IC50 determination

1. Preparation of test compound solution
   a. The test compounds was dissolved in and diluted with dimethylsulfoxide to a 100X solution. This solution was further diluted to a 4X compound solution plate in assay buffer. Reference compounds for assay control were prepared similarly.
2. Assay regents and procedures
   a. Off-chip mobility shift assay
      i. The 5 µL of 4X compound solution, 5 µL of 4X substrate/ATP/Metal solution, and 10 µL of 2X kinase solution were prepared with assay buffer (20mM HEPES, 0.01% Triton X-100, 2mM DTT, pH7.5) and mixed and incubated in a well of polypropylene 384 well microplate for 1 hour at room temperature.
      ii. 60 µL of termination buffer (QuickScout screening assist MSA; Carna Biosciences) was added to each well.
      iii. The reaction mixture was applied to LabChip3000 system (Caliper Life Sciences), and the product and substrate peptide peaks were separated and quantitated.
      iv. The kinase reaction was evaluated by the product ratio calculated from peak heights of product (P) and substrate(S) peptides (P/(P+S)).

beta-Catenin Nuclear translocation Assay

Outline:

A standard protocol using U2-OS cells stably expressing two complimentary β-Galactosidase fragments: one on beta-catenin and the other constitutively expressed in the cell nucleus. When beta-catenin translocates to the nucleus, the complimentary fragments form a complete beta-Galactosidase that is then quantified by a luminescent-based assay.

Reagents:

3. **PathHunter Detection Kit from PathHunter (93-0001)**
   a. Galacton Star Substrate
   b. Emerald II Solution
   c. PathHunter Cell Assay Buffer
   d. Cell plating reagent CP22

Plate Type:

Corning 384 well white, TC treated culture plates (3707)

Protocol:
24. Seed 10,000 cells in 20 µL cell plating reagent CP22
25. Incubate cells overnight @ 37 °C

26. Induce cells with appropriate doses of GSK3 inhibitors
27. Incubate for 6 hrs @ 37 °C
28. Prepare PathHunter Detection Reagent by combining 1 part Galacton Star Substrate with 5 parts Emerald II Solution and 19 Parts PathHunter Cell Assay Buffer as described in product insert
    a. Calculations are made by diving total volume desired for the assay by 25, then multiplying the resulting number (vol. for 1 part) by the appropriate number of parts
    b. Reagents are stable for 24 hrs at room temperature
    c. PathHunter recommends preparing 30% more reagent to account for loading waste
    d. Example for a single 96-well plate (7.5 ml/25 = 0.3 ml per part):
        i. Cell Assay Buffer- 5.7 ml (19 Parts)
        ii. Emerald II Solution (Substrate Reagent 1)- 1.5 ml (5 Parts)
        iii. Galacton Star Substrate (Reagent 2)- 0.3 ml (1 Part)
    e. Example for a single 384-well plate (6 ml/25 = 0.24 ml per part):
        i. Cell Assay Buffer- 4.56 ml (19 Parts)
        ii. Emerald II Solution (Substrate Reagent 1)- 1.2 ml (5 Parts)
        iii. Galacton Star Substrate (Reagent 2)- 0.24 ml (1 Part)
29. Add 12 µL PathHunter Detection Reagent per well
30. Incubate for 1 hr @ room temperature
31. Read luminescent signal on the Perkin Elmer EnVision:
    a. Distance between plate & detector (mm) = 0.2
    b. Measurement time(s) = 0.1
    c. Glow (CT2) correction factor = 0

TCF/LEF Reporter Gene Assay

Outline:

A standard protocol for analyzing TCF/LEF gene activity in established cell lines stably expressing the TCF/LEF reporter

Reagents:

4. **Dual-Glo Luciferase Assay Reagent from Promega (E2940)**
    a. Luciferase Buffer
    b. Luciferase Substrate
    c. Stop & Glo Luciferase Buffer
    d. Stop & Glo Luciferase Substrate

Plate Type:

Corning 384 well white, TC treated culture plates (3707)

Protocol:
32. Culture cells in 384 well plates to appropriate density.
    a. Total plating volume should be 40 µL.

33. 24 hours after plating, pin cells with 100 nl compounds.
34. 24 hours after incubation with compounds (48 hours after plating), prepare assay reagents by mixing Luciferase Assay solution with Luciferase substrate and Stop & Glo solution to Stop & Glo substrate
    a. Extra reagents can be aliquoted and frozen for future use and are stable for at least one freeze/thaw cycle.
35. Add a volume of luciferase reagent equal to ¼ the volume of media to each well
    a. For example, in a 384-well plate with 40 µL in each well, add 10 µL. This gives a final volume of 50 µL.
36. Spin the plate down and allow 10 minutes for signal stabilization.
37. Read luciferase signal on the Perkin Elmer EnVision
    a. The following read parameters are used:
        i. Distance between plate & detector (mm) = 0.2
        ii. Measurement time(s) = 0.1
        iii. Glow (CT2) correction factor = 0
38. Once the initial data is secure, add a volume of Stop & Glo equal to each well equal to the volume of Luciferase reagent added above
    a. If 10 µL Luciferase Reagent was added, 10 µL Stop & Glo should also be added
39. Spin the plate down and allow 10 minutes for signal stabilization.
40. Read the plate on the EnVision using the same parameters detailed in step four above.
41. Both reagents remain stable for >2 hours. After that, signal may begin to drop off.

Secondary Surface Plasmon Resonance Analysis

Generation of GSK3β Surface on CM5 SensorChip

Materials/Reagents: SensorChip (GE Healthcare Life Sciences, BR-1000-12), Glycine 2.0 buffer (GE Healthcare Life Sciences, BR-1003-55), NaOH 50 (GE Healthcare Life Sciences, BR-1003-58), Phosphate Buffered Saline running/immobilization buffer (PBS, Invitrogen, 70011-044), anti GST-antibody (GE Healthcare Life Sciences, GST Capture Kit, BR100223), Tris Buffered Saline (TBS, 10mM Tris, 150mM NaCl, pH7.35, 2%DMSO), Recombinant GST (GE Healthcare Life Sciences, GST Capture Kit, BR100223), Recombinant GST-GSK3b (BPS BioSciences, 40007).

Protocol:

Buffer generation:

1. PBS
    a. Mix 900mL filtered DI water with 100mL 10X PBS buffer solution (Invitrogen)
2. In house TBS
    a. Add 1.21g Tris and 8.7g NaCl to 950mL filtered DI water
    b. pH using 6M HCl to 7.35
    c. Fill to 1000mL mark
    d. Filter and collect 900mL in one bottle
    e. Filter and collect 100mL in second bottle
    f. Add 450 µL P20 detergent (GE Healthcare Life Sciences) to bottle 1
    g. Add 50 µL P20 detergent to bottle 2

h. Mix thoroughly

i. Transfer 18mL buffer from bottle 1 to bottle 2 to make TBS running buffer

j. Add 18mL DMSO (Aldrich) to bottle 1 to make a 2% DMSO running buffer

GSK3b CM5 Sensor Chip Generation

1. Conditioning New Chip
   a. Load PBS immobilization buffer into buffer shelf and insert buffer line A.
   b. Load unused CM5 sensor chip into instrument per user manual
   c. Prime chip with 6 minutes of buffer injection at 30 µL/min
   d. Initiate manual run and inject over flow cell (FC) 1 and 2 alternating injections of Lysine buffer (GE Healthcare Life Sciences) and Sodium Hydroxide buffer (GE Healthcare Life Sciences) at a flow rate of 30 µL/min for 30 seconds per injection.

2. Immobilization of anti GST antibody
   a. Prime chip again per step 1.c.
   b. Generate anti GST antibody solution by mixing 4.5 µL anti GST antibody (GE Healthcare Life Sciences, GST Capture Kit) with 95.5 µL immobilization buffer (GE Healthcare Life Sciences, GST Capture Kit).
   c. Put solution into 700 µL small vial and cap
   d. Repeat 2.b-2.c.
   e. Place both vials in reagent rack 1 of Biacore T100 instrument and insert into machine per user manual
   f. Initiate immobilization of anti GST antibody by utilizing the immobilization Wizard protocol of Biacore T100 software.
   g. Immobilize approximately 20,000 Response Units (RU) of anti GST antibody on FC1 and FC2

3. Capture Reference and Active Proteins on FC1 and FC2 respectively.
   a. Remove PBS immobilization buffer from buffer rack and replace with TBS 2% DMSO running buffer.
   b. Insert buffer line A
   c. Repeat prime procedure from 1.c.
   d. Generate GST protein solution by mixing 2 µL of recombinant GST (GE Healthcare Life Sciences, GST Capture Kit) with 98 µL TBS 2% DMSO buffer
   e. Generate GST- GSK3b protein solution by mixing 5 µL of recombinant GST-GSK3b with 95 µL TBS 2% DMSO running buffer.
   f. Place GST protein solution in position B1 on reagent rack 1
   g. Place GST- GSK3b protein solution in position C1 on reagent rack 1
   h. Initiate a manual injection run and inject for 30 seconds at 5 µL /min GST protein solution on FC1 to generate reference flow cell
   i. Initiate a manual injection run and inject for 30 seconds at 5 µL /min GST-GSK3b protein solution on FC2 to generate active flow cell
   j. Capture approximately 1000 RU GST protein on FC1
   k. Capture approximately 2500 RU GST- GSK3b protein on FC2

Analysis of Small Molecule GSK3b Inhibitors

1. Generation of analyte plate for assay
   a. Using a standard deep volume 384 well plate, place 100 µL of a 10 µM TBS 2% DMSO solution of the desired analyte in wells A1 and A2.
   b. Place 100 µL of a 5 µM TBS 2% DMSO solution of desired analyte in wells A3 and A4
   c. Place 100 µL of a TBS 2% DMSO solution 2.5um solution of desired analyte in wells A5 and A6
   d. Repeat steps 1.a - - 1.c. with serially diluted analytes to 10nM in wells A21 and A22
   e. Place 100 µL of TBS 2% DMSO running buffer in wells A23 and A24
   f. Repeat steps 1.a. - - 1.e. for subsequent analytes
2. Place analyte plate in Biacore T100 per user manual
3. Generate method that consists of the following
   a. Analyte injection over FC1 and FC2 with reference subtraction
   b. 30 µL /min flow rate of analyte
   c. 60 second contact time of analyte
   d. 60 second wash time of running buffer
   e. DMSO standard curve generation using 1, 1.5, 1.75, 2, 2.5, 2.75 and 3% DMSO in TBS running buffer.
4. Run analysis of compounds
5. Compounds were ranked according to K_D determination utilizing the affinity measurement option in Biacore T100 software.

Appendix C: Experimental Procedures for the Synthesis of the Probe

Chemistry Experimental Methods

General details.   All oxygen and/or moisture-sensitive reactions were carried out under nitrogen (N_2) atmosphere in glassware that had been flame-dried under vacuum (approximately 0.5 mm Hg) and purged with N_2 prior to use. All reagents and solvents were purchased from commercial vendors and used as received, or synthesized according to methods already reported. NMR spectra were recorded on a Bruker 300 (300 MHz ^{1}H, 75 MHz ^{13}C) or Varian UNITY INOVA 500 (500 MHz ^{1}H, 125 MHz ^{13}C) spectrometer. Proton and carbon chemical shifts are reported in ppm (δ) referenced to the NMR solvent. Data are reported as follows: chemical shifts, multiplicity (br = broad, s = singlet, d = doublet, t = triplet, q = quartet, m = multiplet; coupling constant(s) in Hz).

Unless otherwise indicated, NMR data were collected at 25 °C. Flash chromatography was performed using 40-60 μm Silica Gel (60 Å mesh) on a Teledyne Isco Combiflash R$_f$. Tandem Liquid Chromatography/Mass Spectrometry (LC/MS) was performed on a Waters 2795 separations module and 3100 mass detector. Analytical thin layer chromatography (TLC) was performed on EM Reagent 0.25 mm silica gel 60-F plates. Visualization was accomplished with ultraviolet (UV) light and aqueous potassium permanganate ($KMnO_4$) stain followed by heating. High-resolution mass spectra were obtained at the MIT Mass Spectrometry Facility (Bruker Daltonics APEXIV 4.7 Tesla Fourier Transform Ion Cyclotron Resonance Mass Spectrometer).

5,5-dimethylcyclohexane-1,3-dione (824 mg, 5.88 mmol), 2-methoxybenzaldehyde (800 mg, 5.88 mmol) and 3-(trifluoromethyl)-1H-pyrazol-5-amine (1199 mg, 7.93 mmol) were mixed together in a microwave vial and Ethanol (Volume: 14.700 ml, Density: 0.81 g/ml) was added to it. The reaction mixture was heated in microwave for 15 min at 150 °C. The mixture was cooled and the solvent was evaporated. The resultant mixture was then purified by column chromatography over silica gel (hexane/ethyl acetate: 100/0 to 20/80) to provide 4-(2-methoxyphenyl)-7,7-dimethyl-3-(trifluoromethyl)-6,7,8,9-tetrahydro-2H-pyrazolo[3,4-b]quinolin-5(4H)-one (372 mg, 16% yield). The racemic mixture was separated by chiral HPLC to provide (*R*)-4-(2-methoxyphenyl)-7,7-dimethyl-3-(trifluoromethyl)-6,7,8,9-tetrahydro-2H-pyrazolo[3,4-b]quinolin-5(4H)-one (ML320).

^{1}H NMR (300 MHz, MeOD) δ 7.19 (d, *J* = 7.4, 1H), 7.08 (t, *J* = 7.0, 1H), 6.78 (dd, *J* = 7.4, 13.8, 2H), 5.39 (s, 1H), 3.67 (s, 3H), 2.49 (dd, *J* = 16.8, 41.7, 2H), 2.14 (dd, *J* = 16.5, 60.4, 2H), 1.08 (s, 3H), 0.97 (s, 3H); ^{13}C NMR (75 MHz, MeOD) δ 197.40, 158.56, 155.95, 135.10, 131.52, 128.59, 120.87, 112.06, 108.93, 55.72, 51.58, 43.92, 42.51, 33.25, 29.70, 26.82.calculated [M$^+$H] 392.151 experimental [M$^+$H] 392.1591.

Appendix D: Experimental Procedures for Analytical Assays

Solubility. Solubility was determined in phosphate buffered saline (PBS) pH 7.4 with 1% DMSO. Each compound was prepared in duplicate at 100 µM in both 100% DMSO and PBS with 1% DMSO. Compounds were allowed to equilibrate at room temperature with a 250 rpm orbital shake for 24 hours. After equilibration, samples were analyzed by UPLC-MS (Waters, Milford, MA) with compounds detected by SIR detection on a single quadrupole mass spectrometer. The DMSO samples were used to create a two point calibration curve to which the response in PBS was fit.

PBS Stability. Stability was determined in the presence of PBS pH 7.4 with 0.1% DMSO. Each compound was prepared in duplicate on six separate plates and allowed to equilibrate at room temperature with a 250 rpm orbital shake for 48 hours. One plate was removed at each time point (0, 2, 4, 8, 24, and 48 hours). An aliquot was removed from each well and analyzed by UPLC-MS (Waters, Milford, MA) with compounds detected by SIR detection on a single quadrupole mass spectrometer. Additionally, to the remaining material at each time point, acetonitrile was added to force dissolution of compound (to test for recovery of compound). An aliquot of this was also analyzed by UPLC-MS.

GSH Stability. Stability was determined in the presence of PBS pH 7.4 µM and 50 µM glutathione with 0.1% DMSO. Each compound was prepared in duplicate on six separate plates and allowed to equilibrate at room temperature with a 250 rpm orbital shake for 48 hours. One plate was removed at each time point (0, 2, 4, 8, 24, and 48 hours). An aliquot was removed from each well and analyzed by UPLC-MS (Waters, Milford, MA) with compounds detected by SIR detection on a single quadrupole mass spectrometer. Additionally, to the remaining material at each time point, acetonitrile was added to force dissolution of compound (to test for recovery of compound). An aliquot of this was also analyzed by UPLC-MS.

Plasma Protein Binding. Plasma protein binding was determined by equilibrium dialysis using the Rapid Equilibrium Dialysis (RED) device (Pierce Biotechnology, Rockford, IL) for both human and mouse plasma. Each compound was prepared in duplicate at 5 µM in plasma (0.95% acetonitrile, 0.05% DMSO) and added to one side of the membrane (200 µl) with PBS pH 7.4 added to the other side (350 µl). Compounds were incubated at 37º C for 5 hours with a 250 rpm orbital shake. After incubation, samples were analyzed by UPLC-MS (Waters, Milford, MA) with compounds detected by SIR detection on a single quadrupole mass spectrometer.

Plasma Stability. Plasma stability was determined at 37º C at 5 hours in both human and mouse plasma. Each compound was prepared in duplicate at 5 µM in plasma diluted 50/50 (v/v) with PBS pH 7.4 (0.95% acetonitrile, 0.05% DMSO). Compounds were incubated at 37º C for 5 hours with a 250 rpm orbital shake with time points taken at 0 and 5 hours. Samples were analyzed by UPLC-MS (Waters, Milford, MA) with compounds detected by SIR detection on a single quadrupole mass spectrometer.
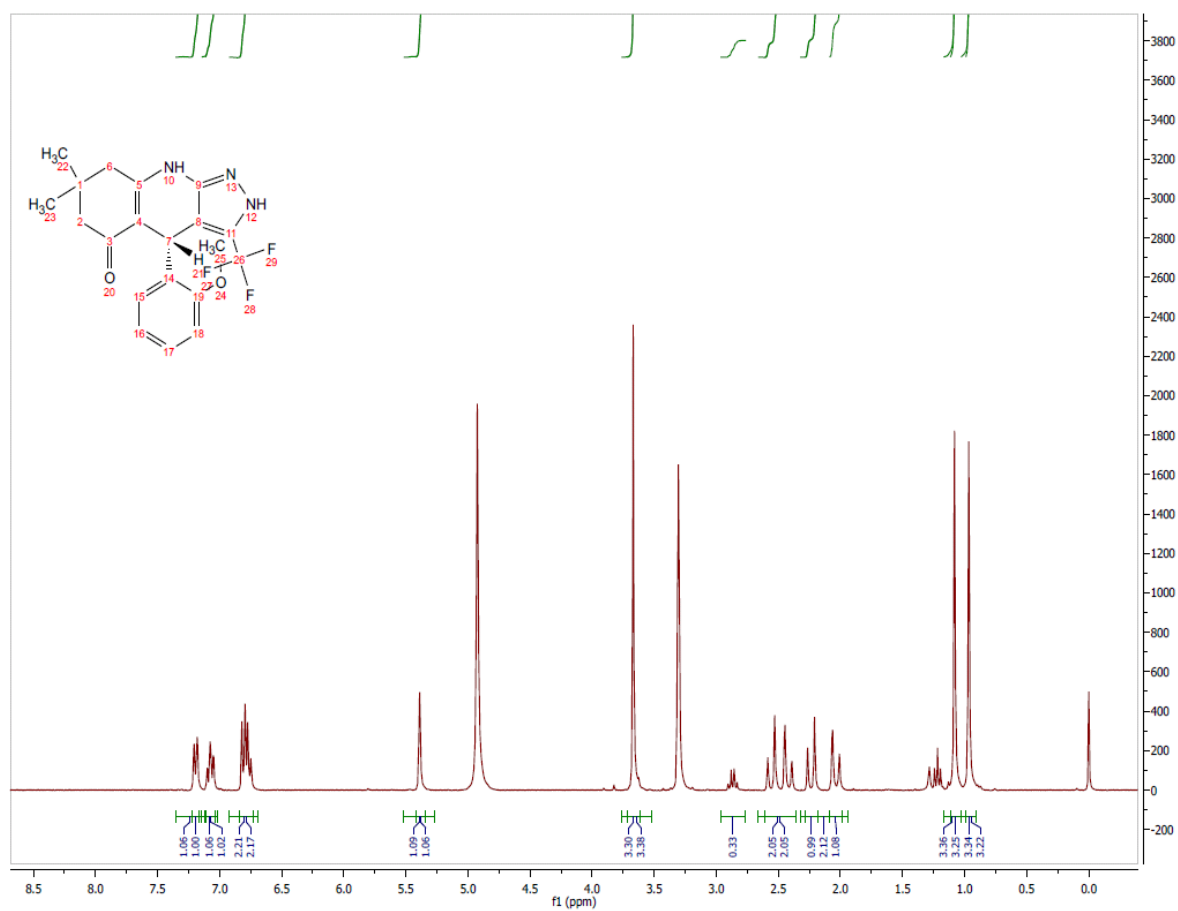
^{1}H NMR Spectrum (300 MHz, CDCl$_3$) of Probe CID 56840716/ML320
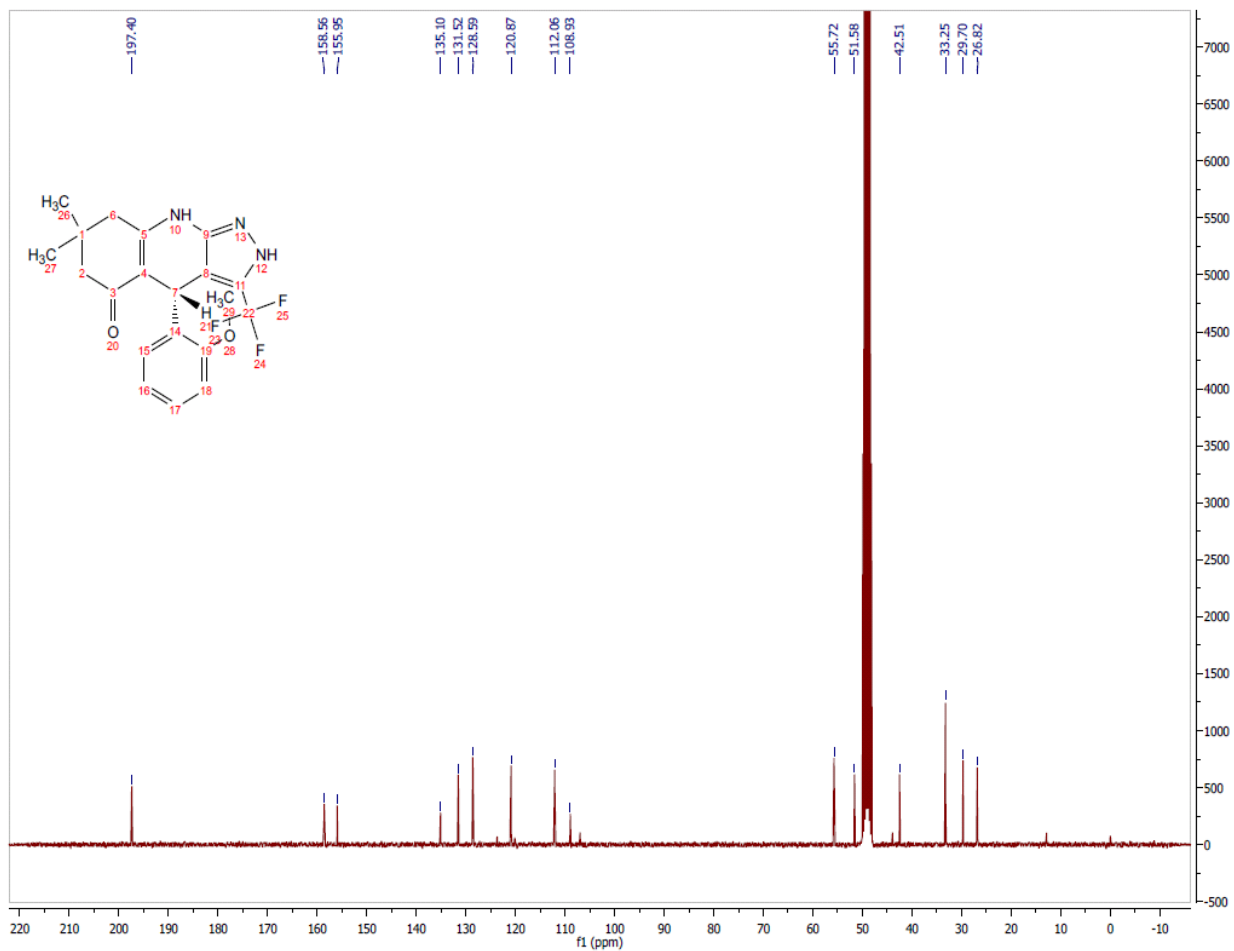
^{19}F NMR Spectrum (300 MHz, CDCl$_3$) of Probe CID 56840716/ML320
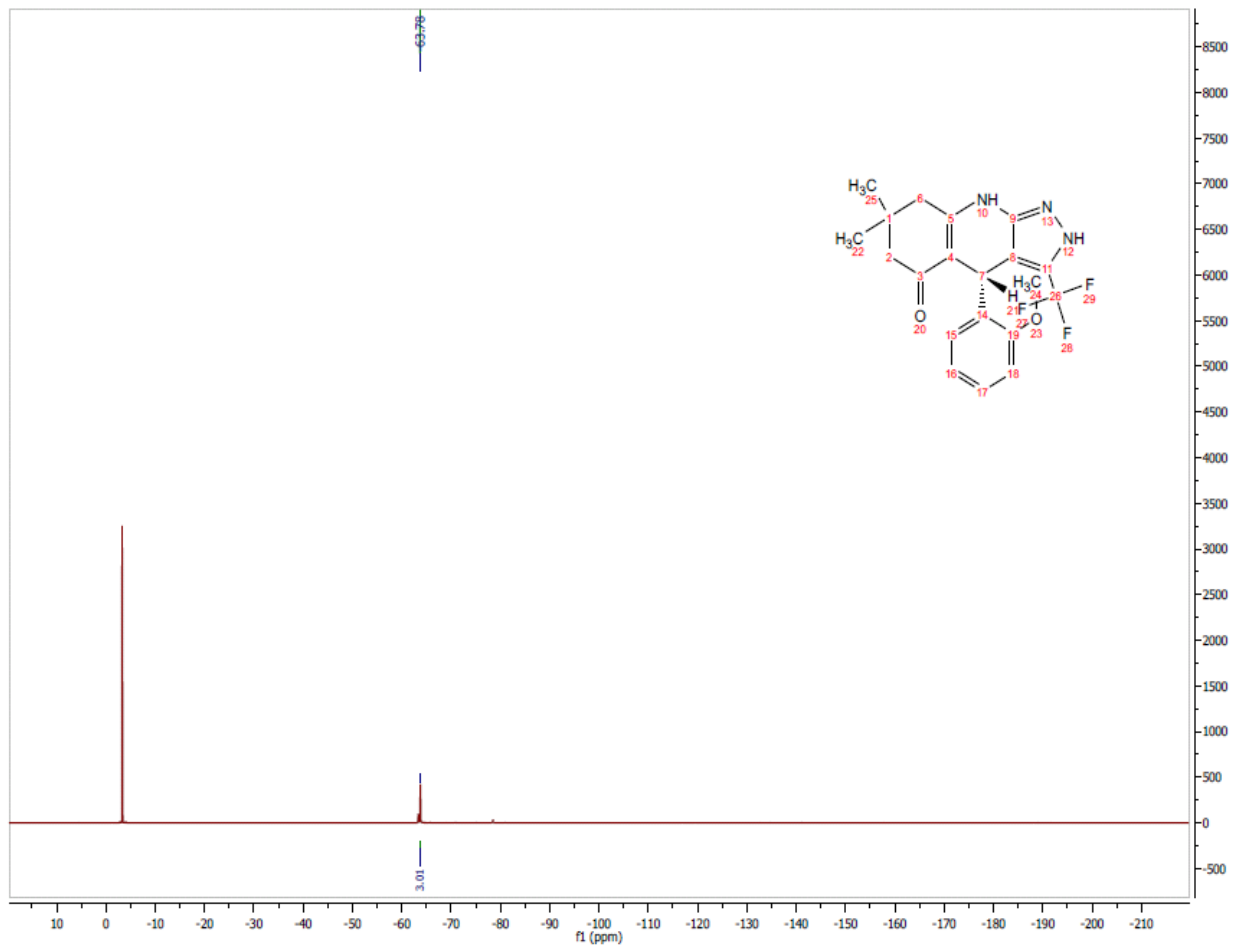
UPLC-MS Chromatogram of Probe CID 56840716/ML320
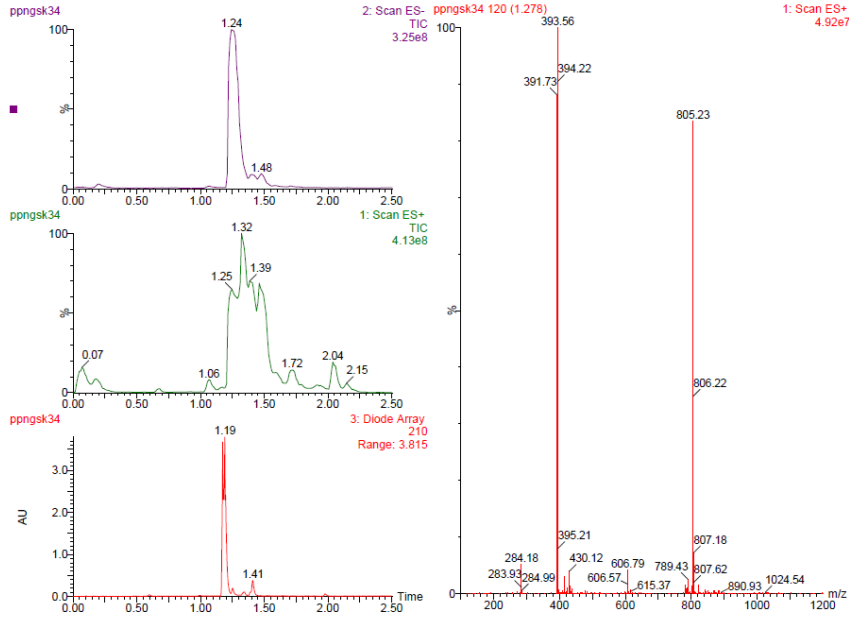
HRMS of Probe CID 56840716/ML320

^{1}H NMR Spectrum (300 MHz, CDCl$_3$) of CID 5706819
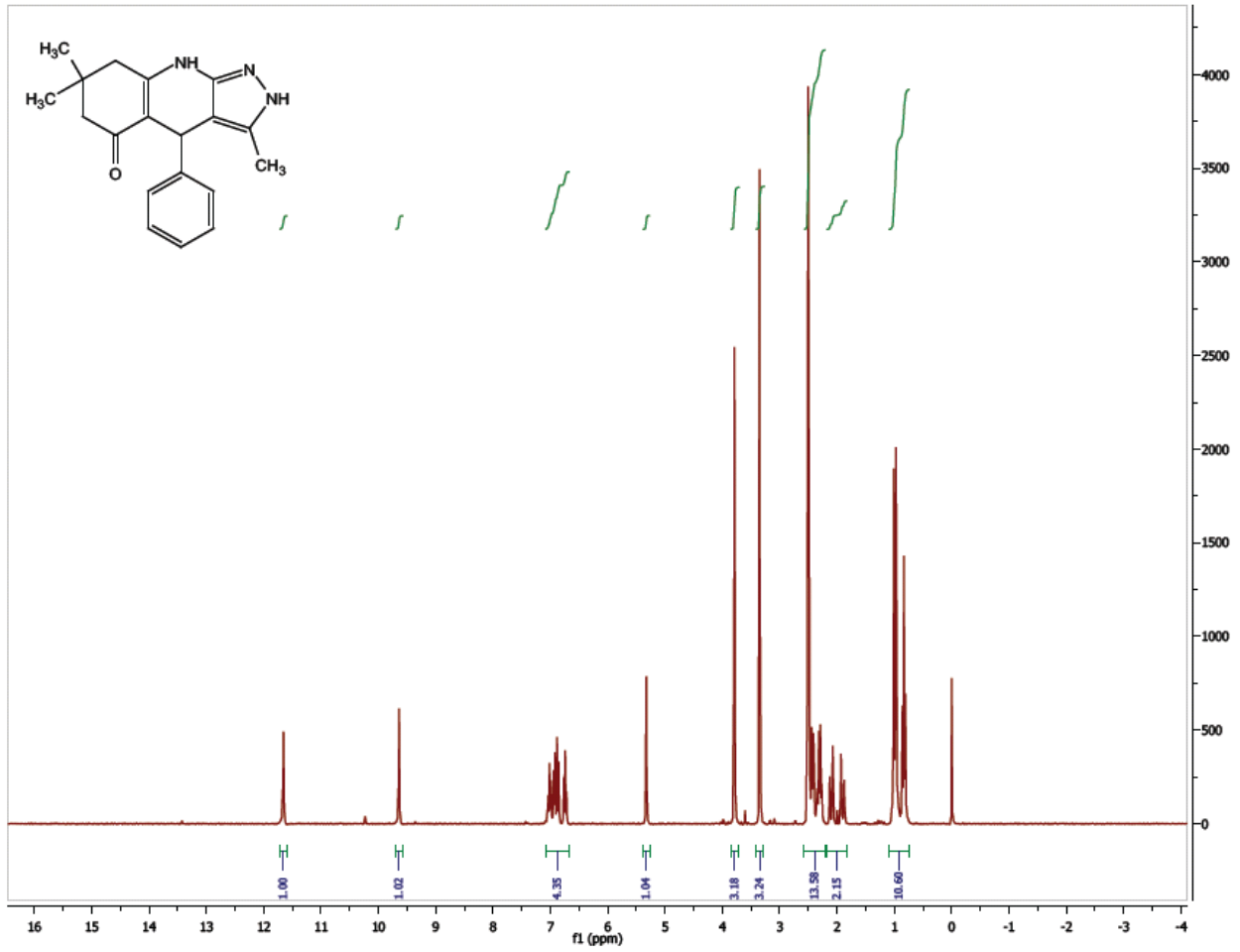
UPLC-MS Chromatogram of CID 5706819
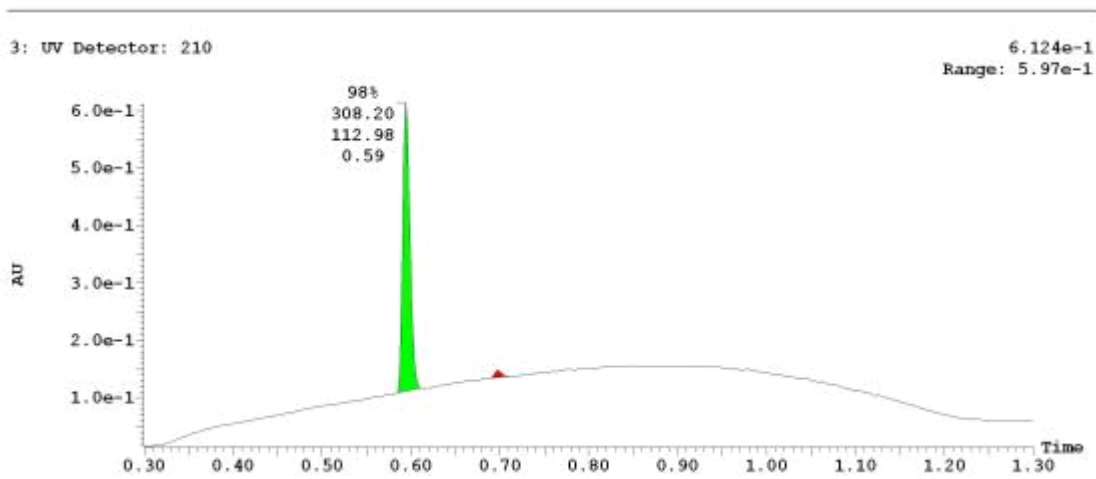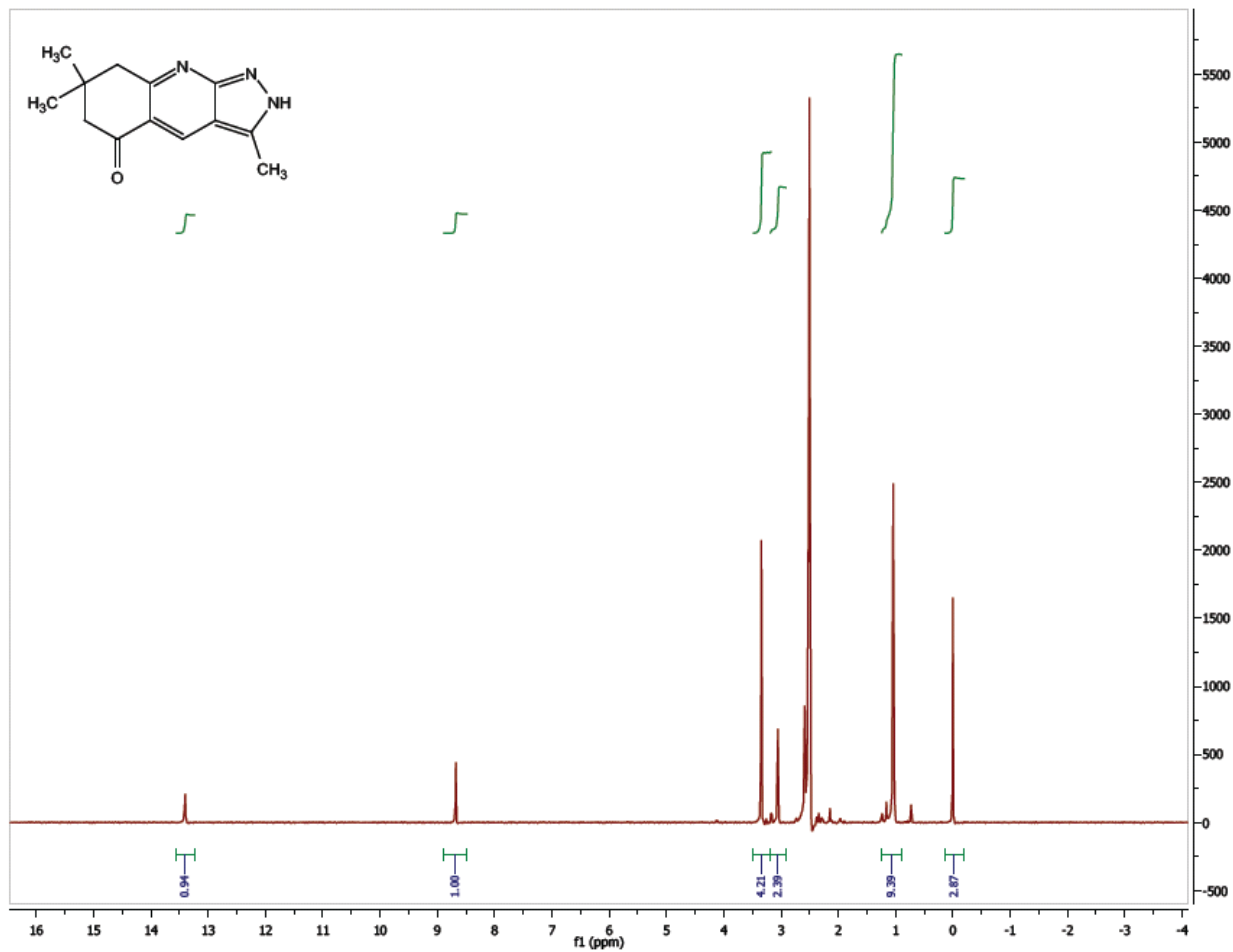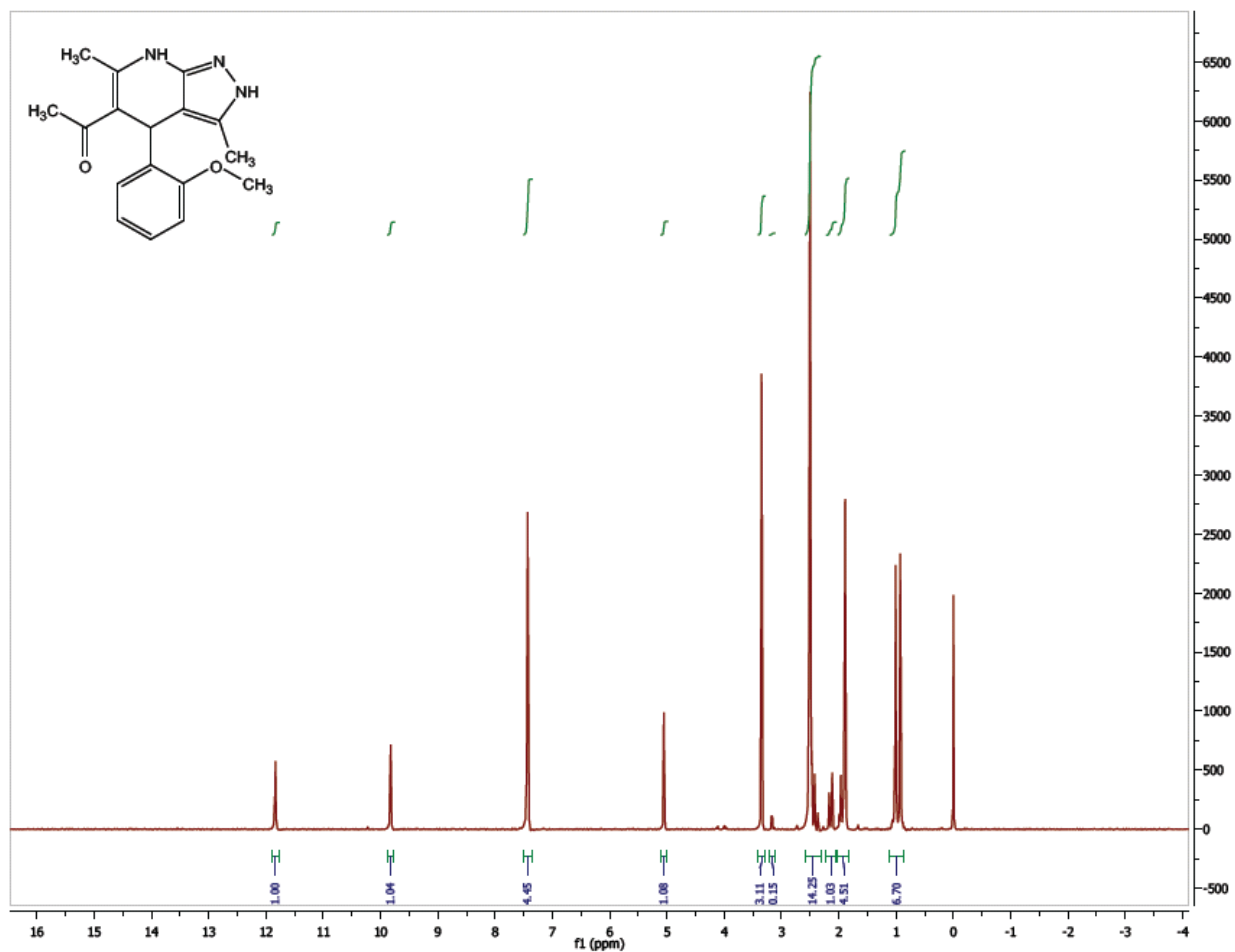
UPLC-MS Chromatogram of CID 21600856
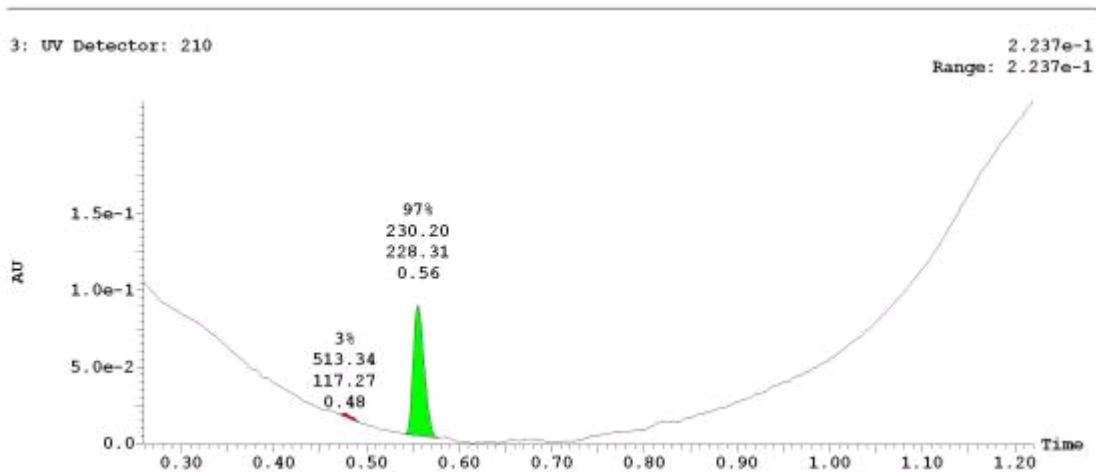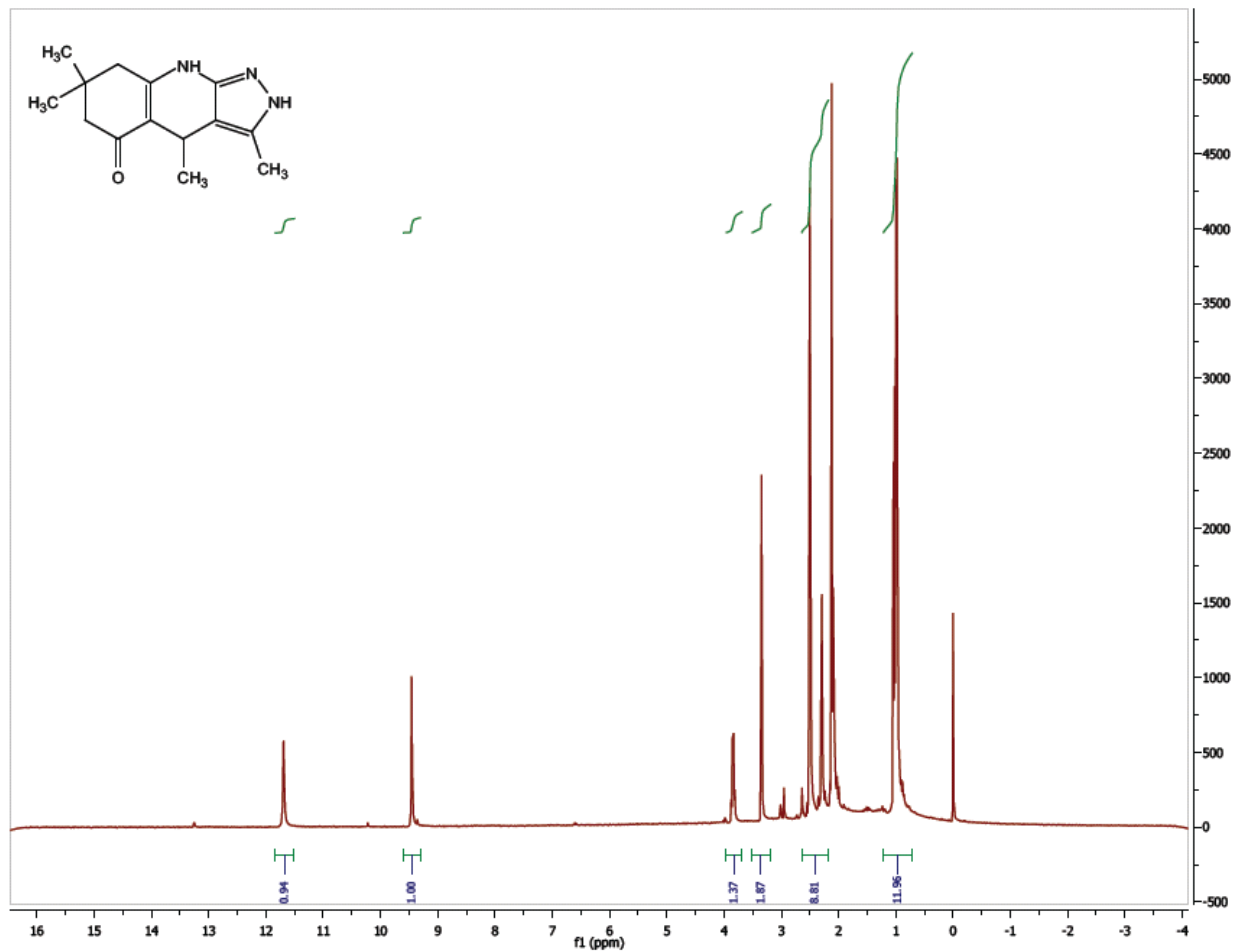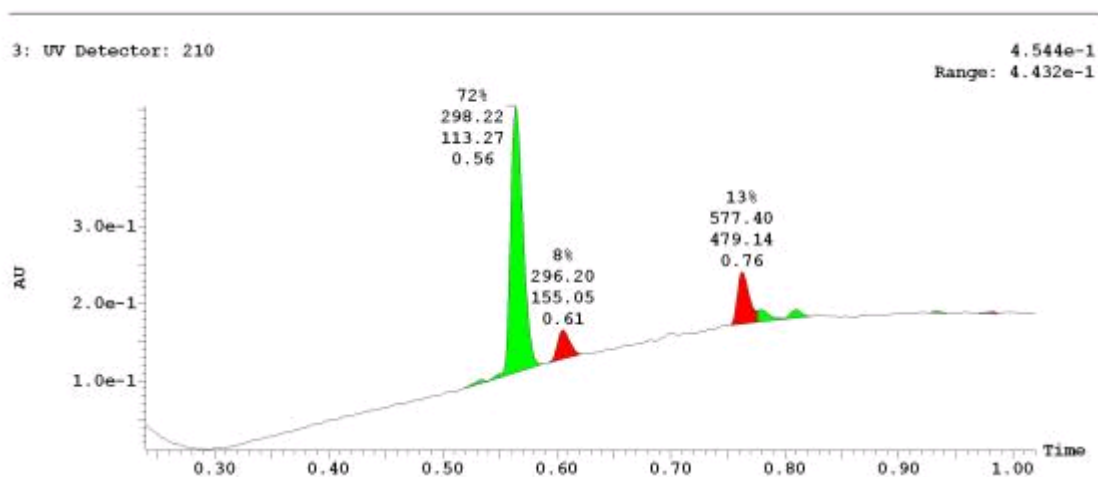
UPLC-MS Chromatogram of CID 56589407
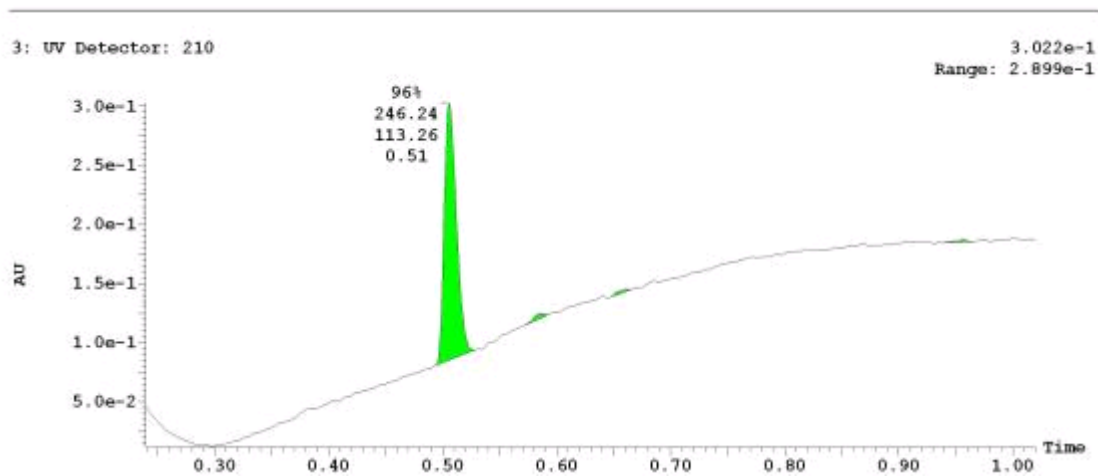
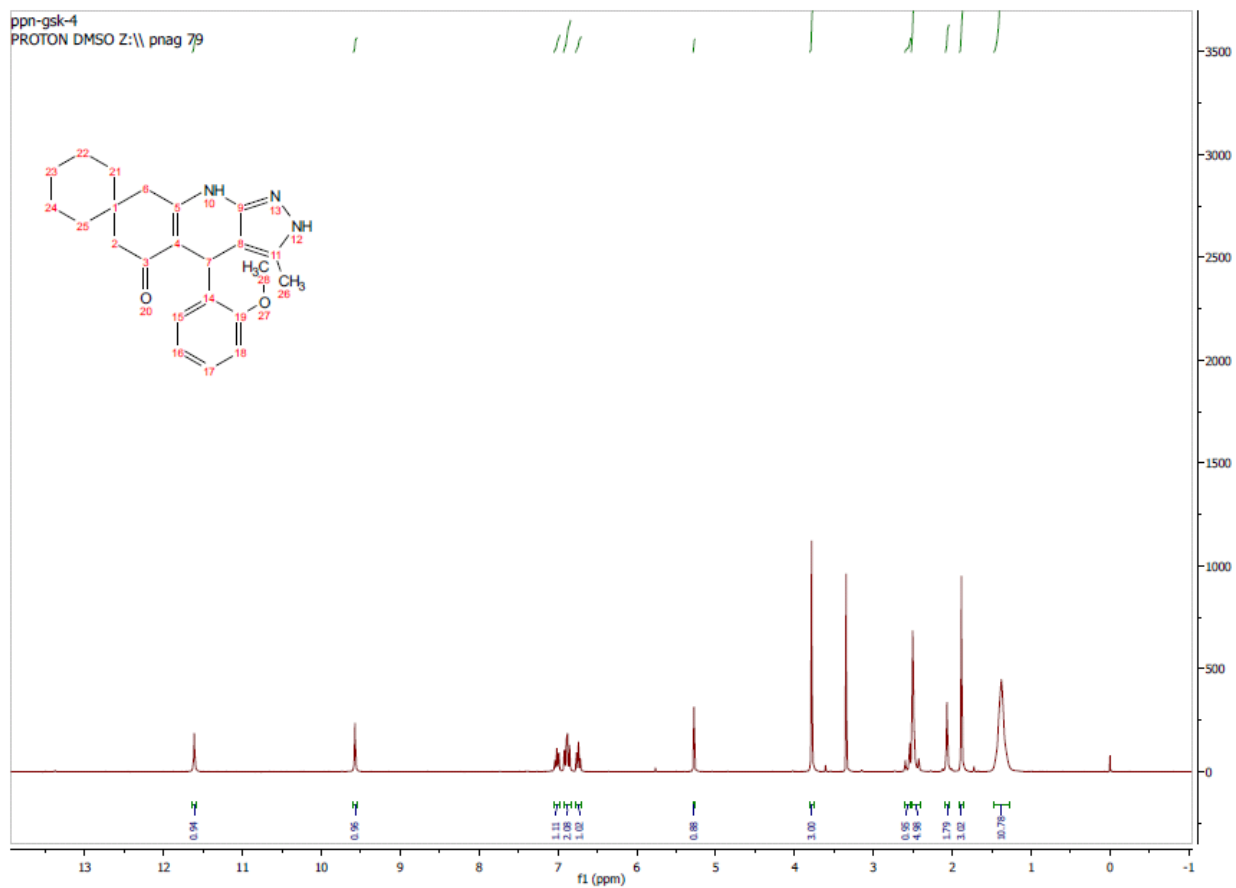## ¹H NMR Spectrum (300 MHz, CDCl₃) of CID 56589416
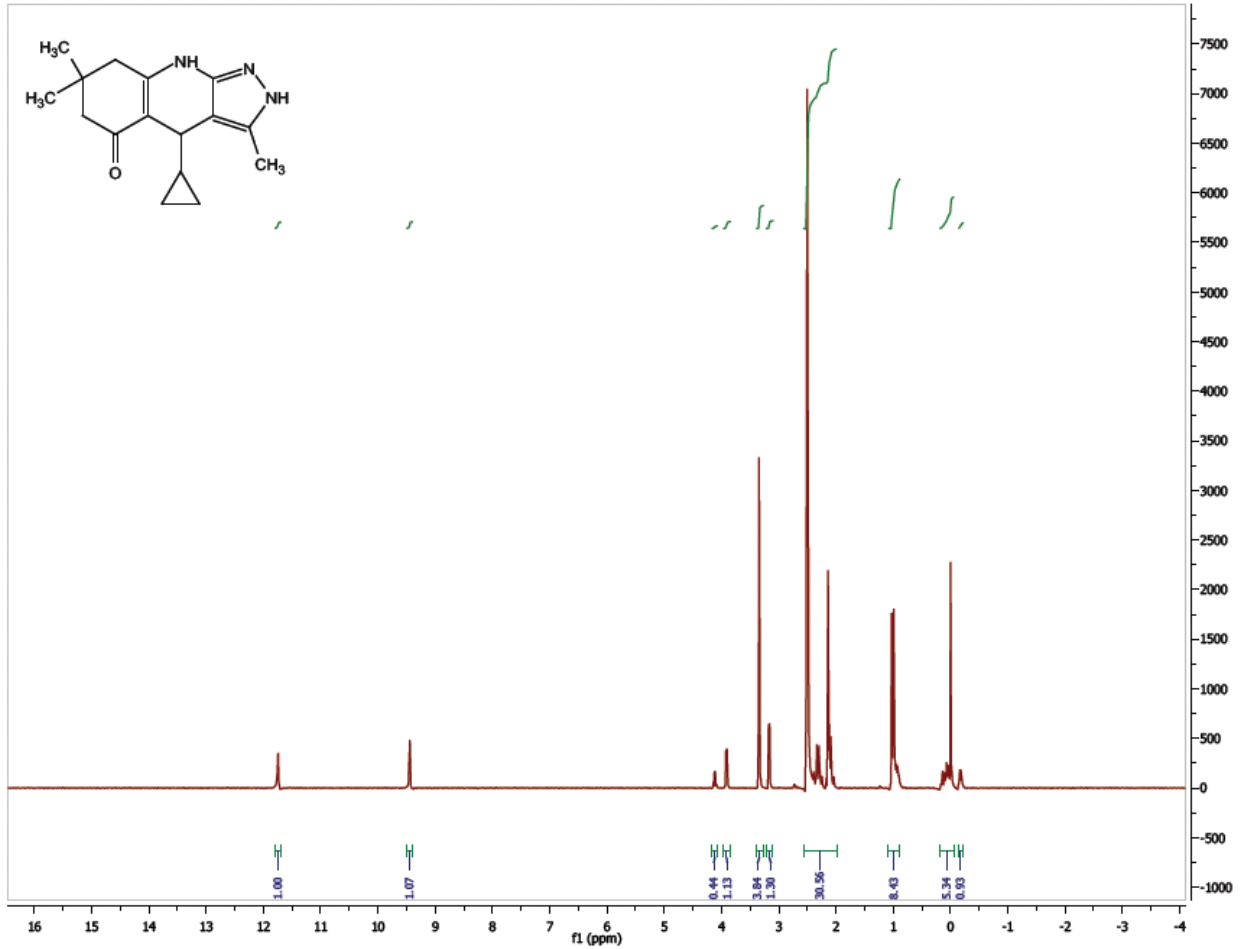
UPLC-MS Chromatogram of CID 56589416

¹H NMR Spectrum (300 MHz, CDCl₃) of CID 56589404
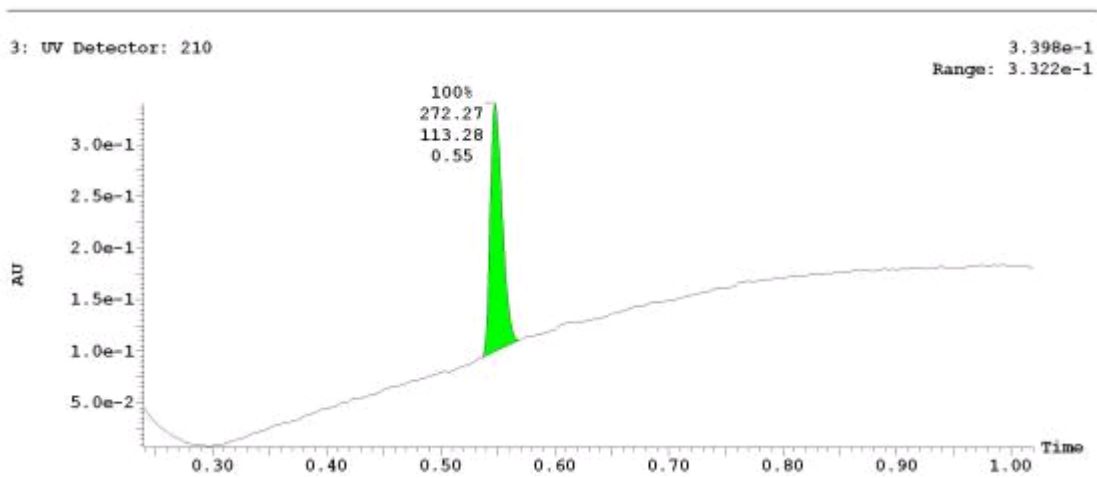
^{1}H NMR Spectrum (300 MHz, CDCl$_3$) of CID 56589404
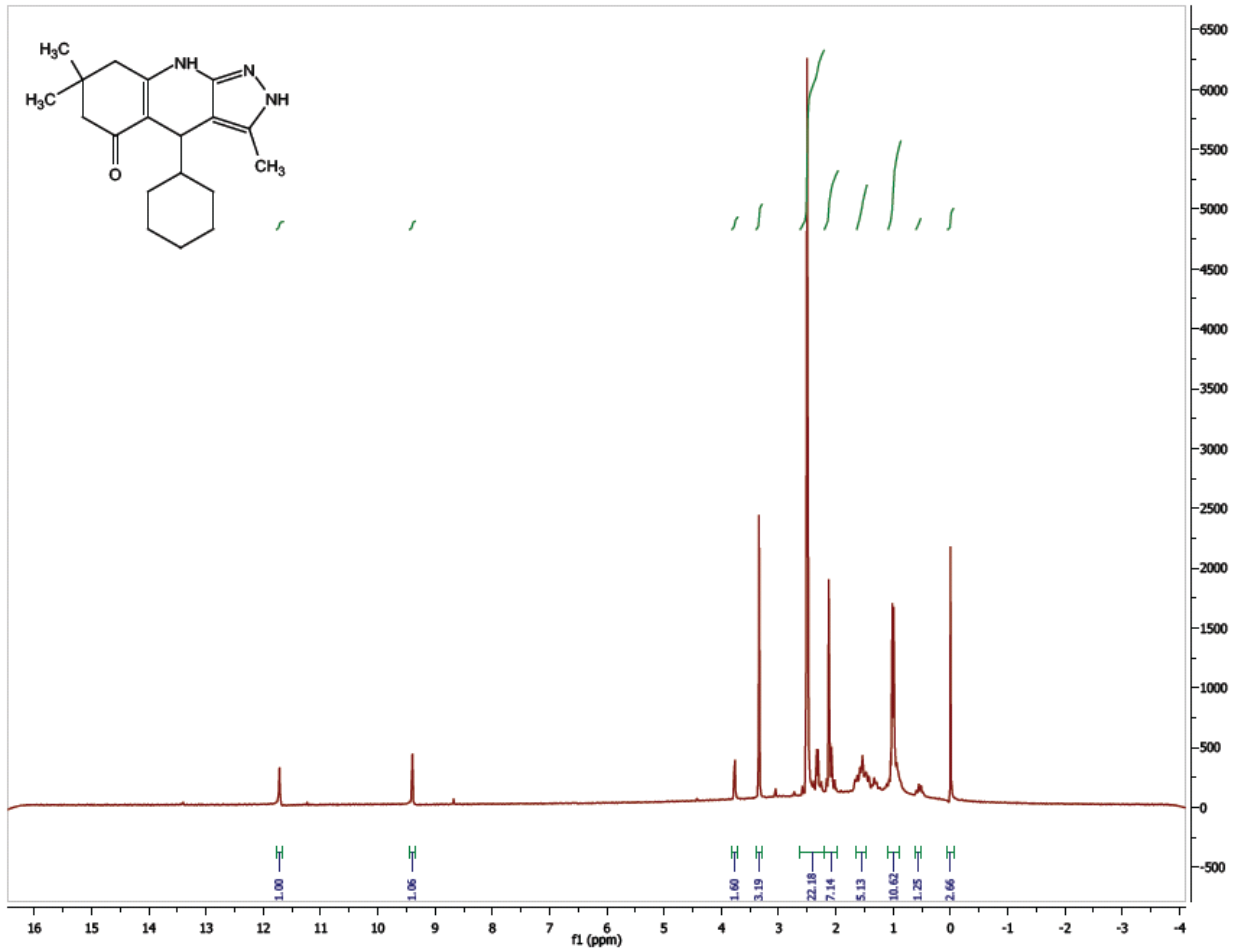
UPLC-MS Chromatogram of CID 56589404

JAB_NB3_0016_pure
PROTON DMSO Z:\\ jbishop 45
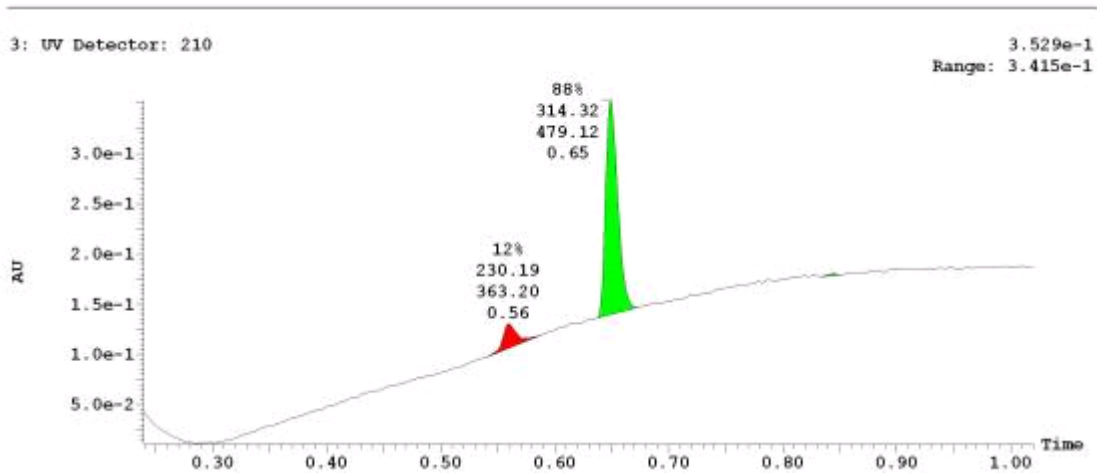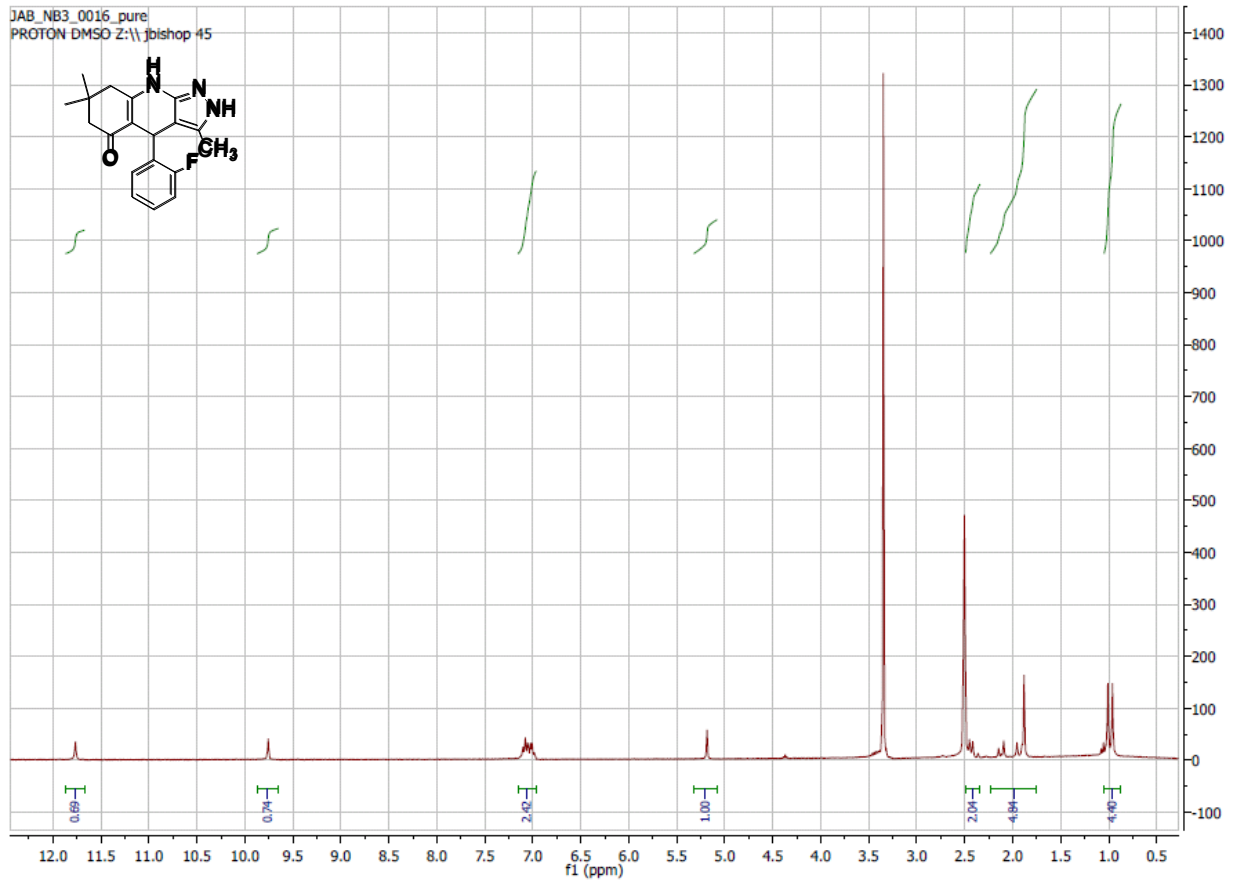
UPLC-MS Chromatogram of CID 5830978

3: UV Detector: 210

4.924e-1
Range: 4.661e-1
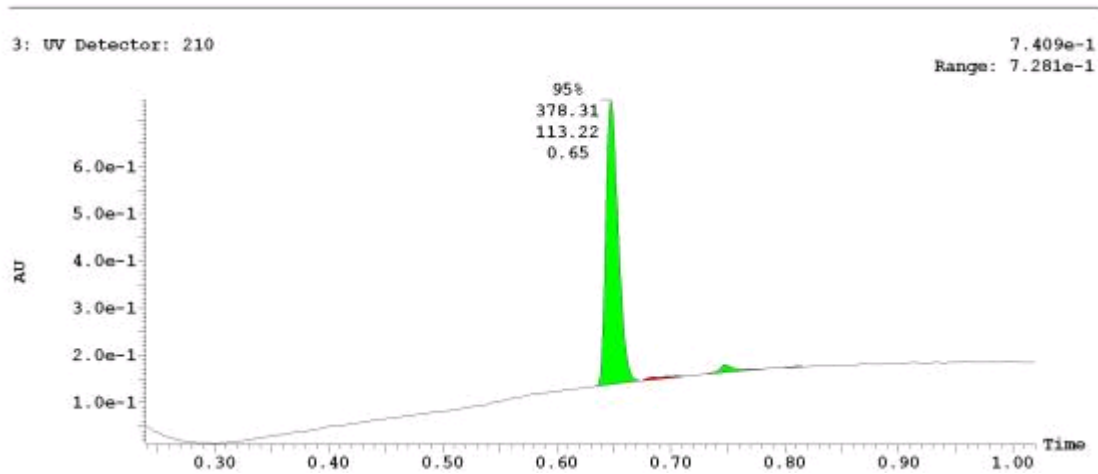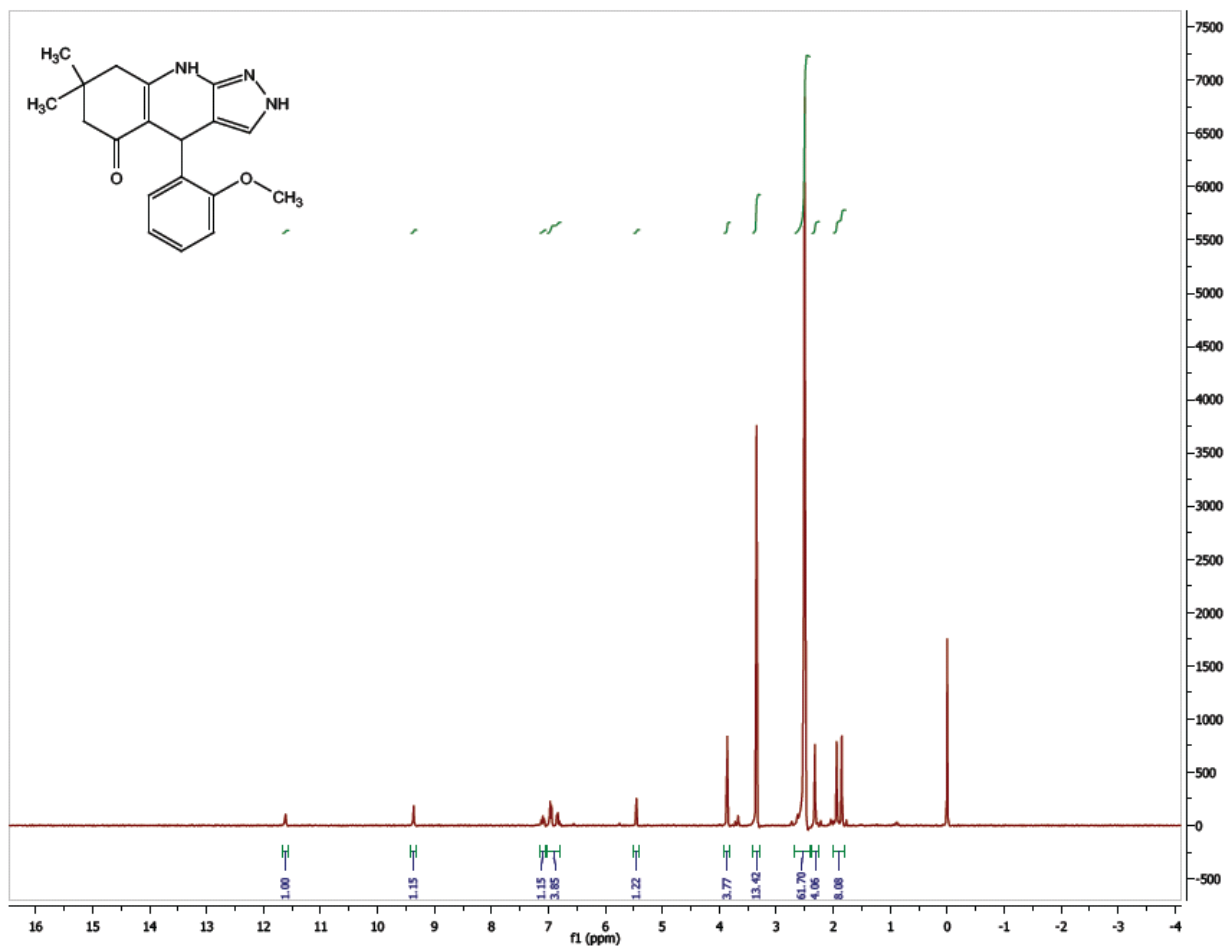
93%
326.26
113.13
0.58

6%
324.33
479.11
0.67
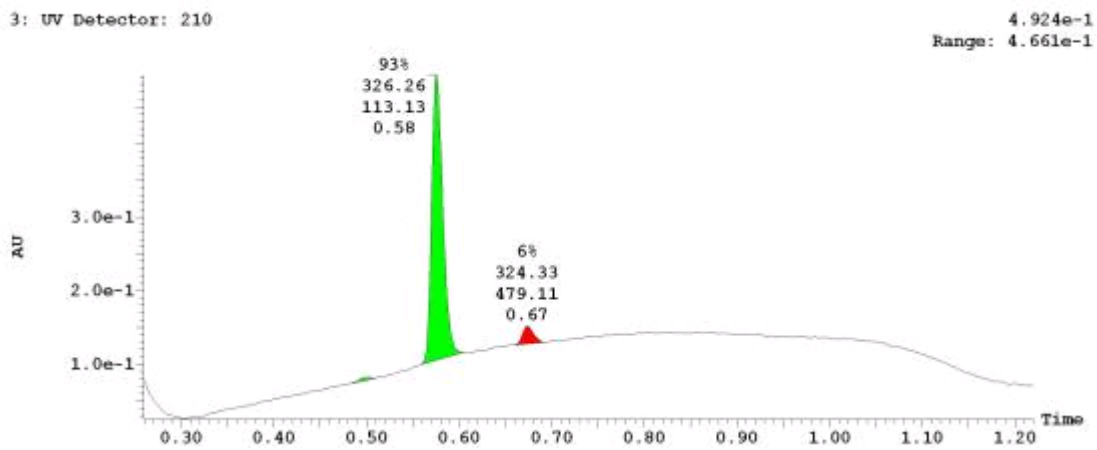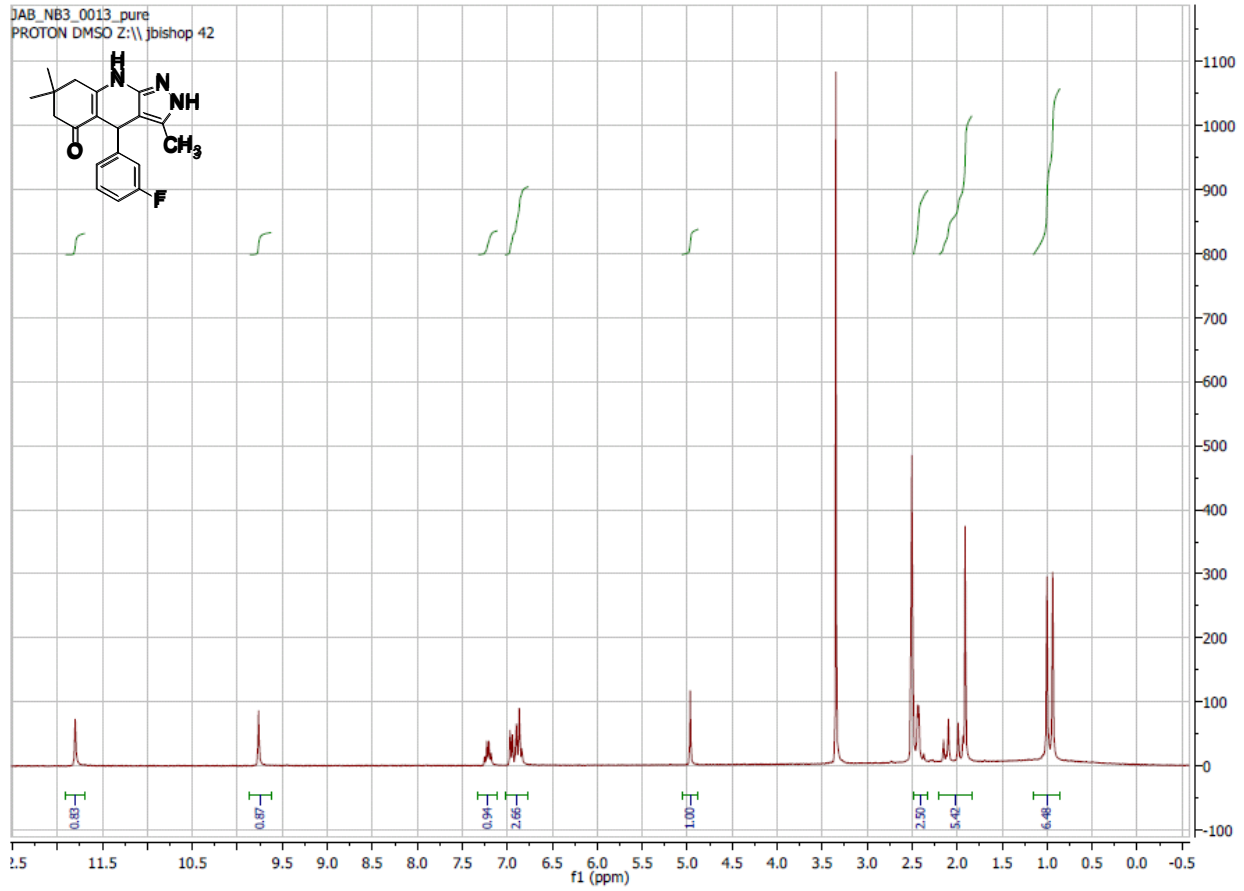
UPLC-MS Chromatogram of CID 56846672
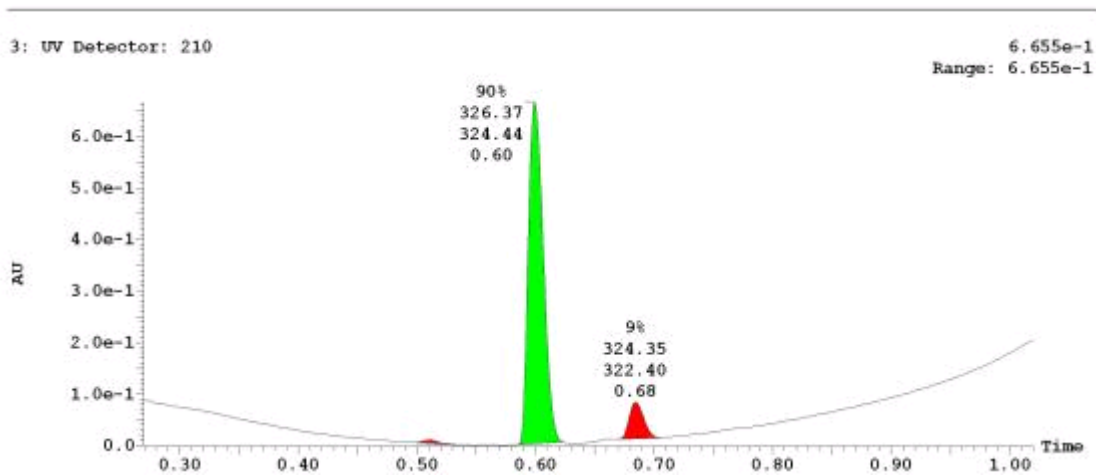
^{1}H NMR Spectrum (300 MHz, CDCl$_3$) of CID 5771498
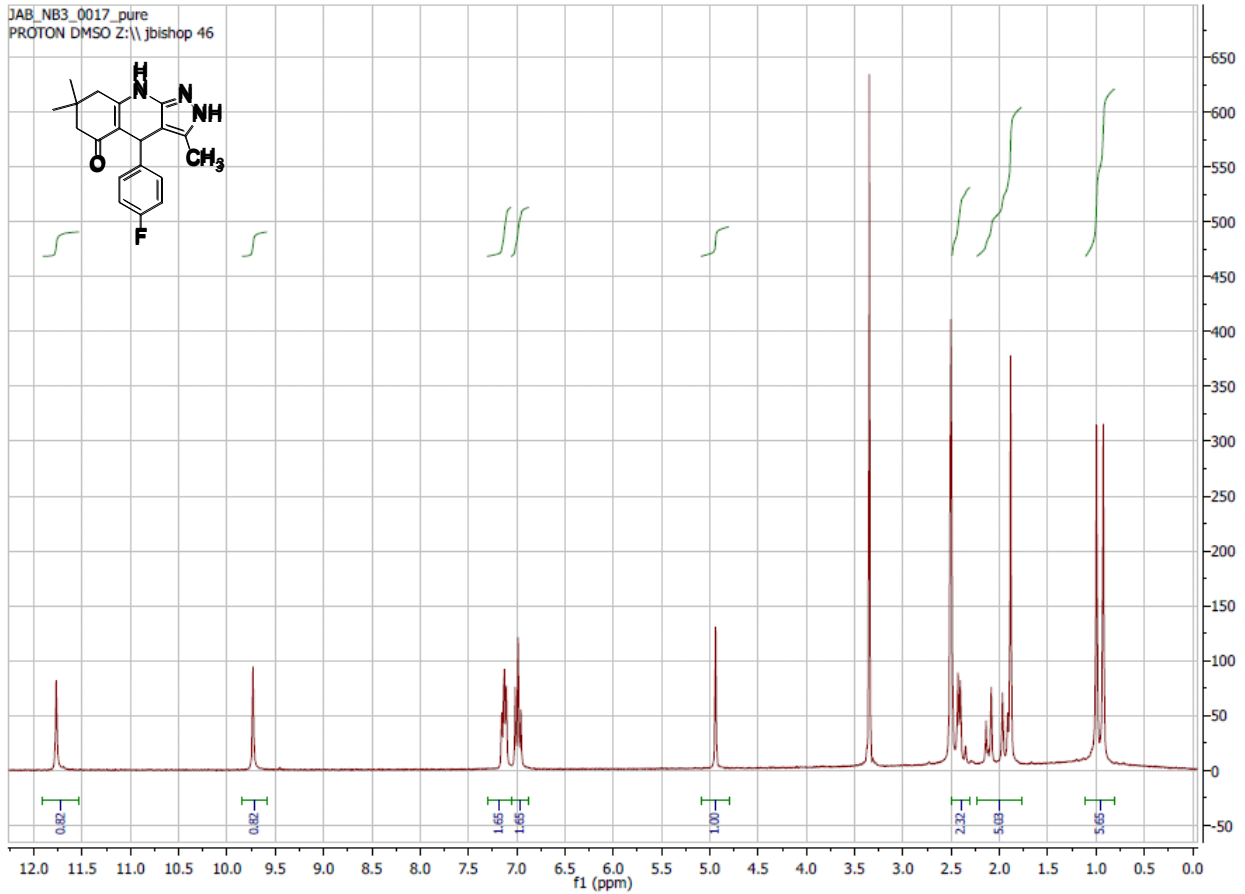
UPLC-MS Chromatogram of CID 5771498
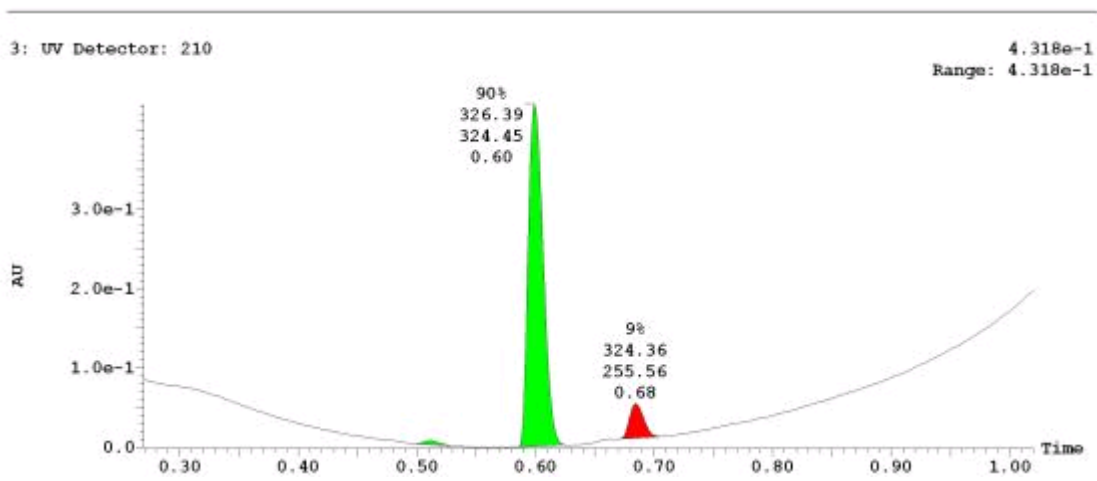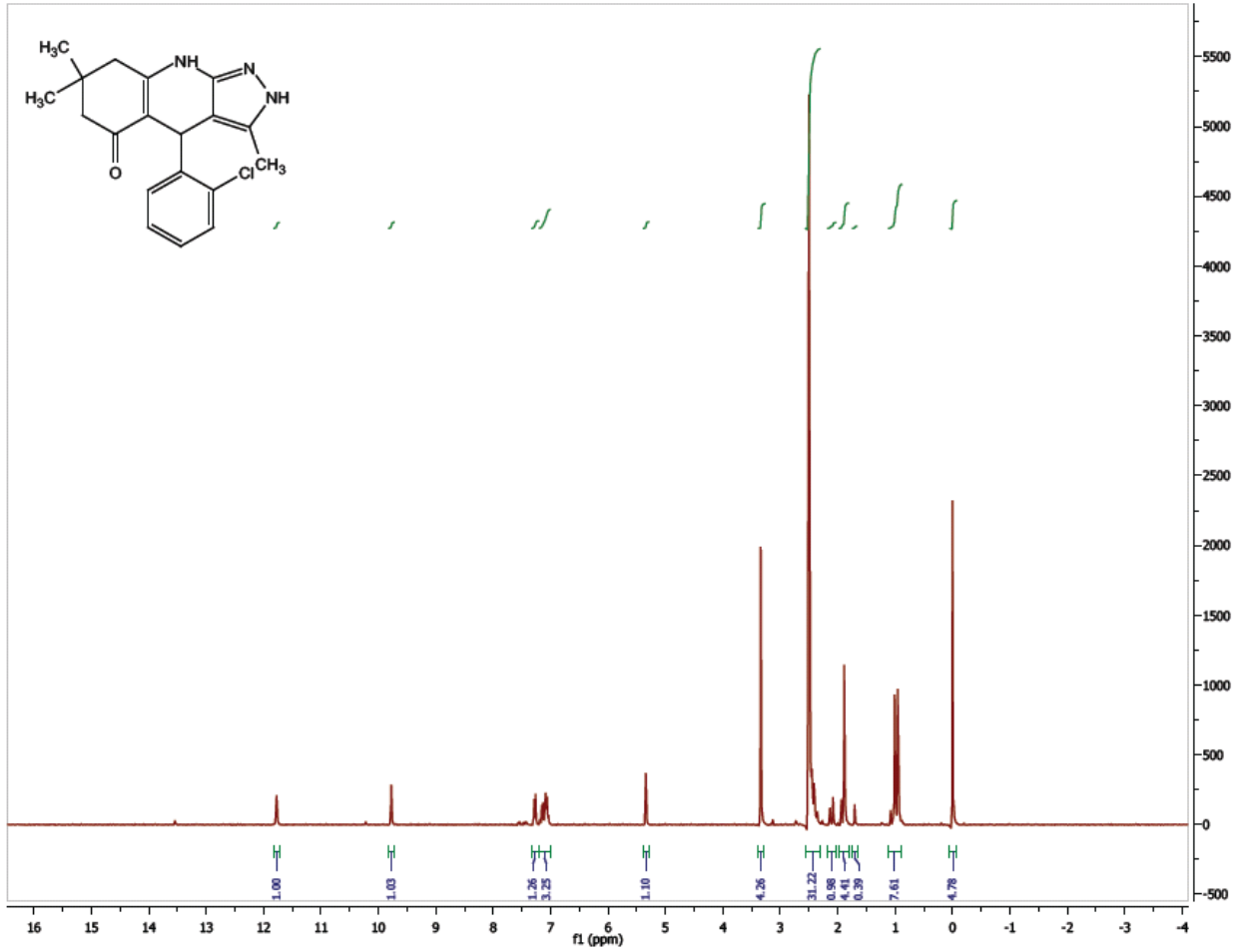
UPLC-MS Chromatogram of CID 56589396
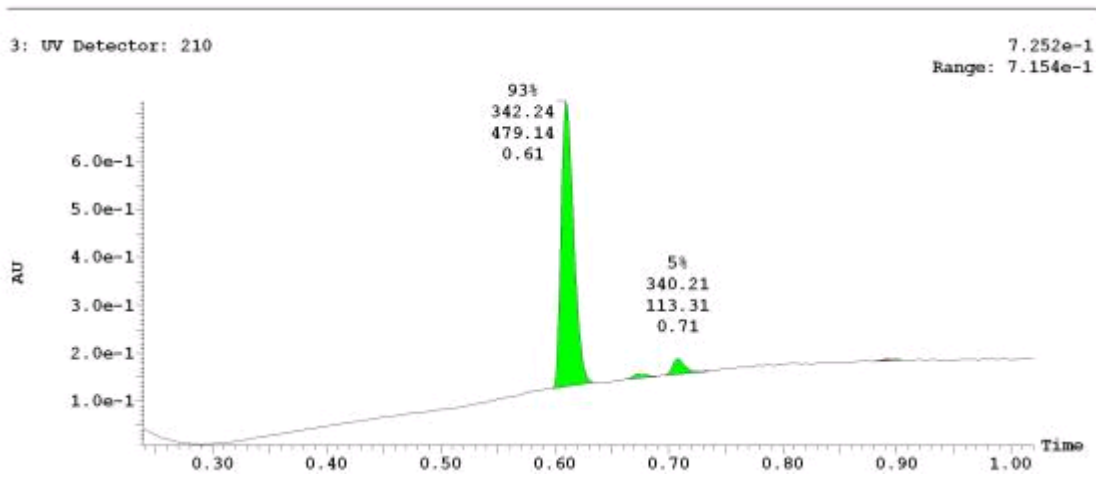
^{1}H NMR Spectrum (300 MHz, CDCl$_3$) of CID 5841835

JAB_NB3_0014_pure
PROTON DMSO Z:\\ jbishop 43
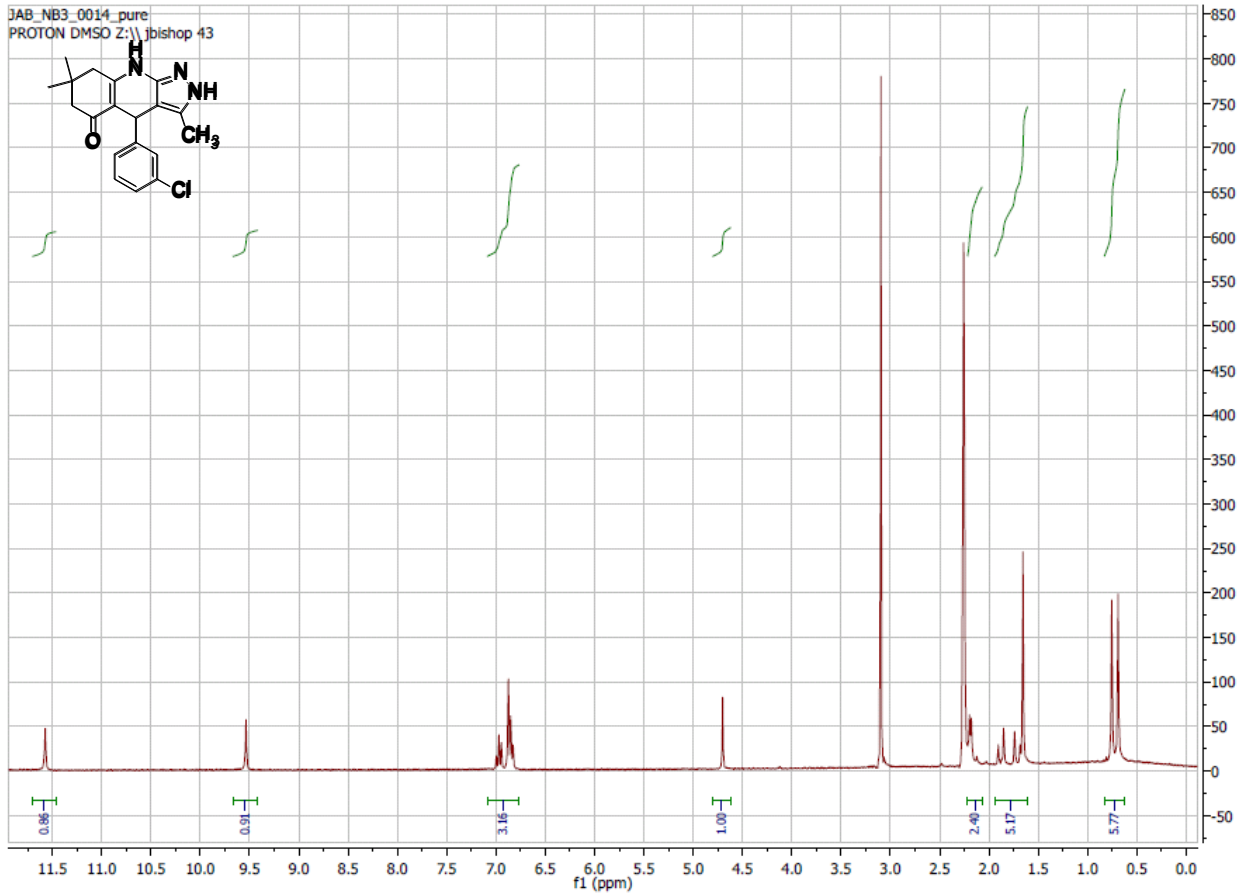
UPLC-MS Chromatogram of CID 5841835

3: UV Detector: 210

7.2e-1
Range: 6.968e-1

97%
342.28
454.36
0.62
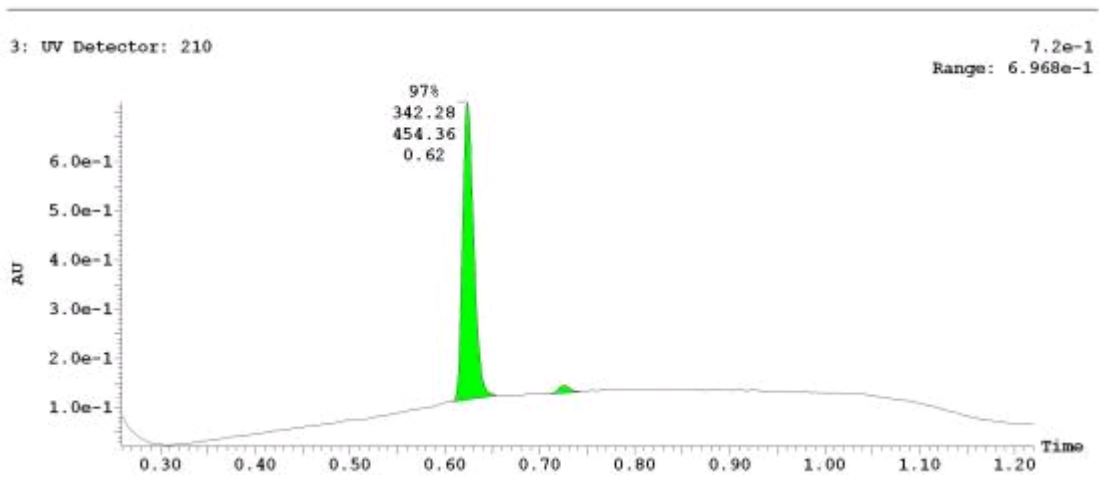
^{1}H NMR Spectrum (300 MHz, CDCl$_3$) of CID 6030657

JAB_NB3_0003_pure
PROTON DMSO Z:\ jbishop 21
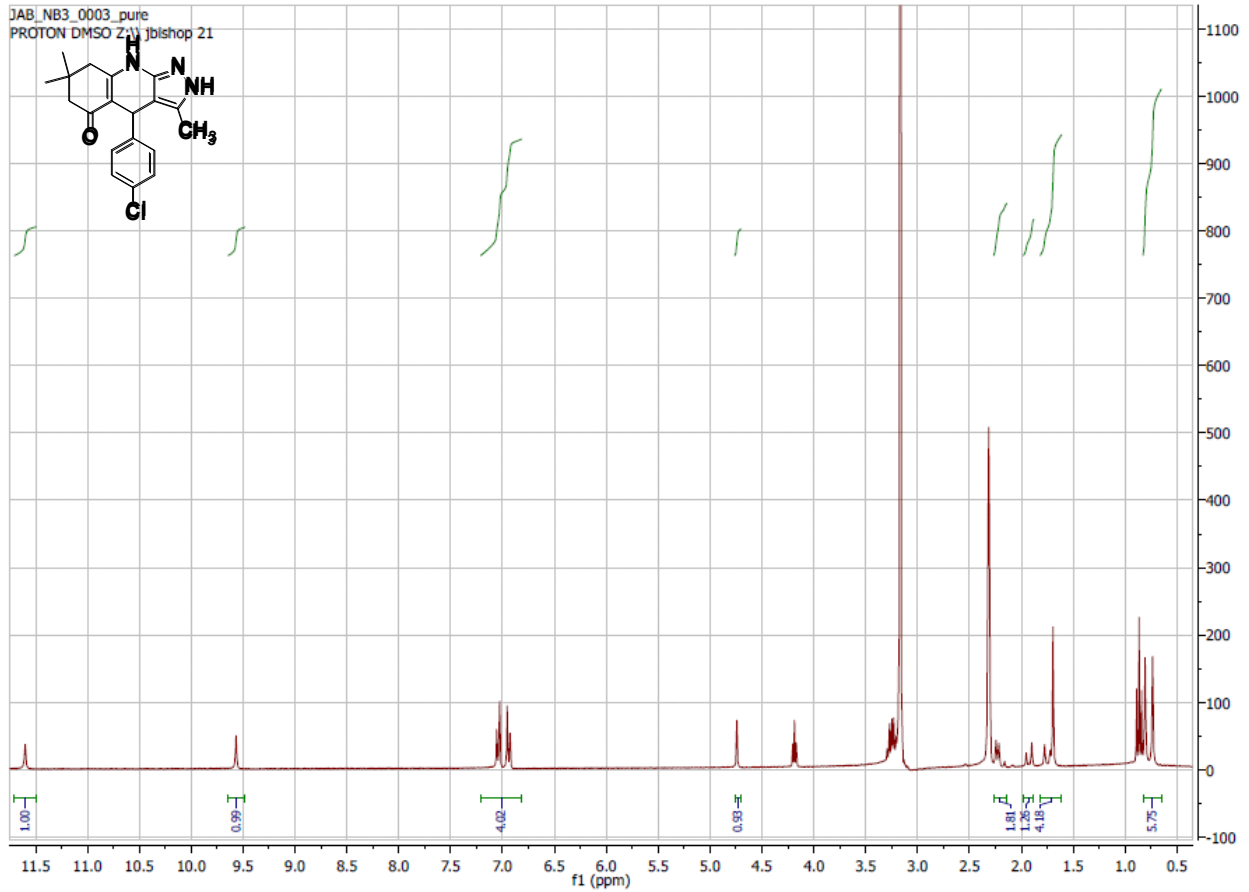
UPLC-MS Chromatogram of CID 6030657

3: UV Detector: 210

4.08e-1
Range: 4.08e-1

89%
342.37
340.42
0.64

11%
340.33
338.40
0.73
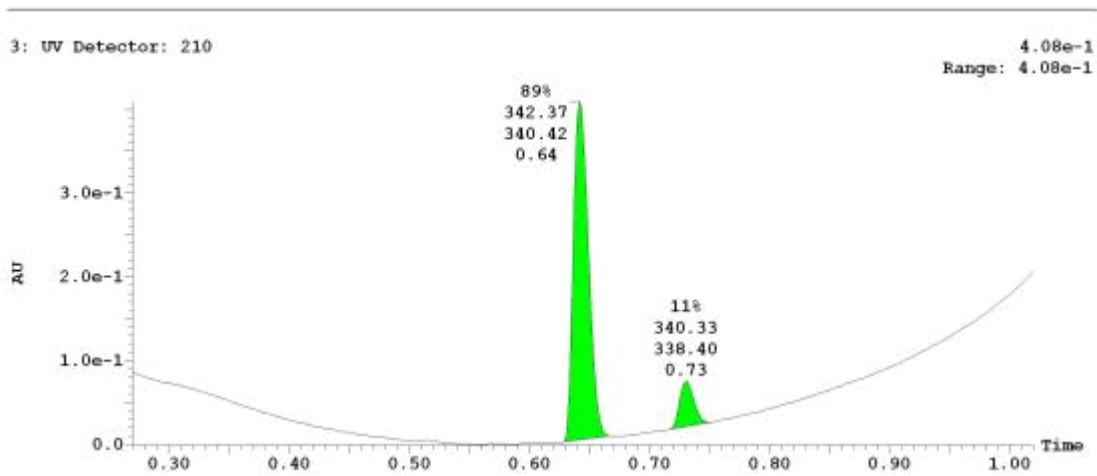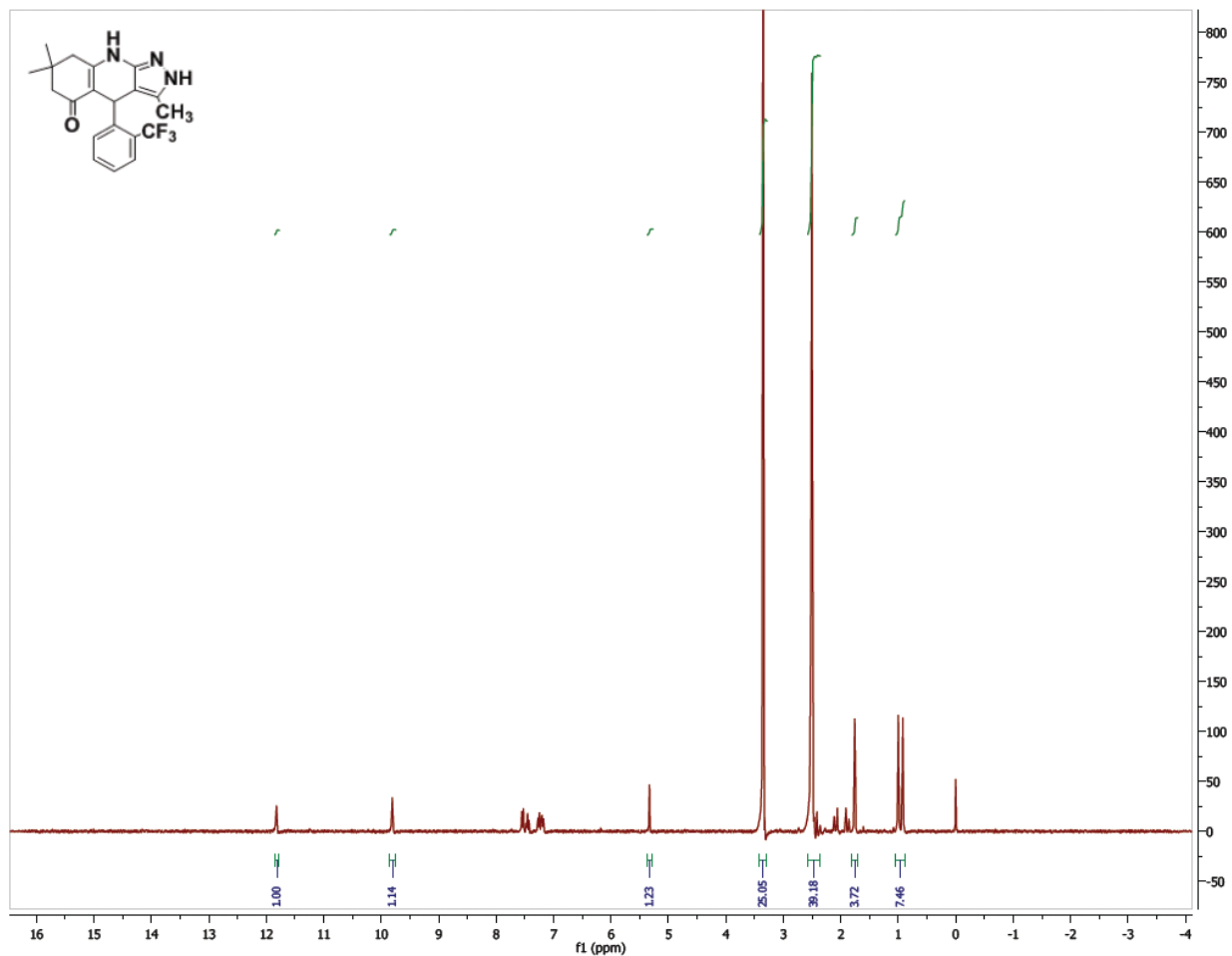
UPLC-MS Chromatogram of CID 56589435
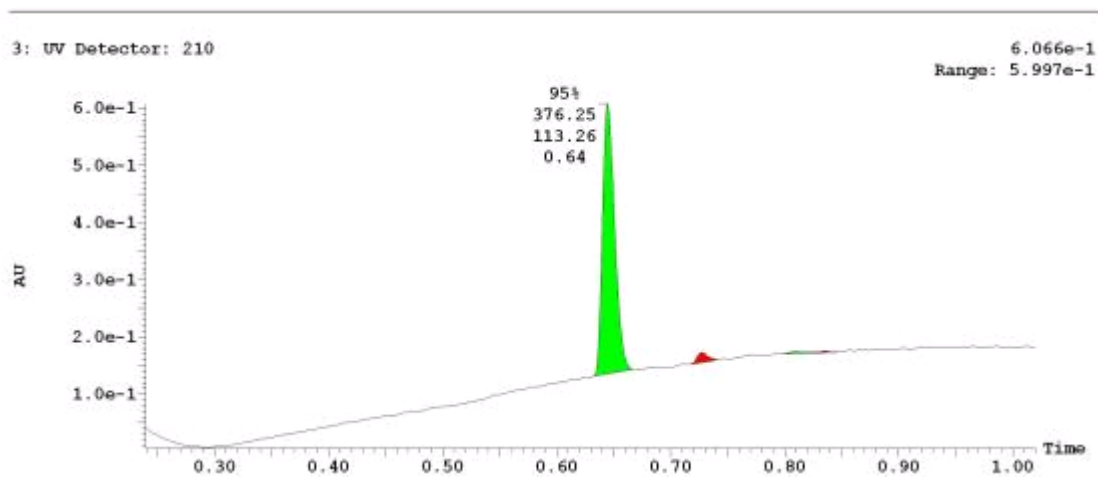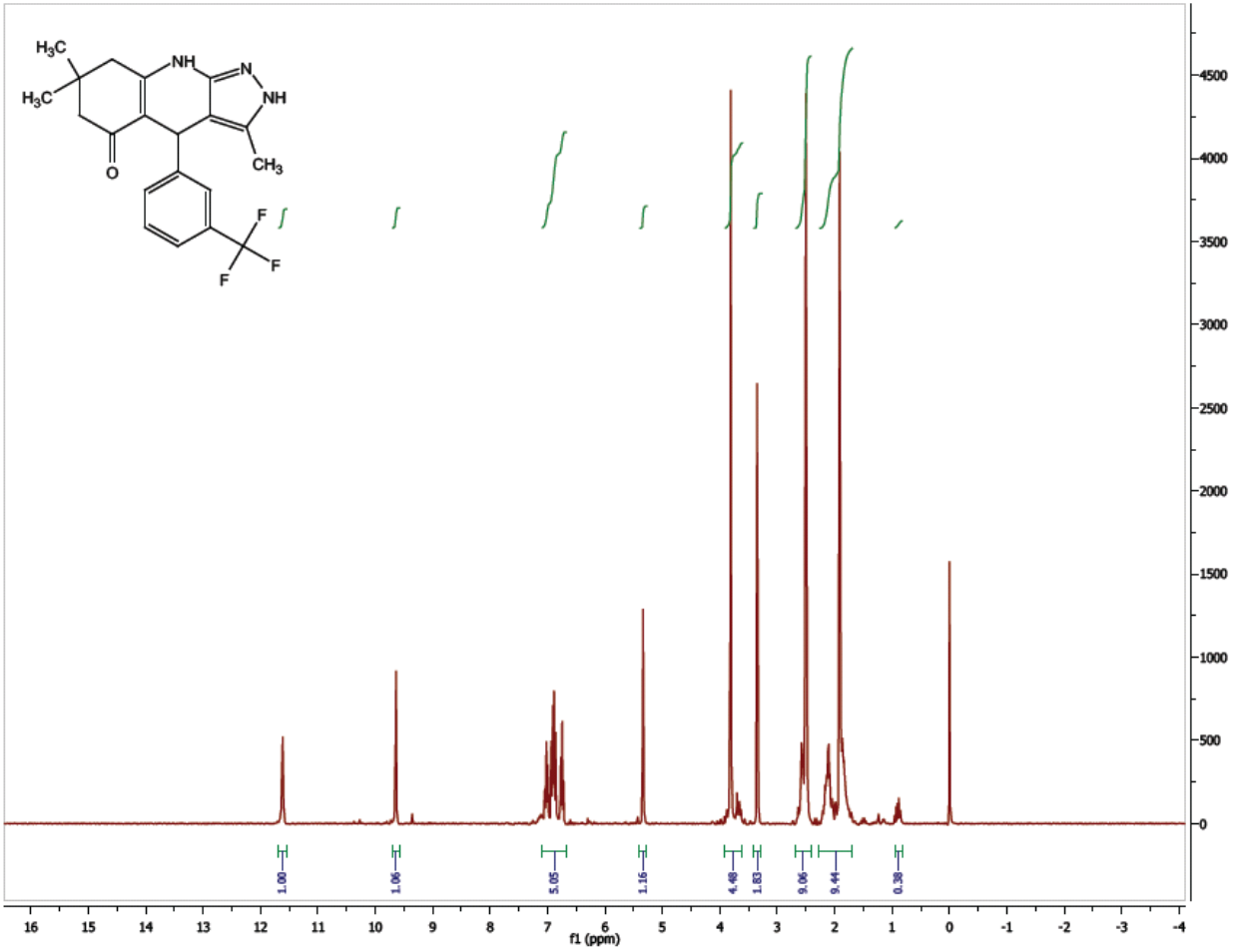
UPLC-MS Chromatogram of CID 56589400
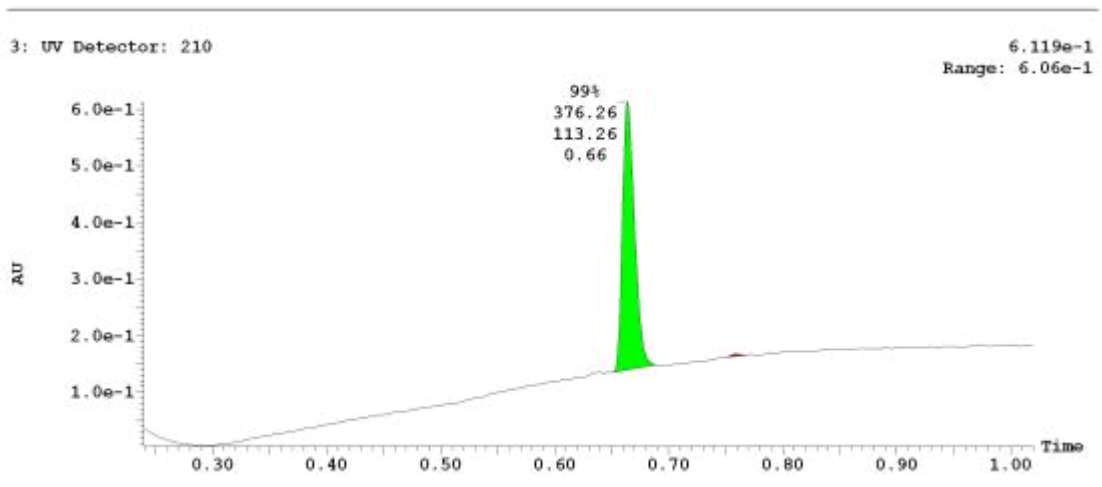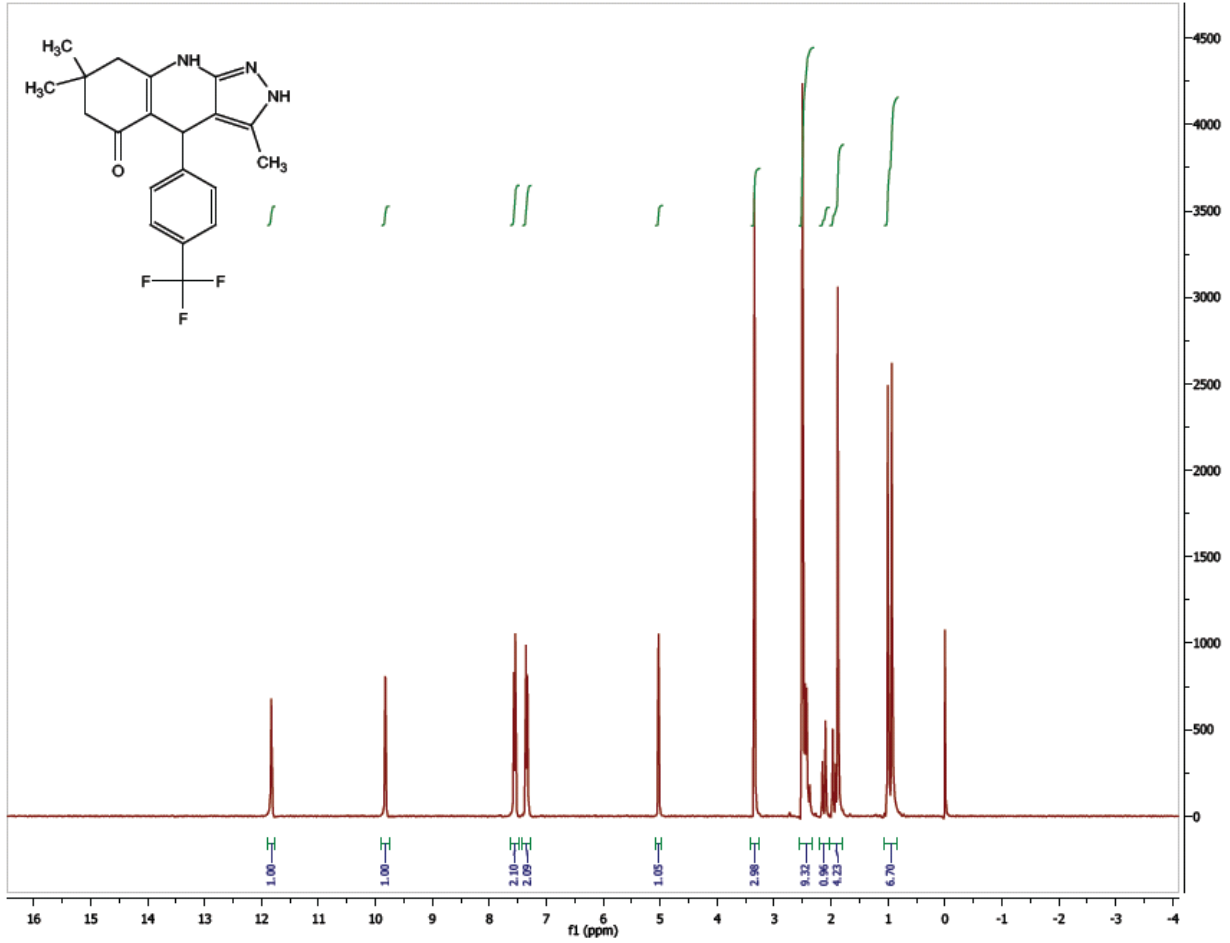
UPLC-MS Chromatogram of CID 56589424
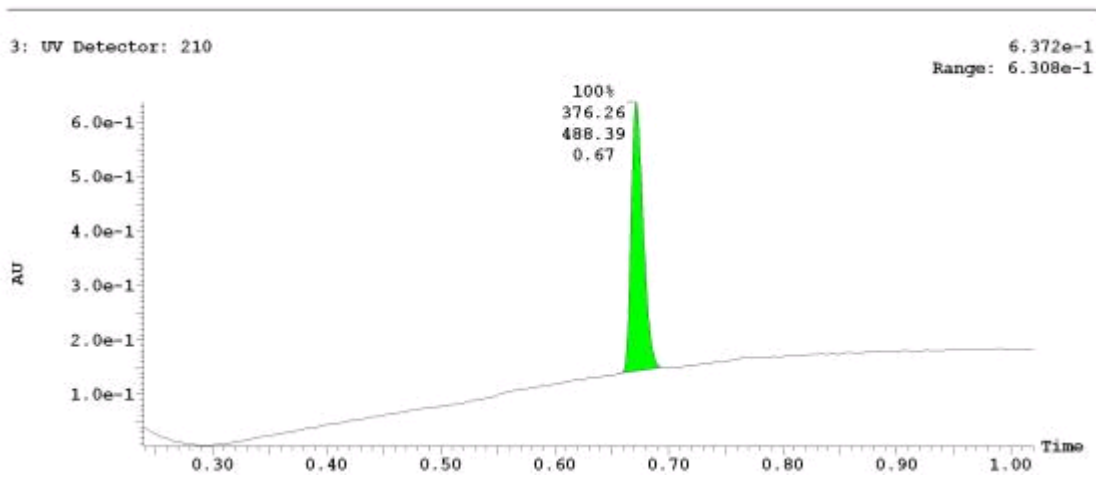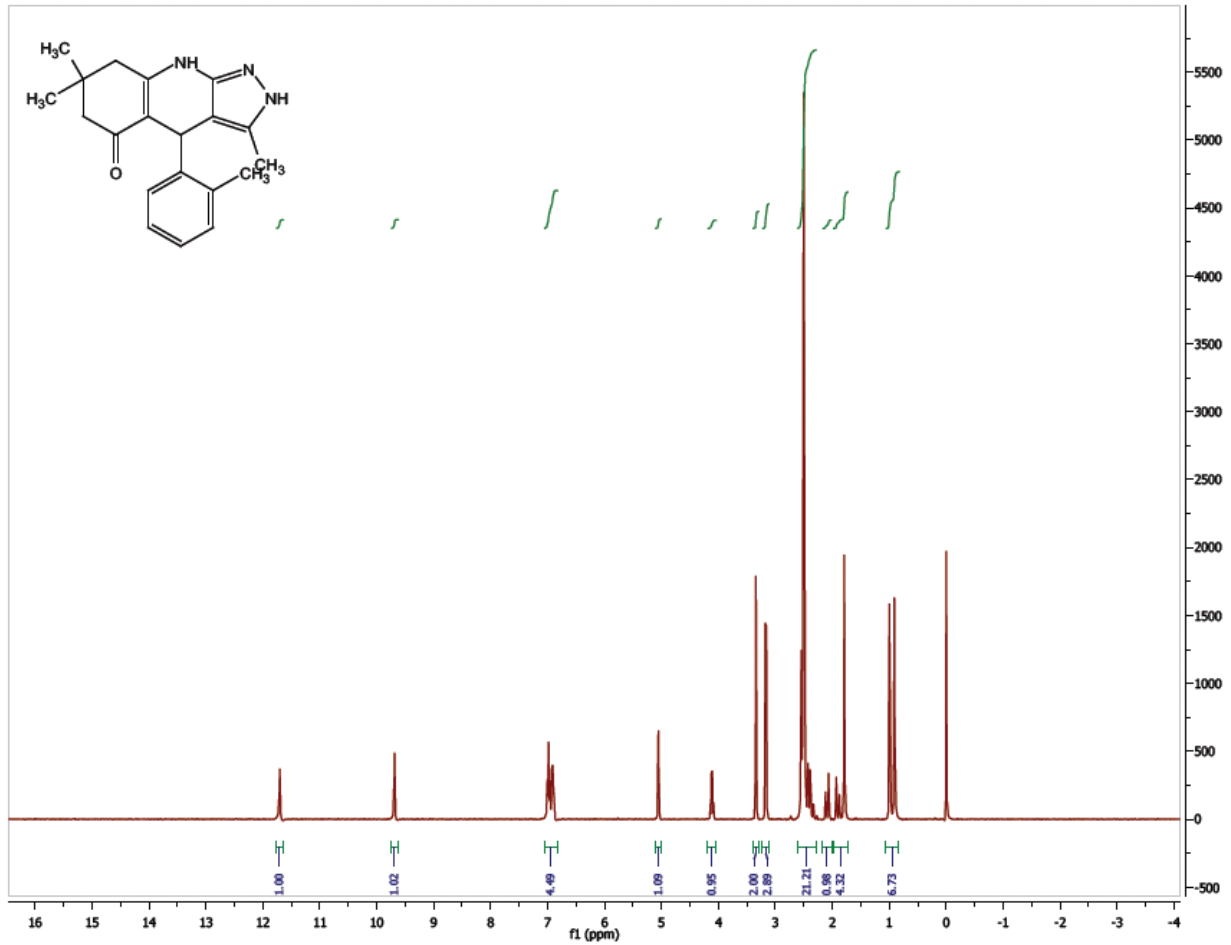
UPLC-MS Chromatogram of CID 56589427
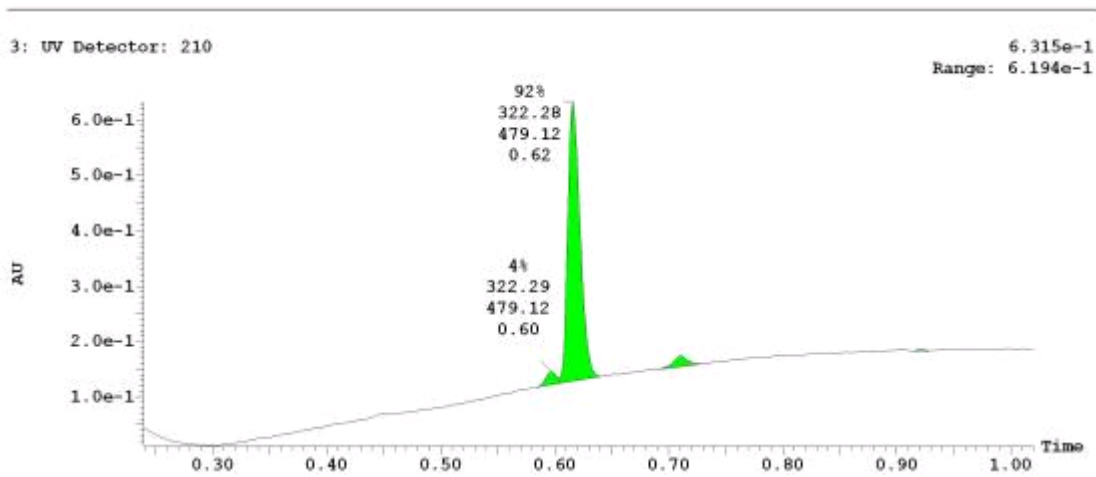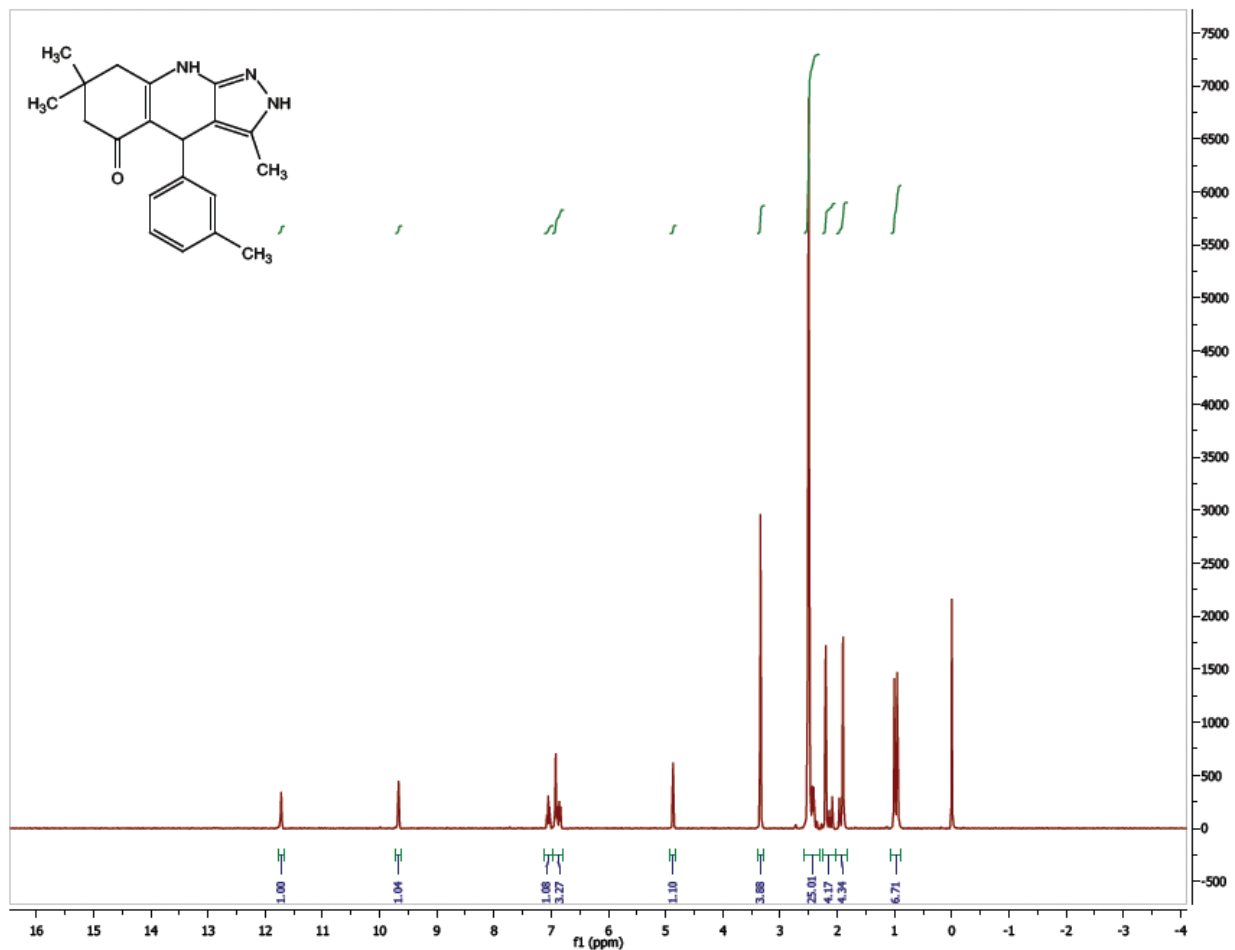
UPLC-MS Chromatogram of CID 56589421
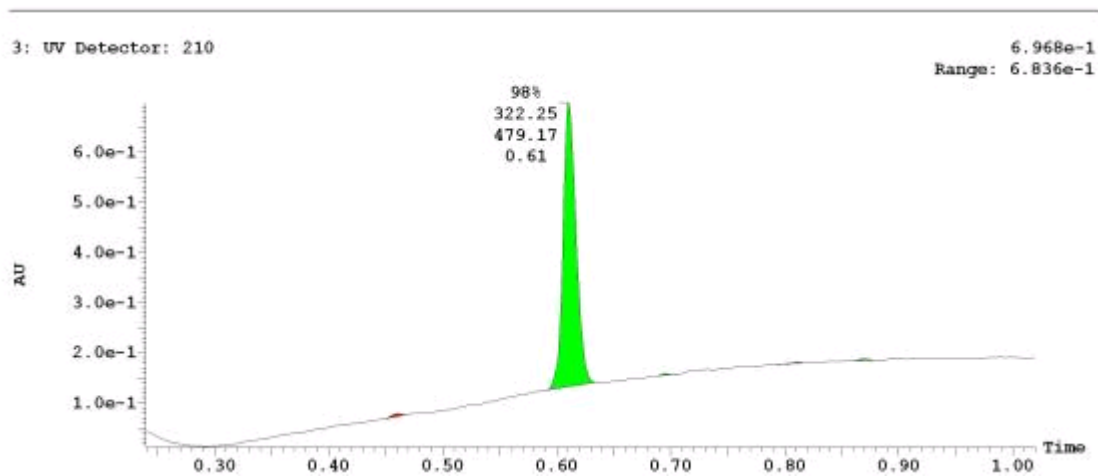
^{1}H NMR Spectrum (300 MHz, CDCl$_3$) of CID 5742470

JAB_NB3_0012_pure
PROTON CDCl3 Z:\\ jbishop 29
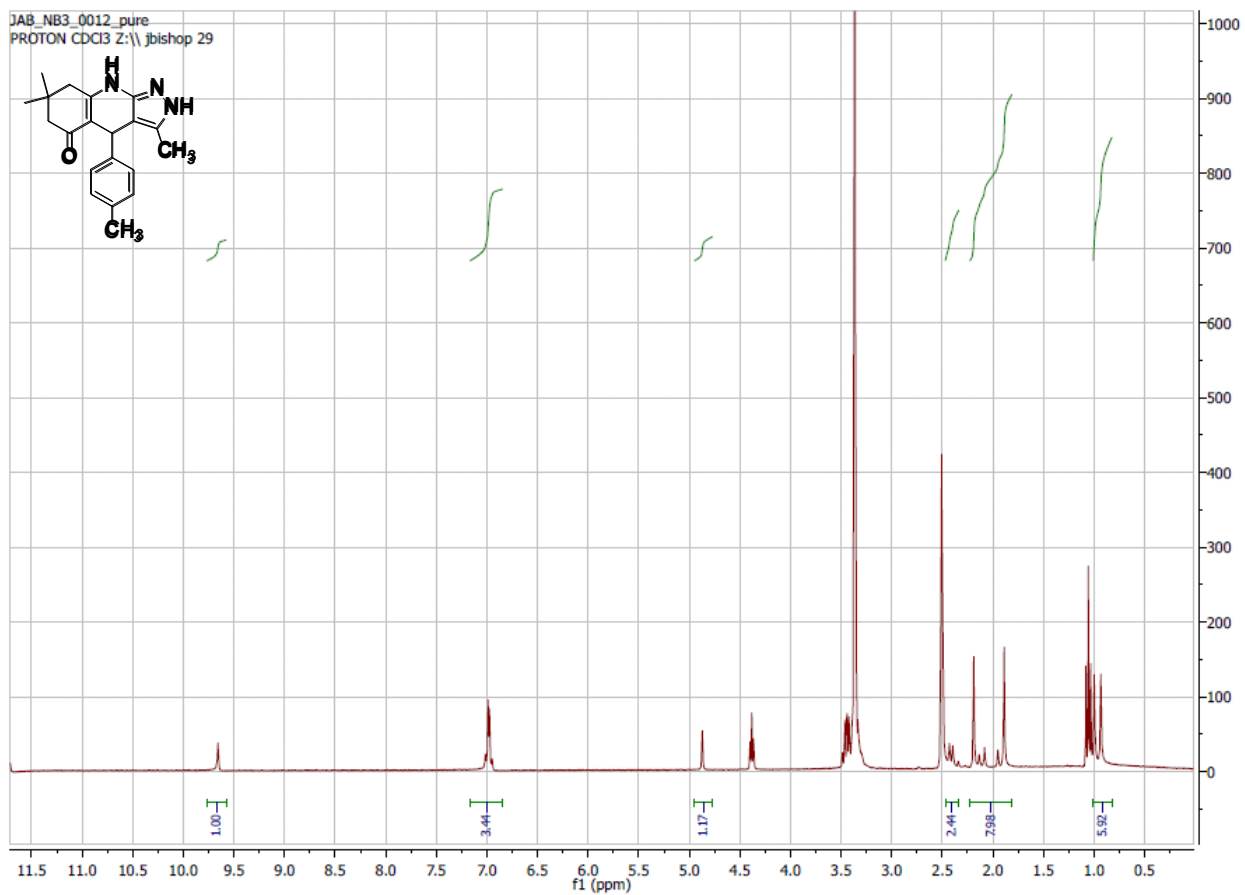
UPLC-MS Chromatogram of CID 5742470

3: UV Detector: 210

6.034e-1
Range: 6.034e-1

89%
322.40
320.46
0.62

11%
320.37
318.42
0.72
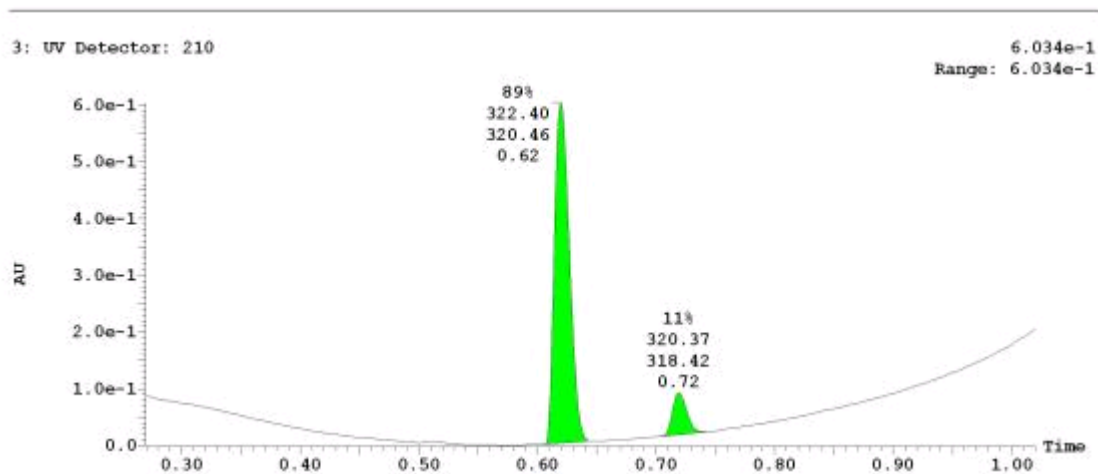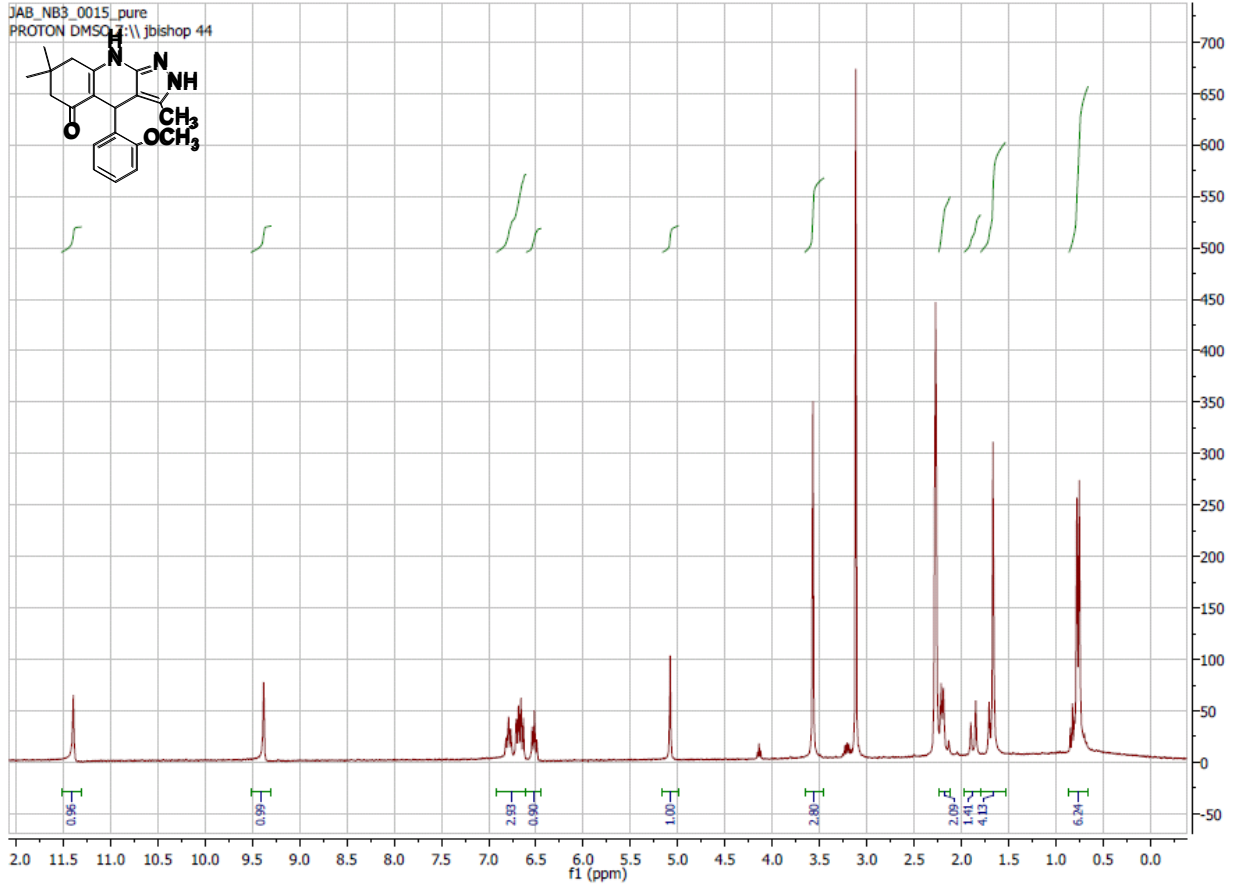
UPLC-MS Chromatogram of CID 5928898
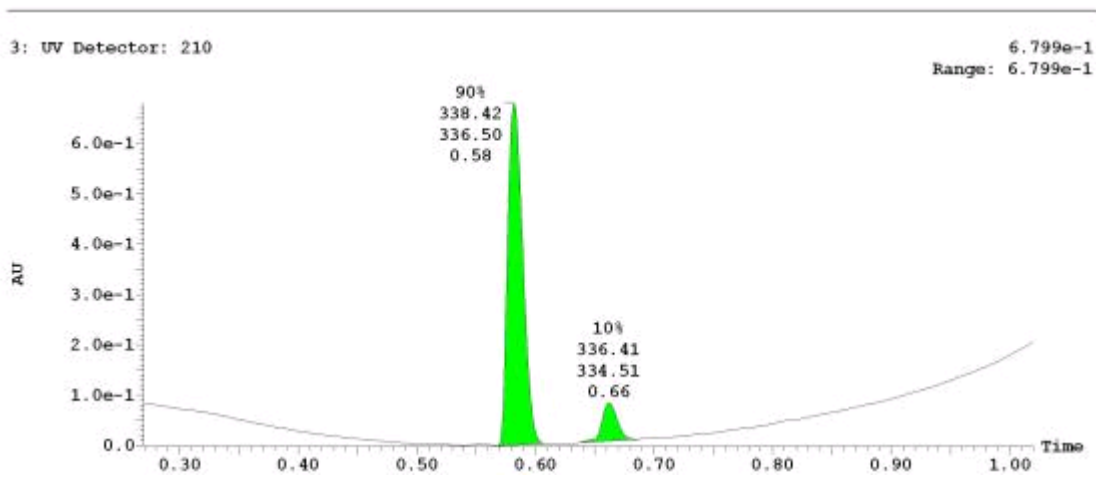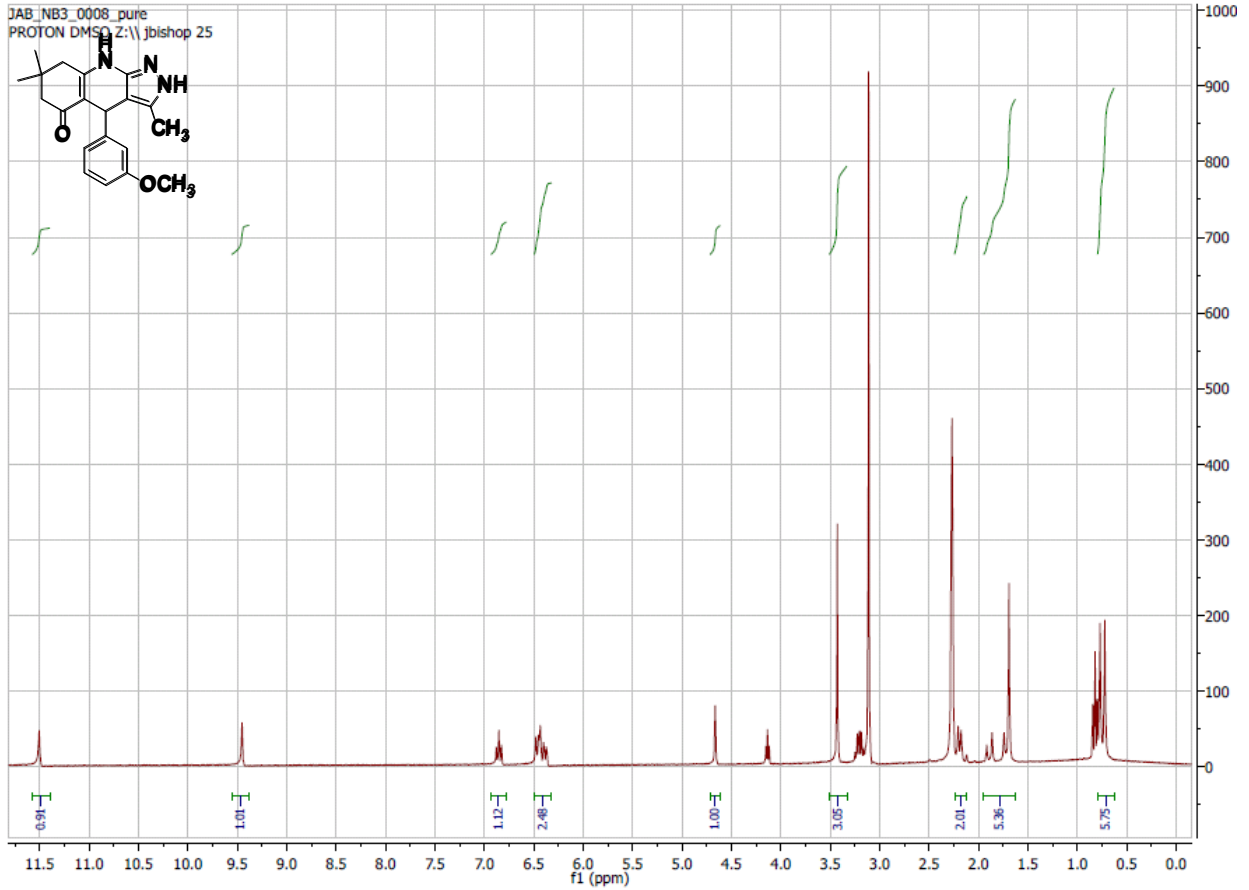
UPLC-MS Chromatogram of CID 6260725
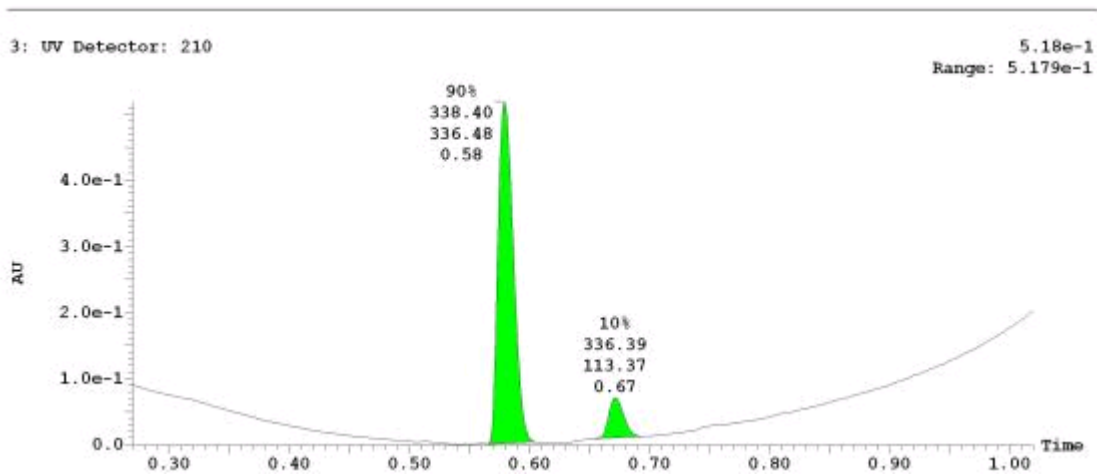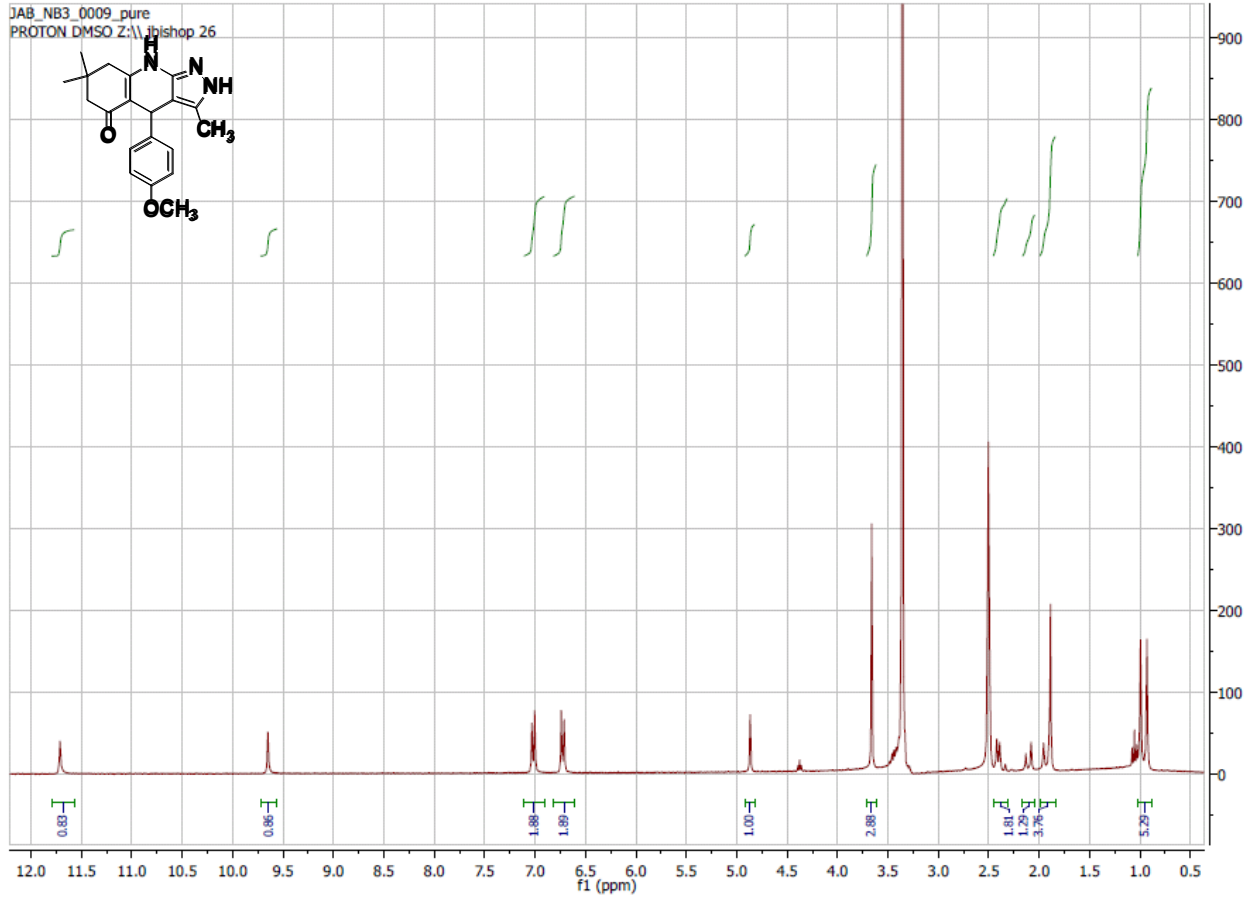
UPLC-MS Chromatogram of CID 5742535
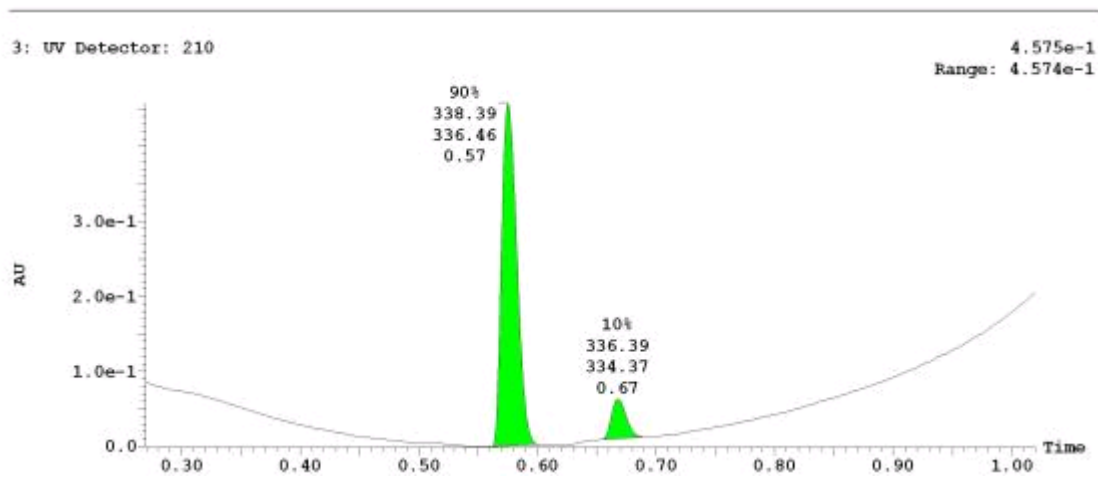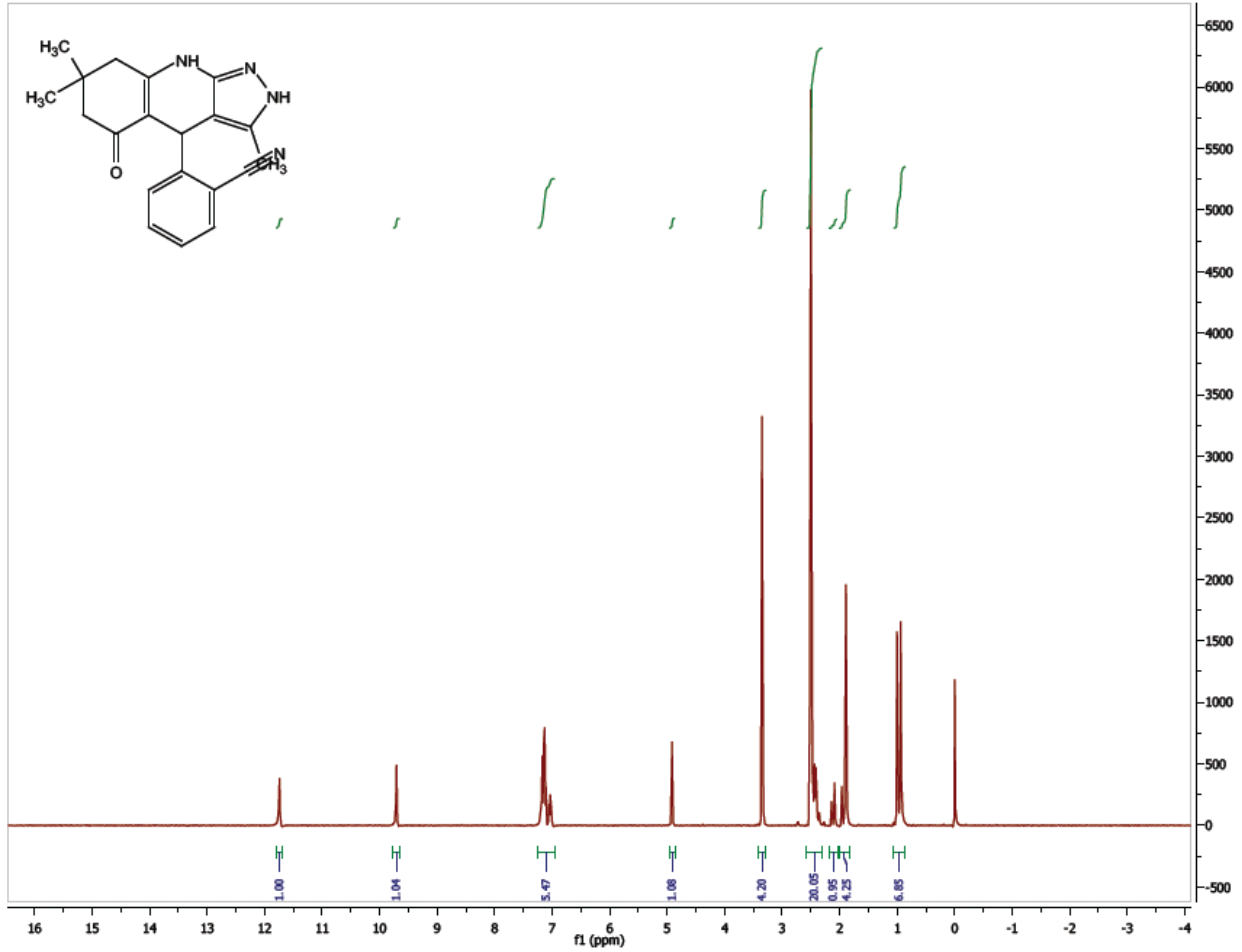
UPLC-MS Chromatogram of CID 56846661
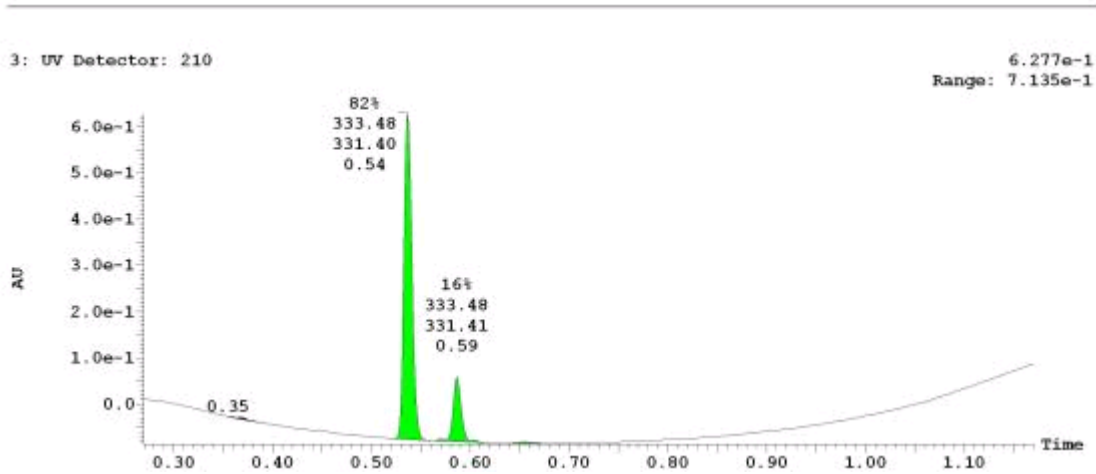
¹H NMR Spectrum (300 MHz, CDCl₃) of CID 56846667
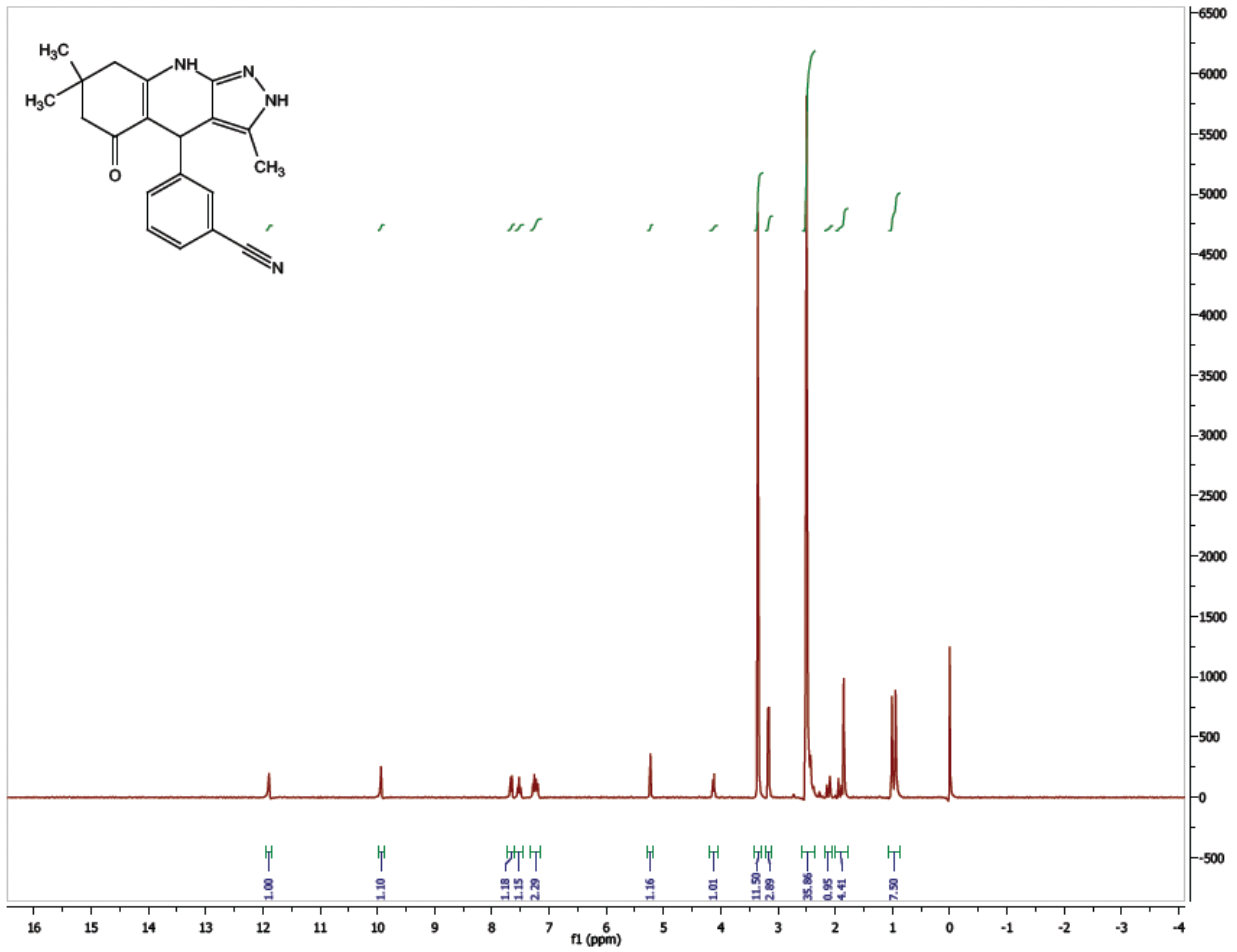
UPLC-MS Chromatogram of CID 56846667

3: UV Detector: 210

4.691e-1
Range: 5.55e-1

78%
333.49
331.42
0.54

22%
333.49
331.41
0.60
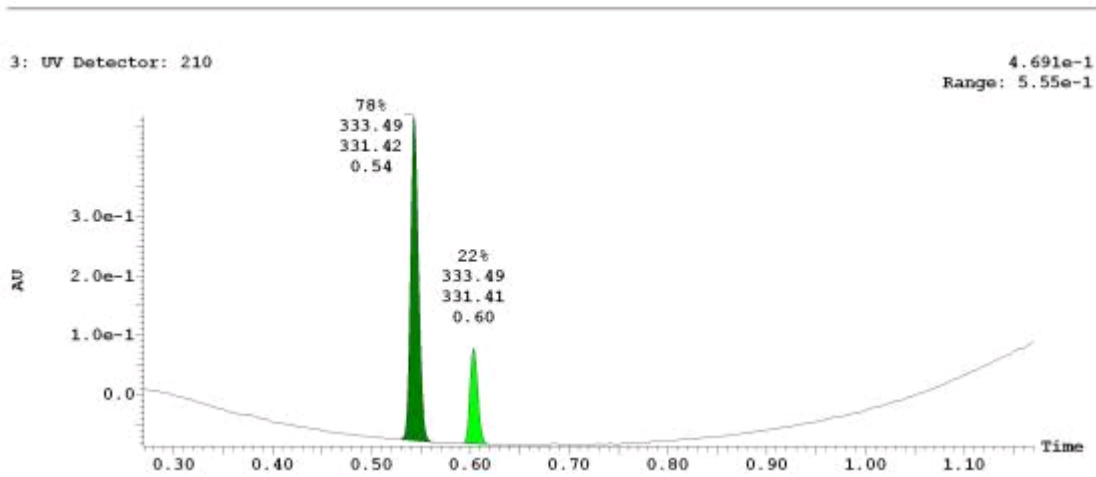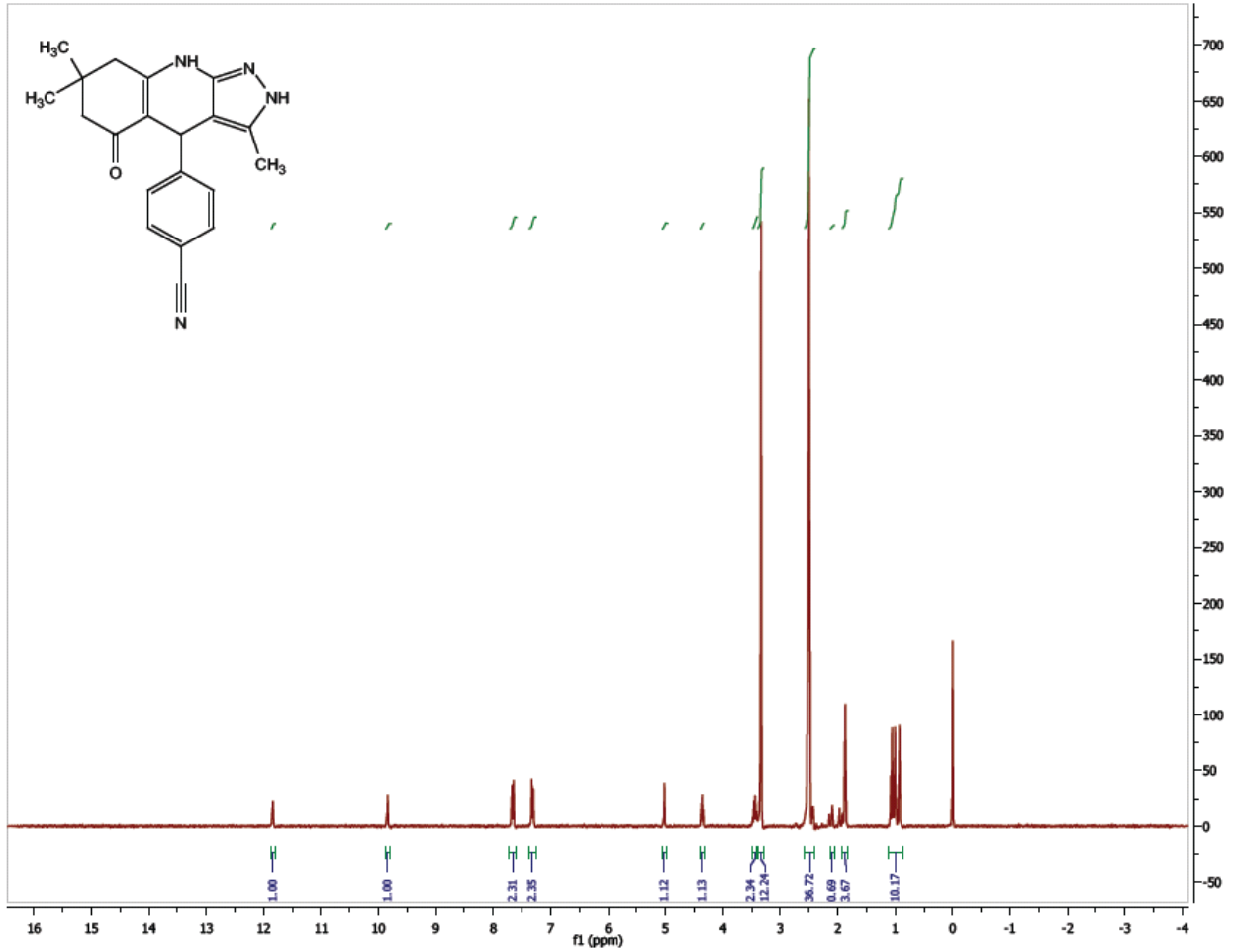
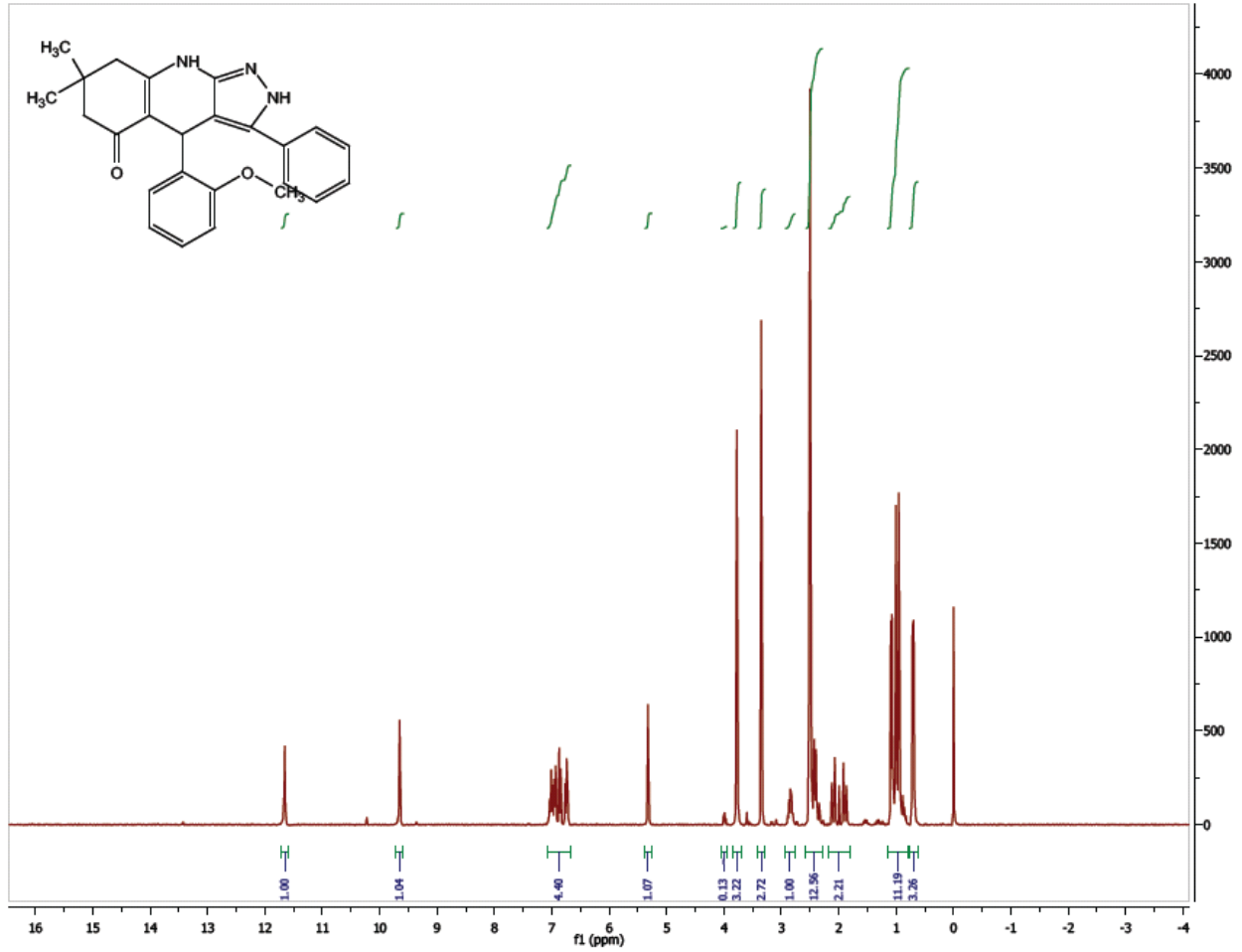**UPLC-MS Chromatogram of CID 56846675**
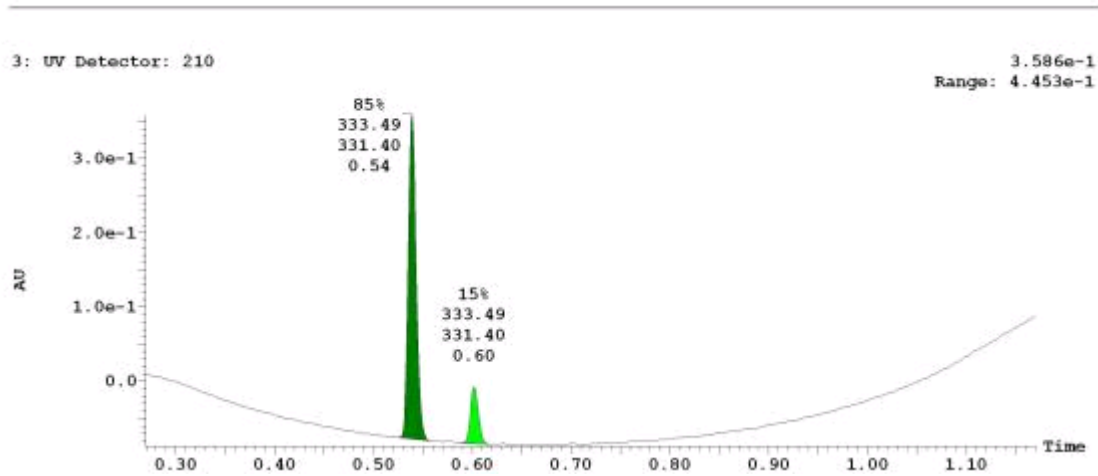
^{1}H NMR Spectrum (300 MHz, CDCl$_3$) of CID 5908141
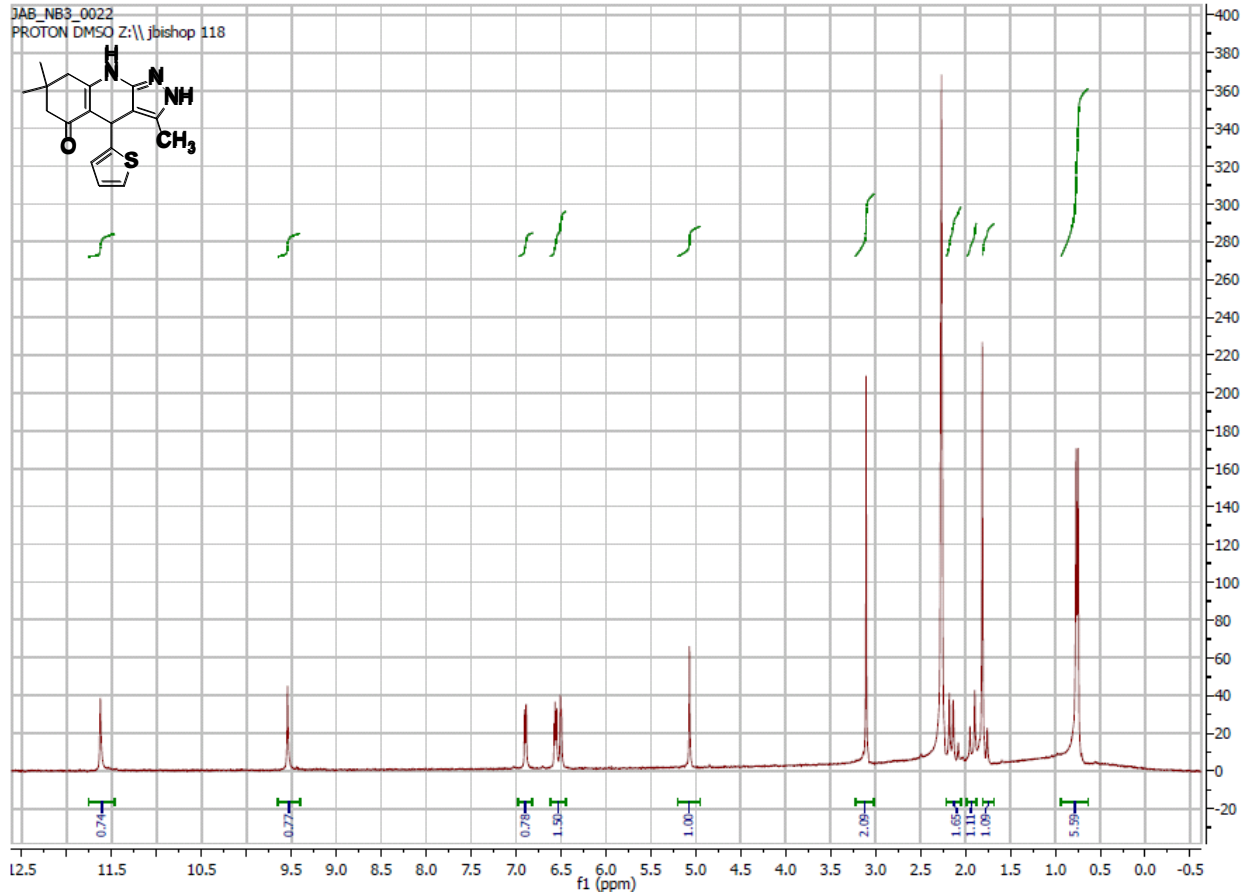
UPLC-MS Chromatogram of CID 5908141
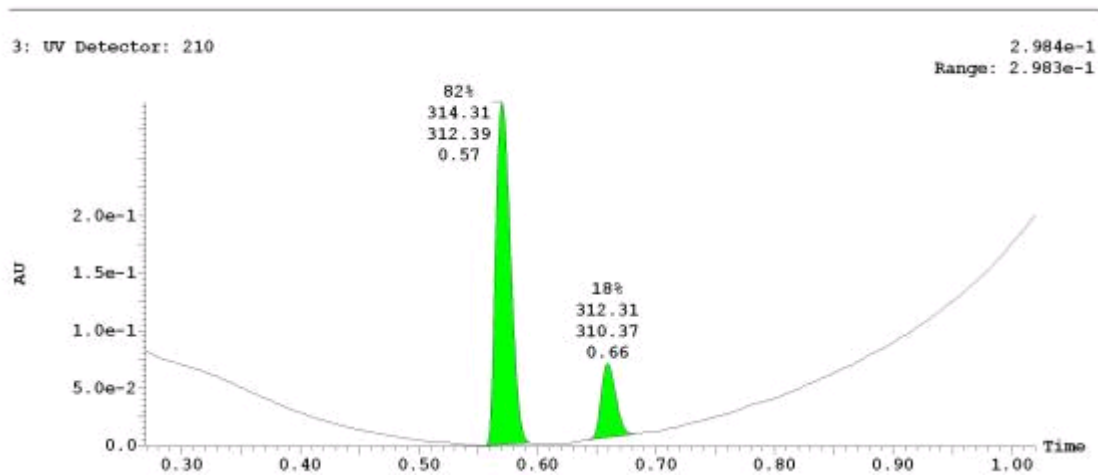
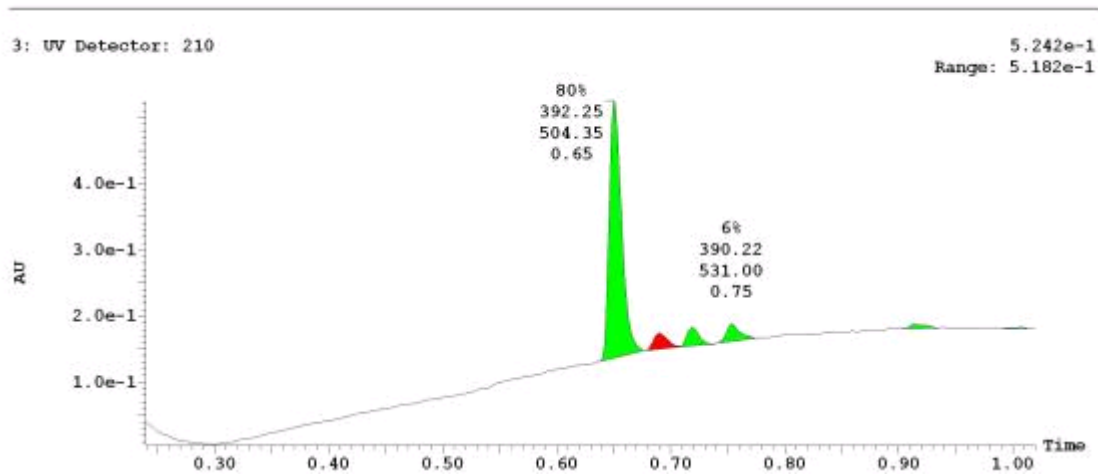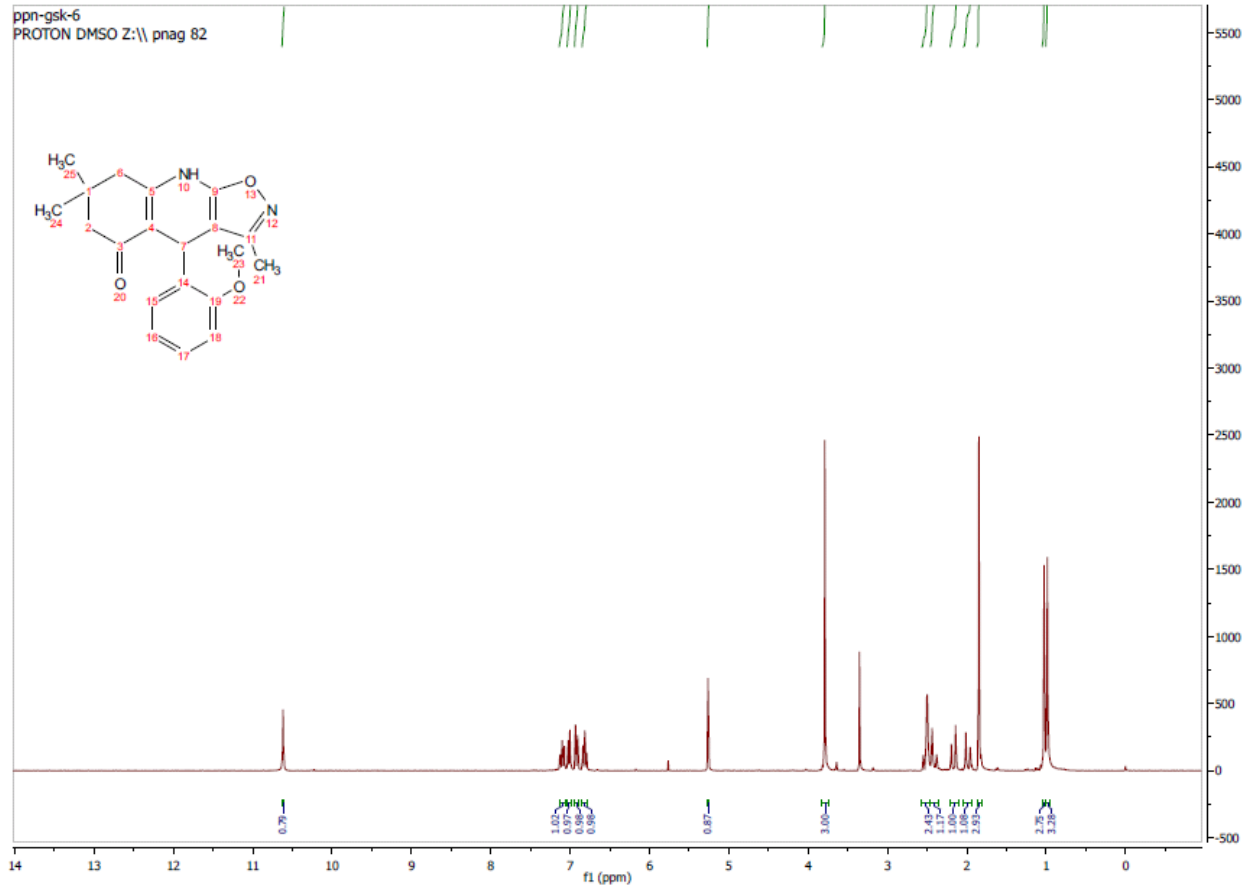## ¹H NMR Spectrum (300 MHz, CDCl₃) of CID 6012776

JAB_NB3_0023
PROTON DMSO Z:\\ jbishop 119

UPLC-MS Chromatogram of CID 6012776

3: UV Detector: 210
4.068e-1
Range: 4.067e-1

91%
314.33
312.43
0.57

9%
312.32
310.38
0.65
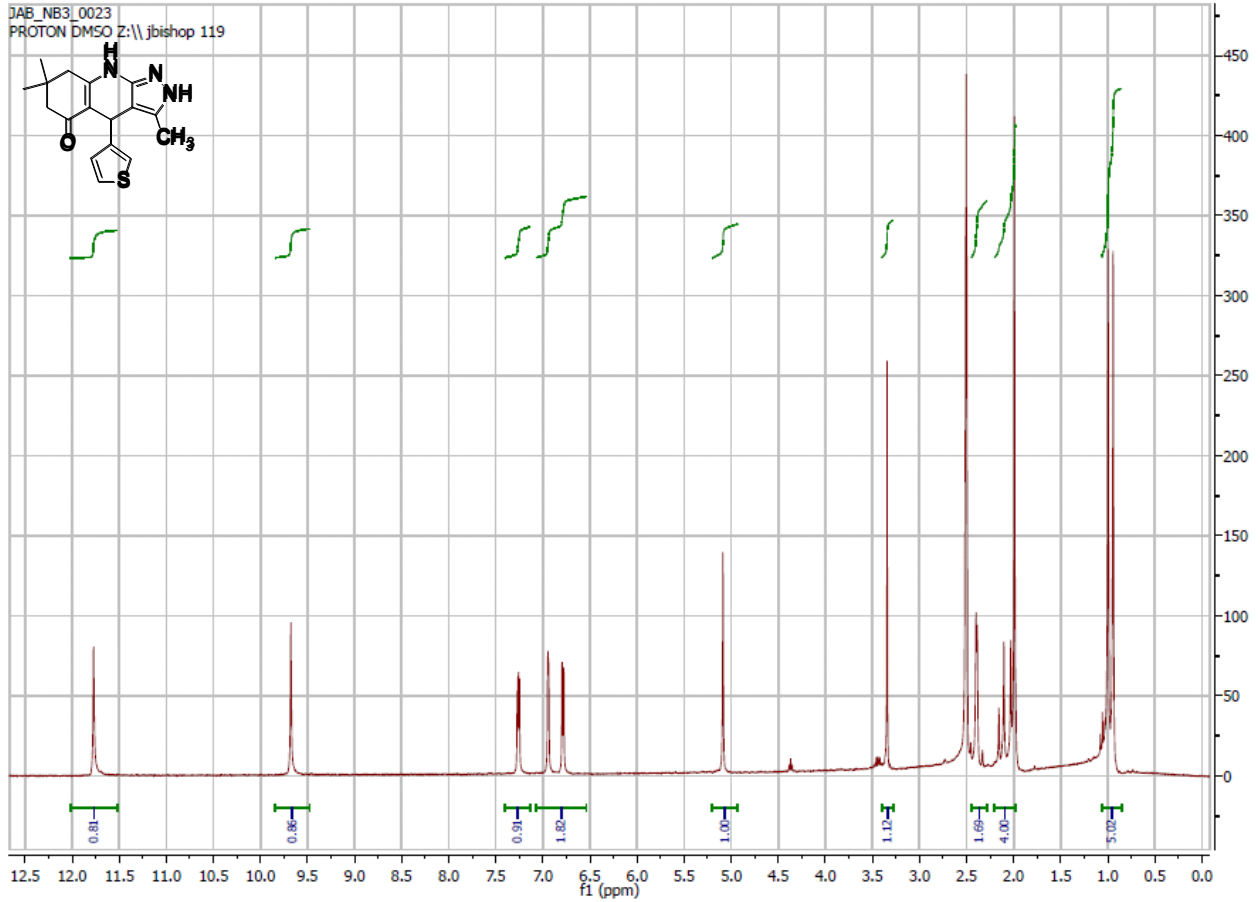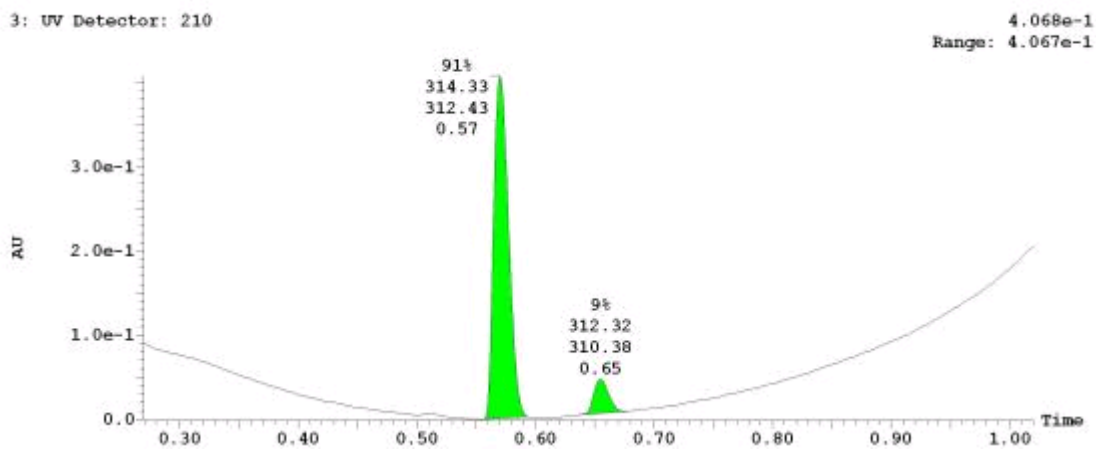
^{1}H NMR Spectrum (300 MHz, CDCl$_3$) of CID 56846658

UPLC-MS Chromatogram of CID 56846658
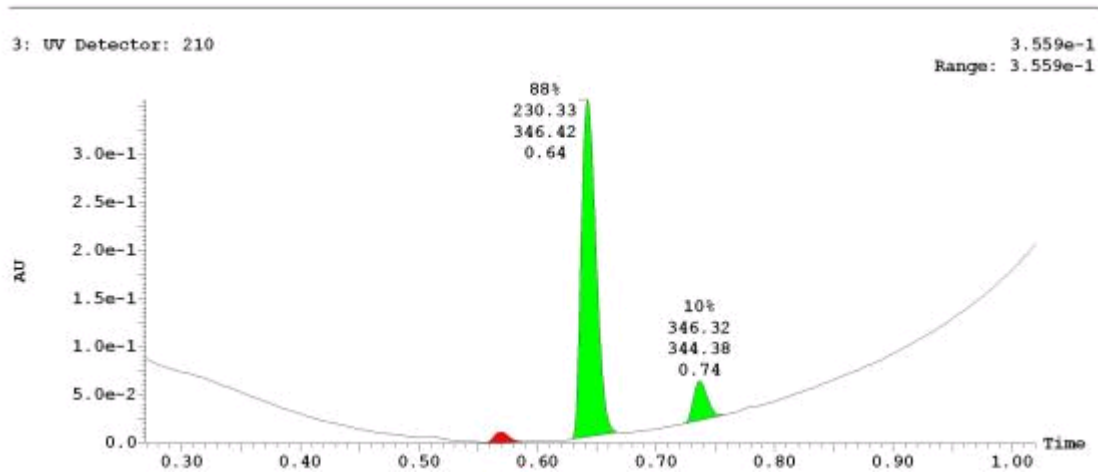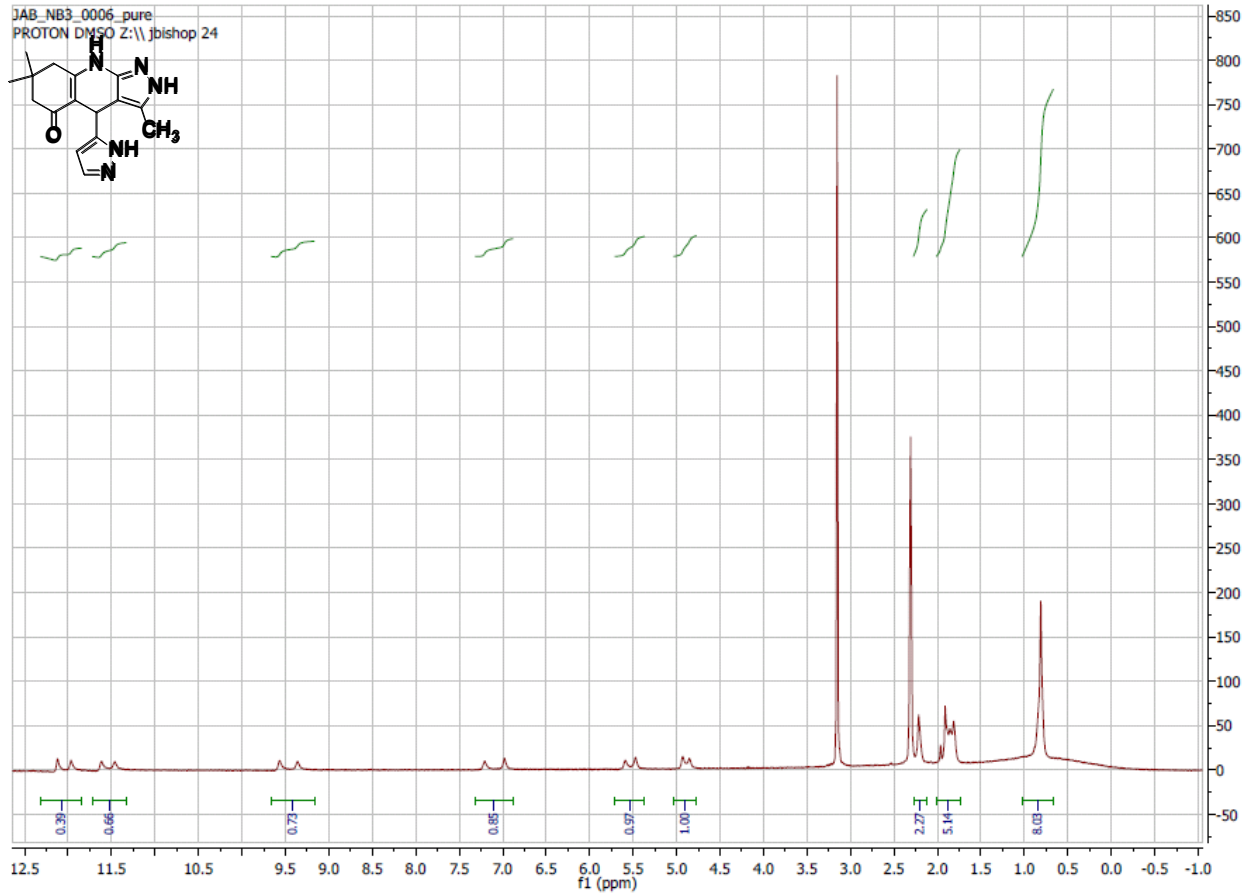
JAB_NB3_0006_pure
PROTON DMSO Z:\\ jbishop 24

UPLC-MS Chromatogram of CID 56846666
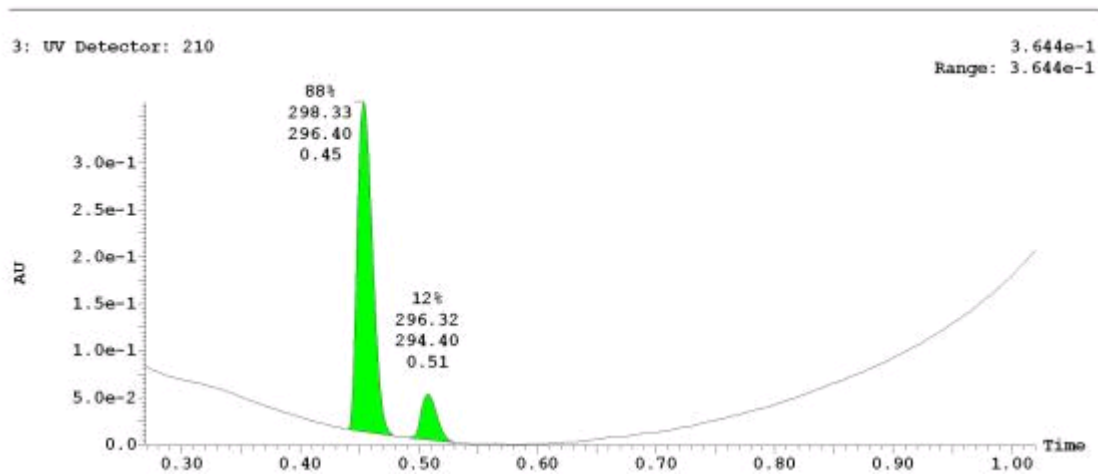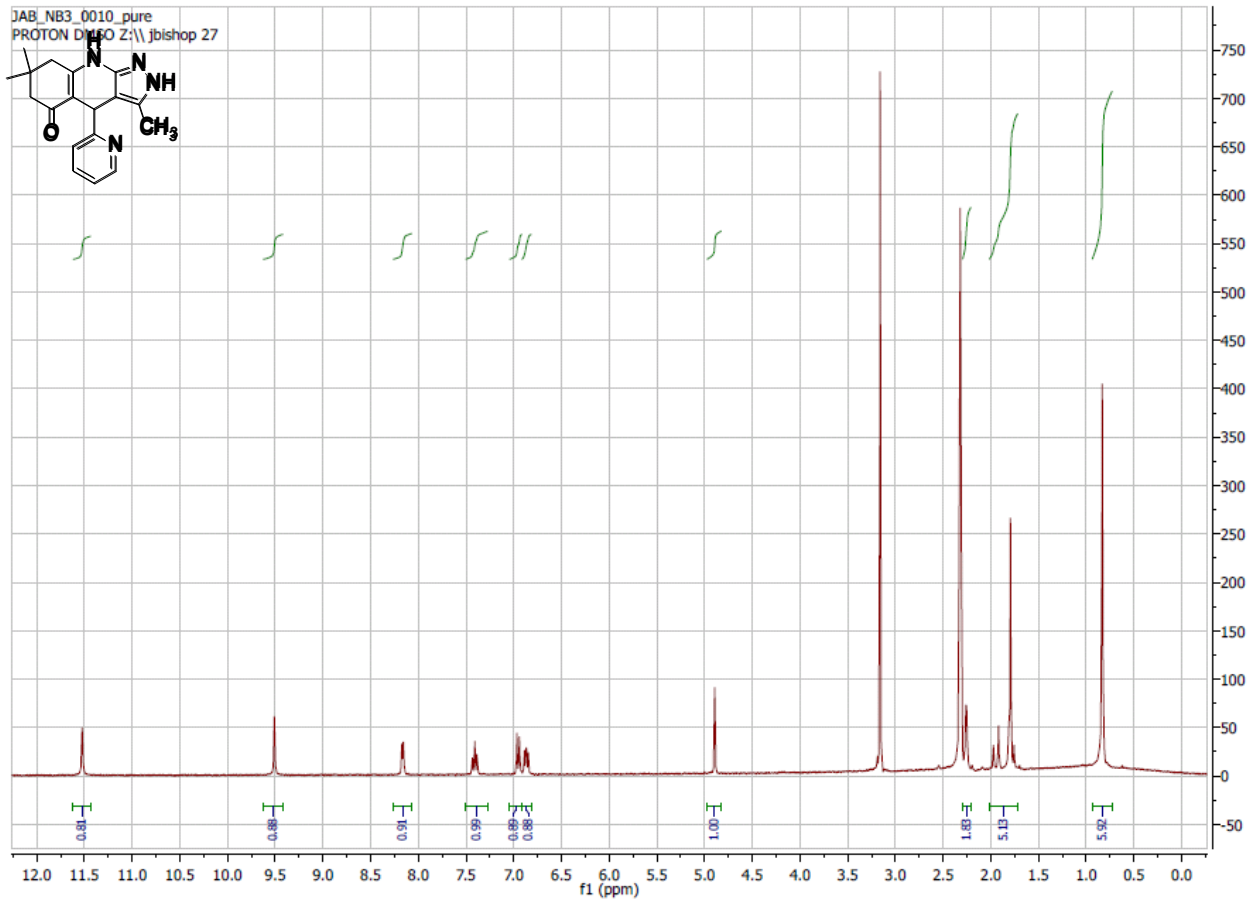
3: UV Detector: 210

3.644e-1
Range: 3.644e-1

88%
298.33
296.40
0.45

12%
296.32
294.40
0.51

Time

JAB_NB3_0010_pure
PROTON DMSO Z:\\ jbishop 27

UPLC-MS Chromatogram of CID 5779597

3: UV Detector: 210

3.324e-1
Range: 3.323e-1

88%
309.37
307.44
0.49

12%
307.34
113.40
0.55

^{1}H NMR Spectrum (300 MHz, CDCl$_3$) of CID 5928899

JAB_NB3_0011_pure
PROTON DMSO Z:\\ jbishop 28

UPLC-MS Chromatogram of CID 5928899

3: UV Detector: 210

3.392e-1
Range: 3.391e-1

89%
309.36
307.42
0.49

11%
307.34
305.42
0.54

¹H NMR Spectrum (300 MHz, CDCl₃) of CID 5776323

JAB_NB3_0018_pure
PROTON DMSO Z:\\ jbishop 13
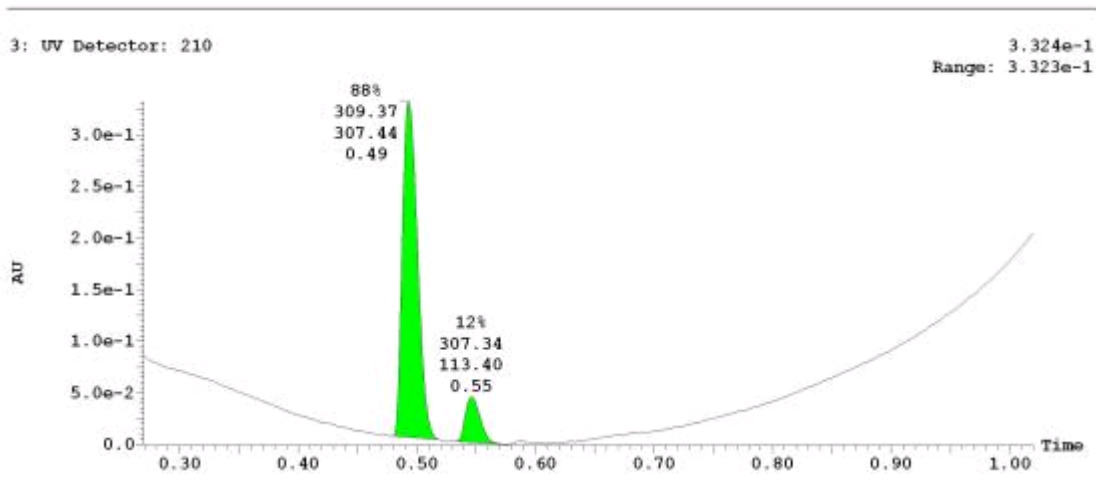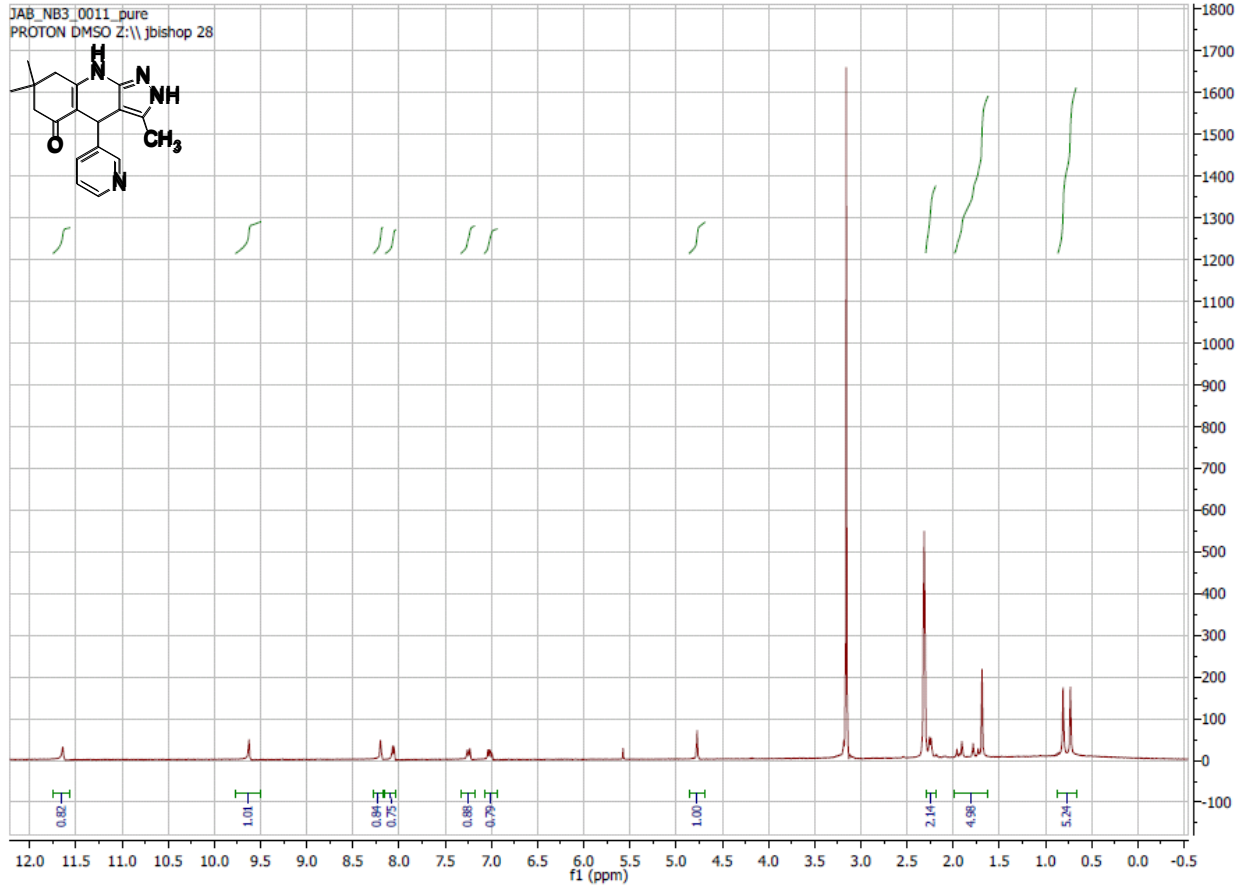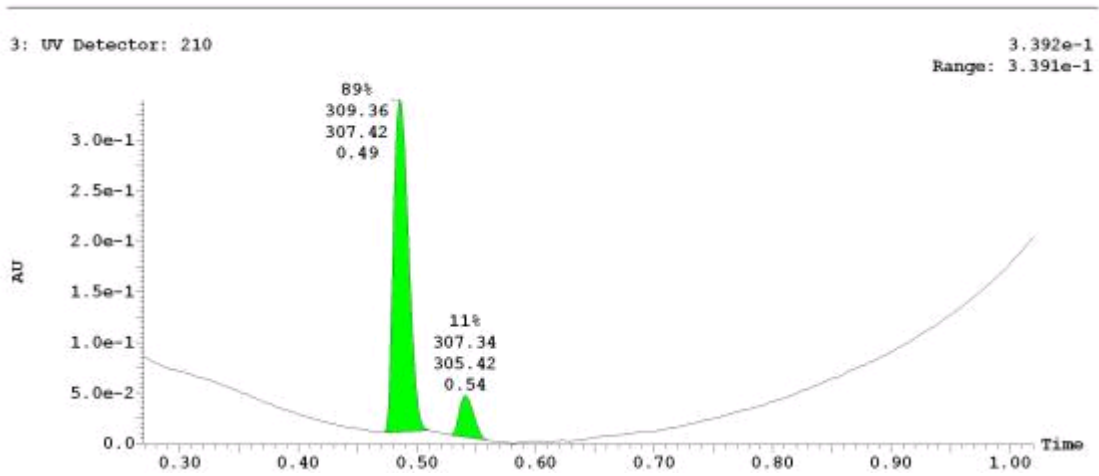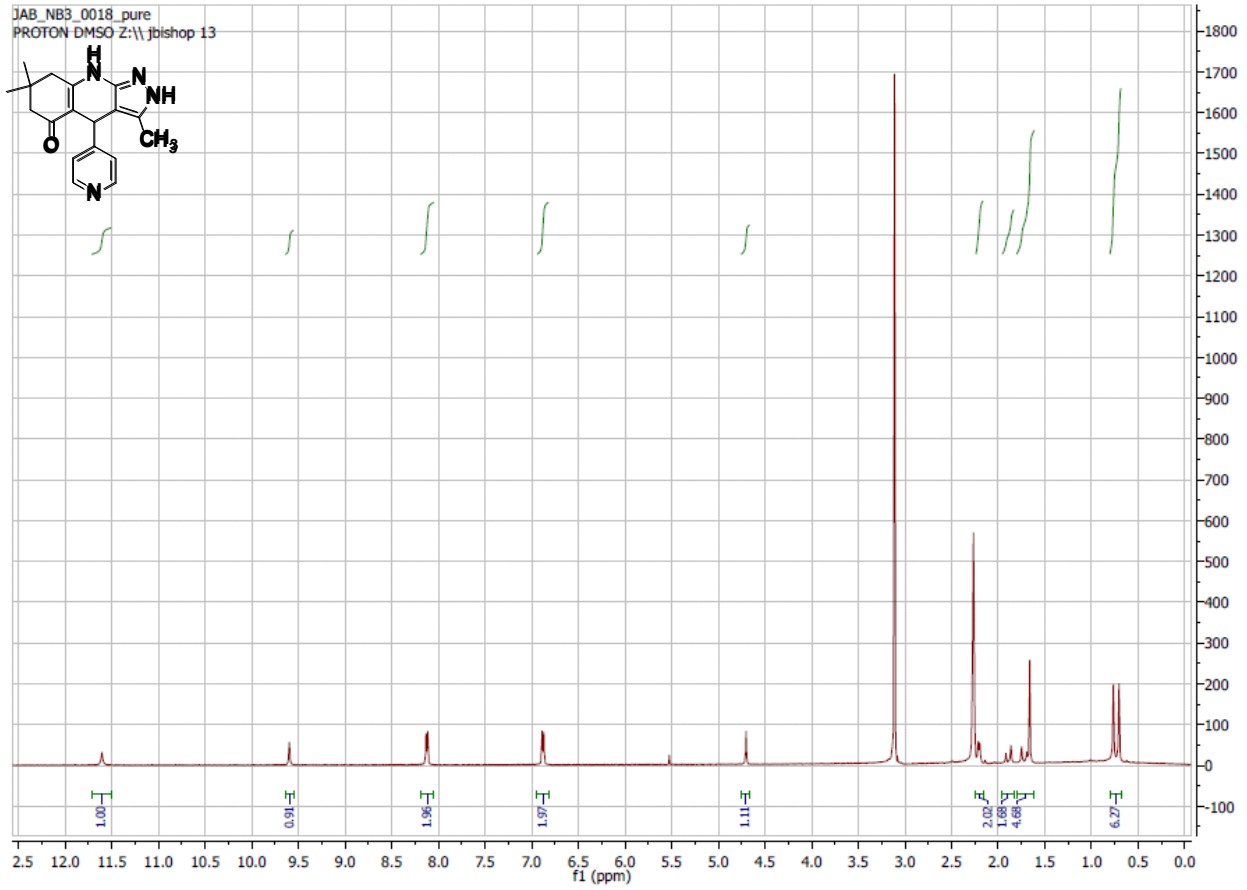
UPLC-MS Chromatogram of CID 5776323

3: UV Detector: 210

4.117e-1
Range: 4.117e-1

88%
309.38
307.45
0.48

11%
307.36
305.45
0.53
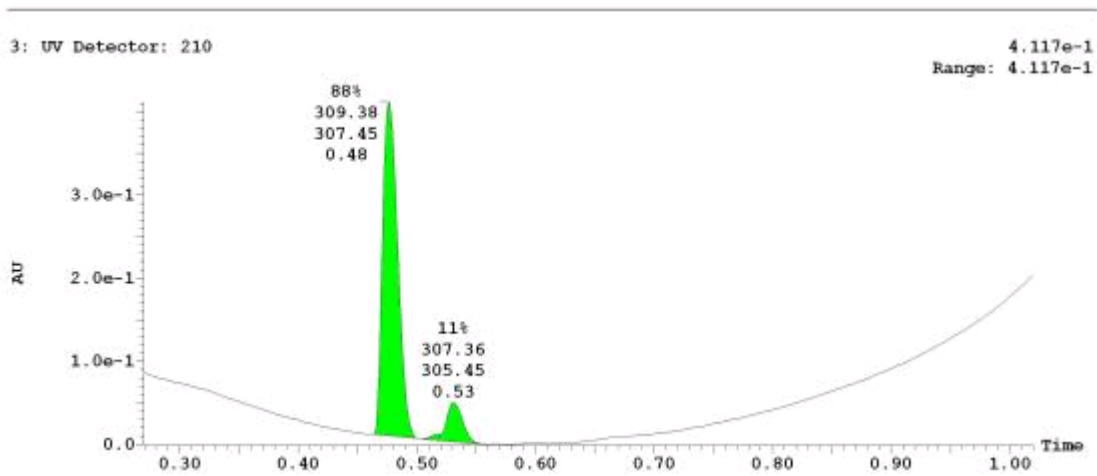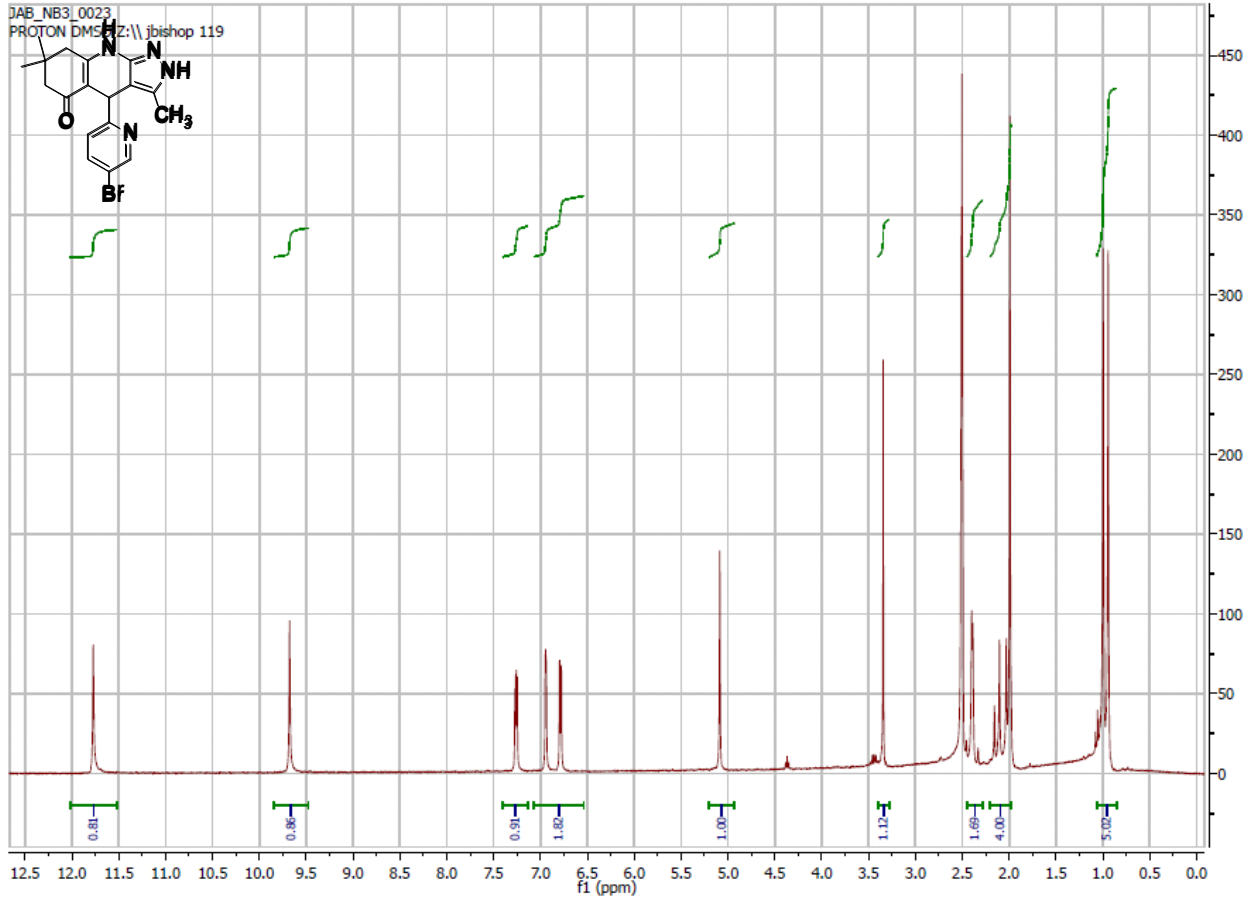
UPLC-MS Chromatogram of CID 56846664
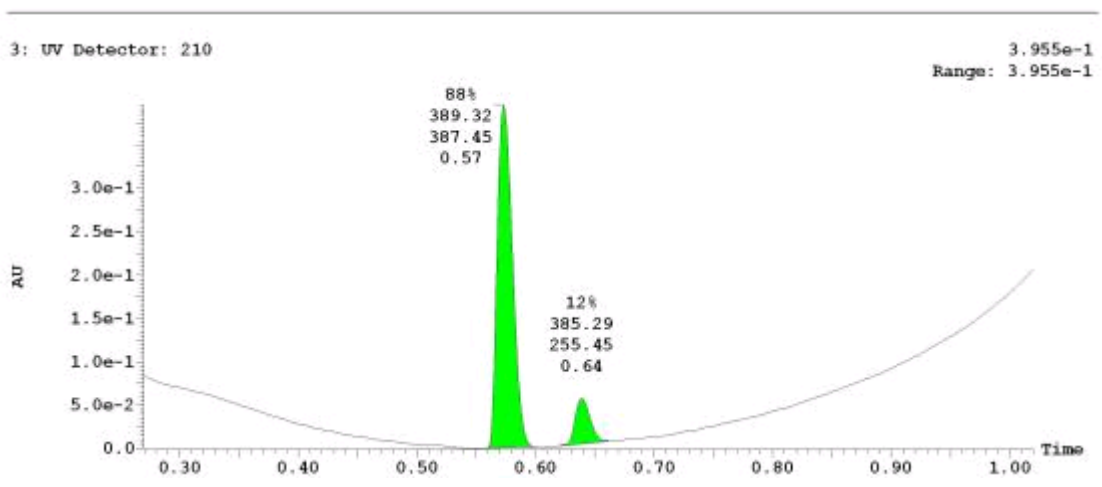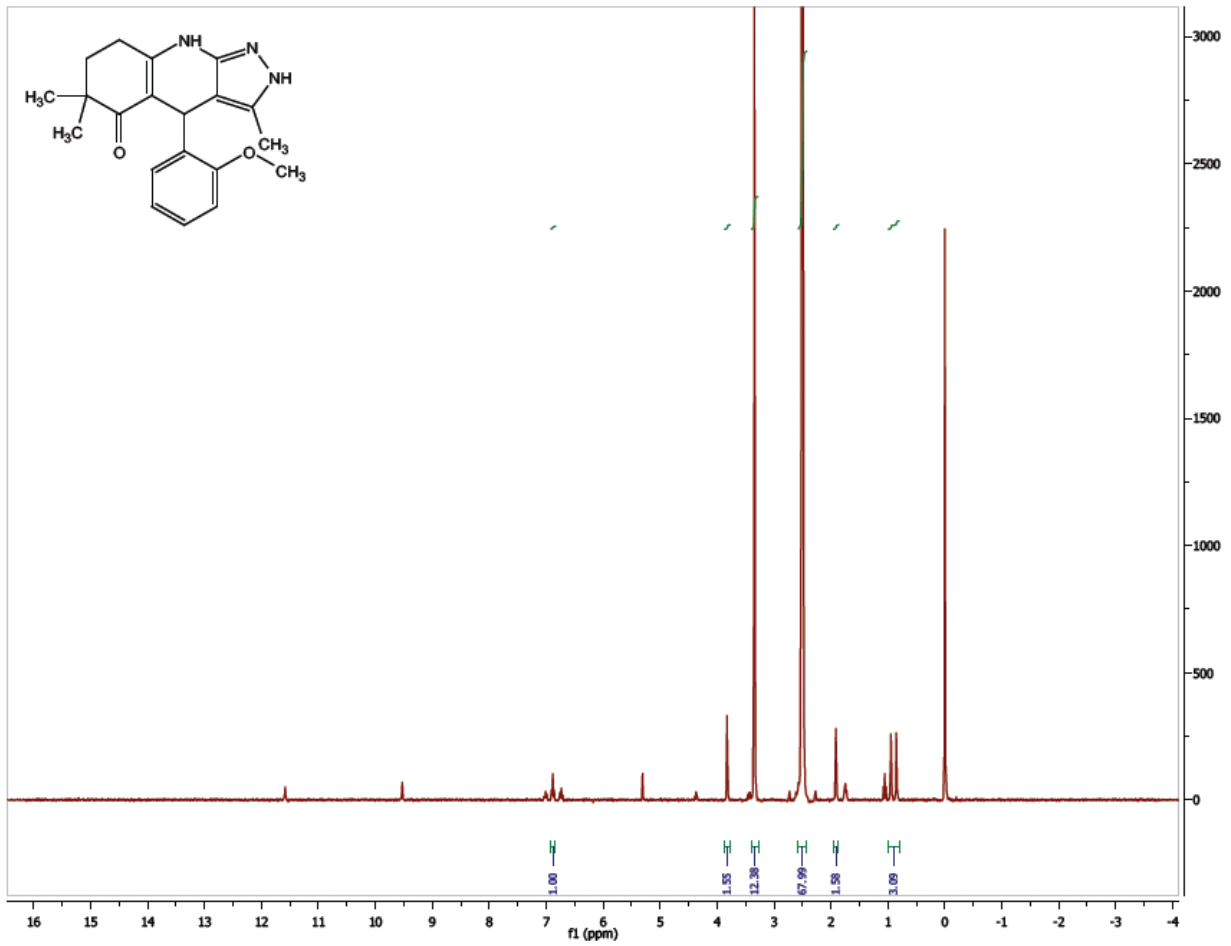
UPLC-MS Chromatogram of CID 56589417

UPLC-MS Chromatogram of CID 56589434
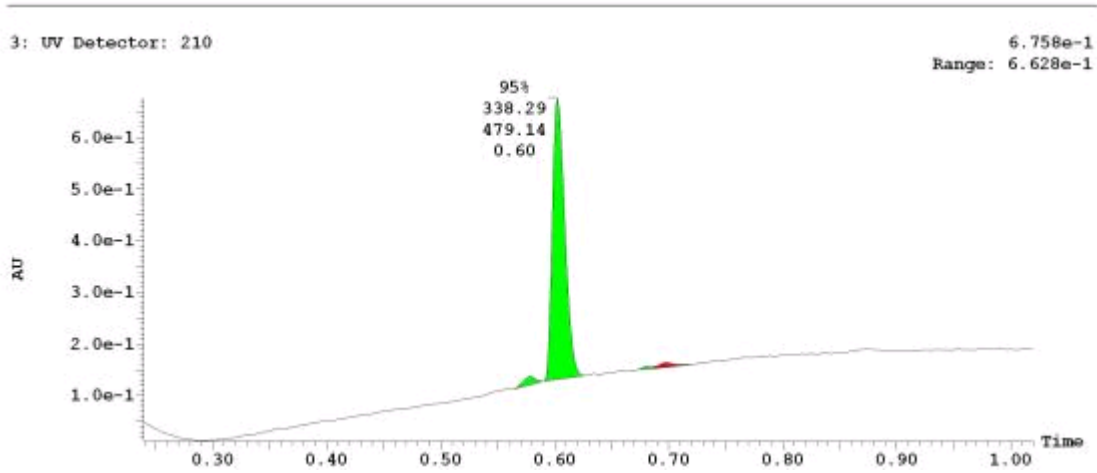
3: UV Detector: 210

5.325e-1
Range: 5.223e-1

83%
310.26
479.11
0.52

¹H NMR Spectrum (300 MHz, CDCl$_3$) of CID 56589433
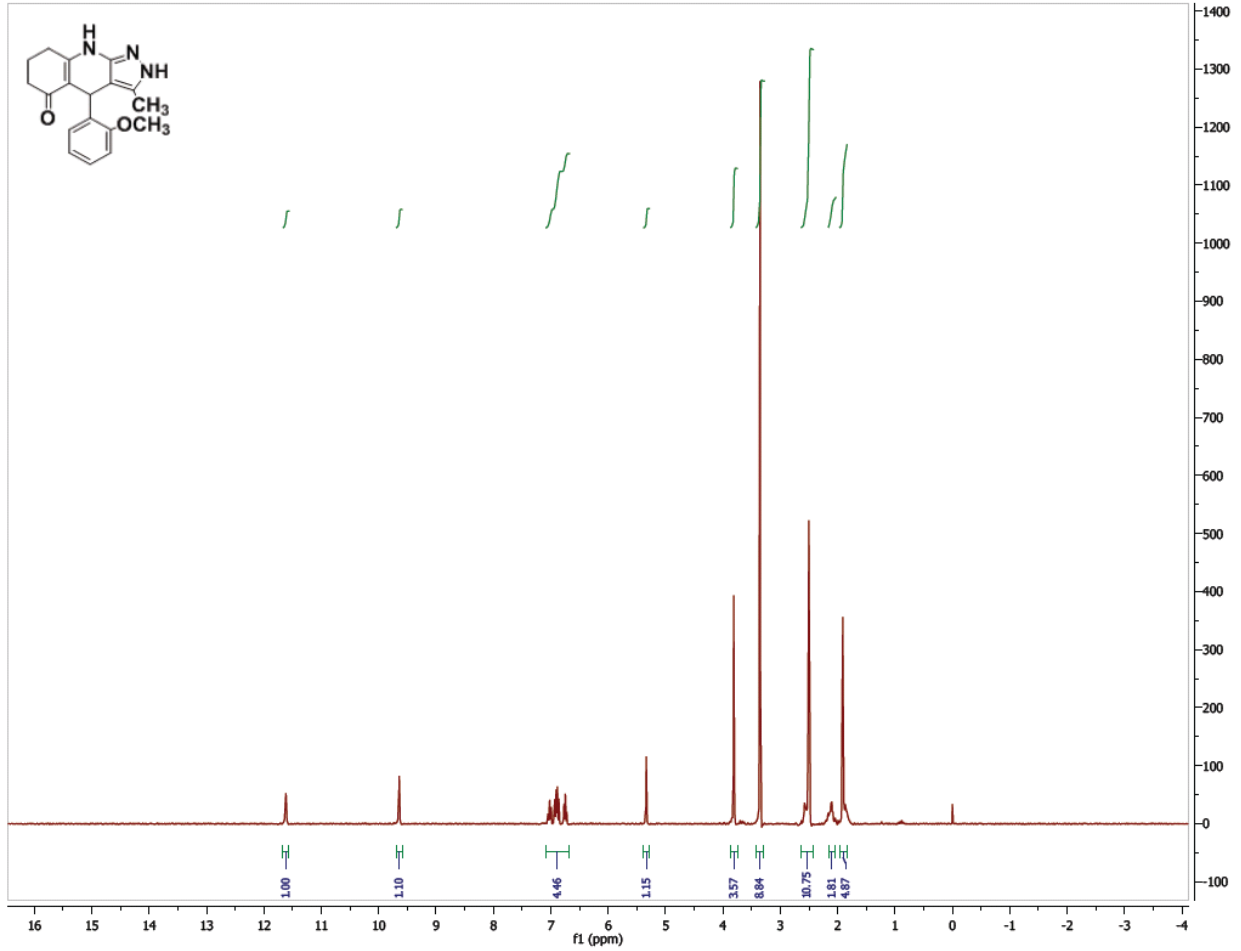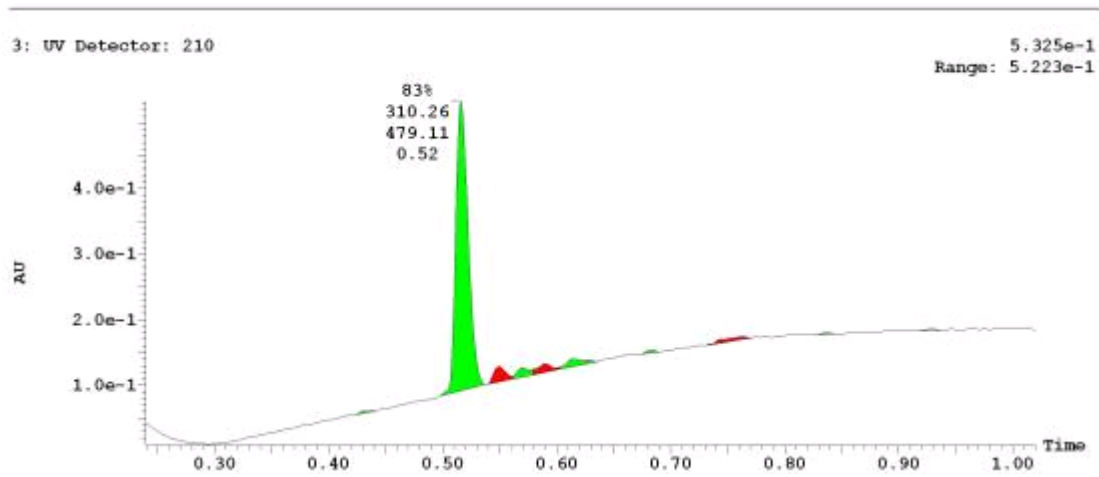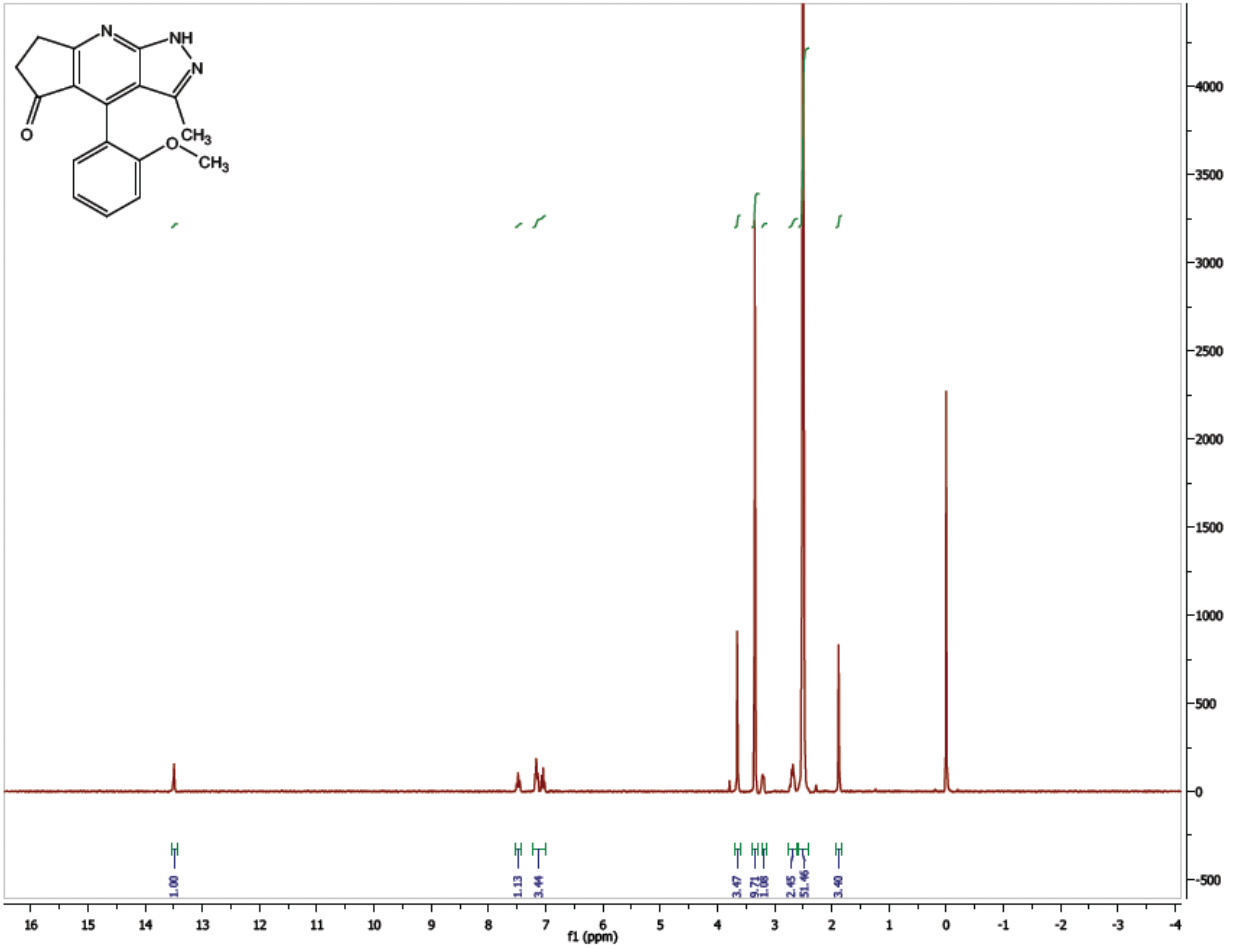
UPLC-MS Chromatogram of CID 56589433

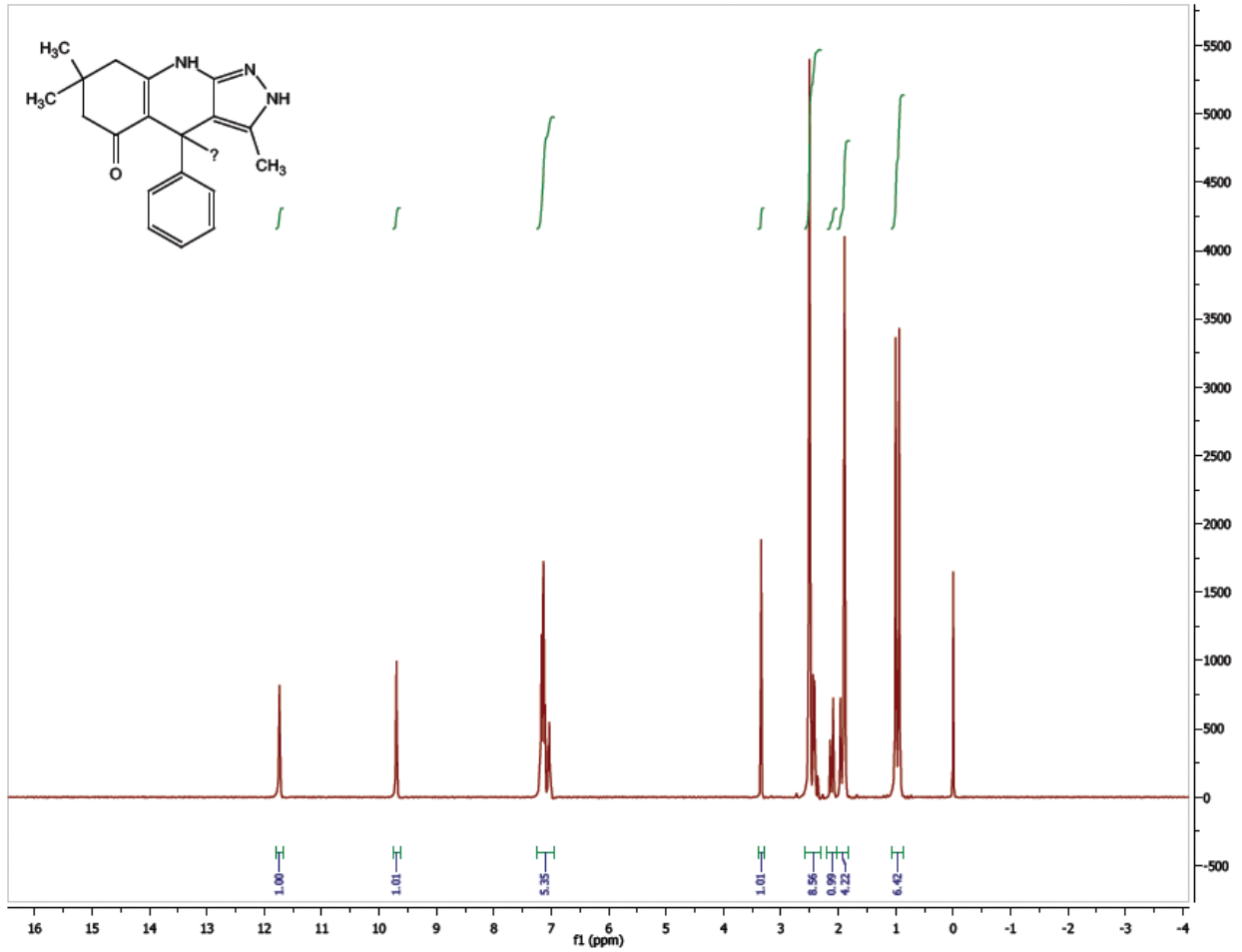3: UV Detector: 210

5.979e-1
Range: 5.978e-1

100%
294.23
292.30
0.55
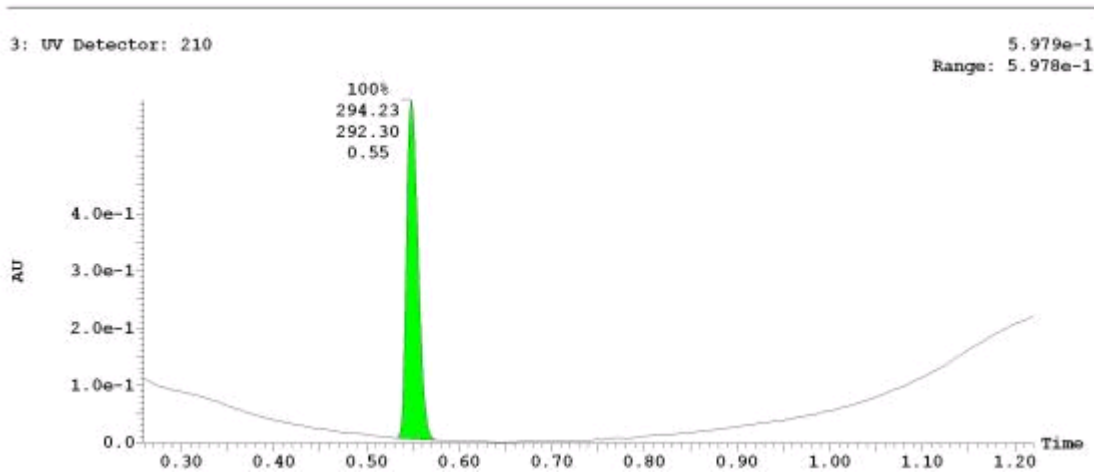
¹H NMR Spectrum (300 MHz, CDCl₃) of CID 56589422

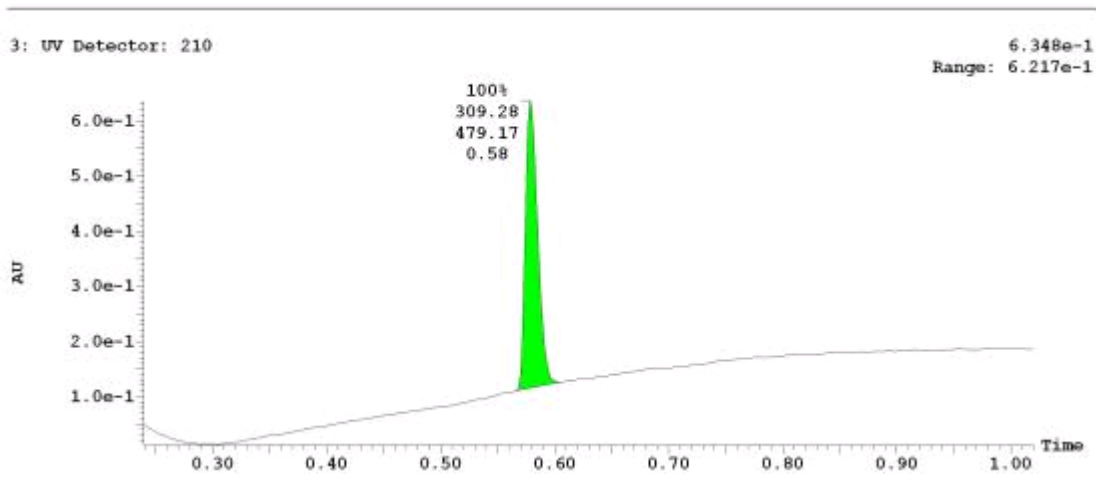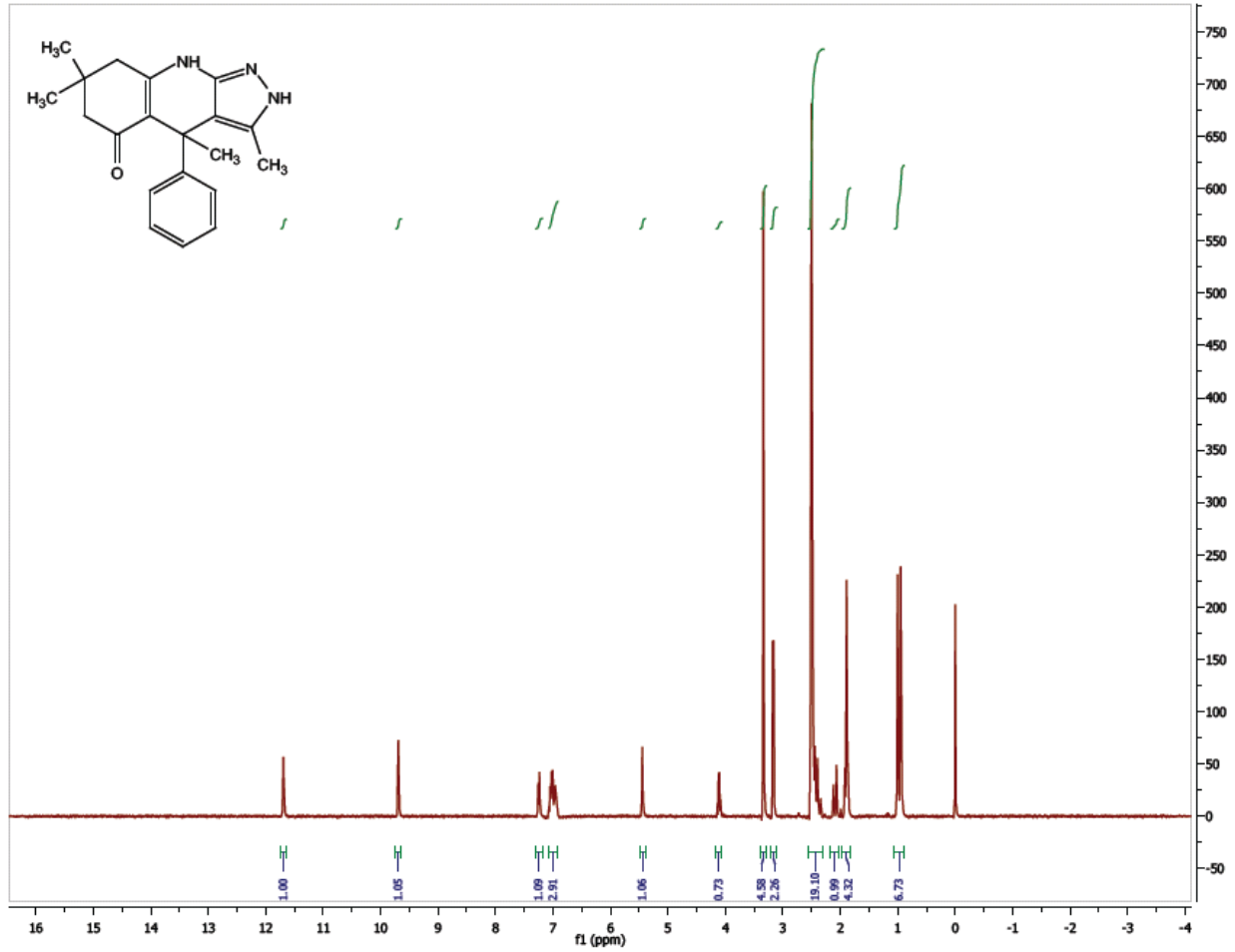**UPLC-MS Chromatogram of CID 56589422**

¹H NMR Spectrum (300 MHz, CDCl₃) of CID 56589428

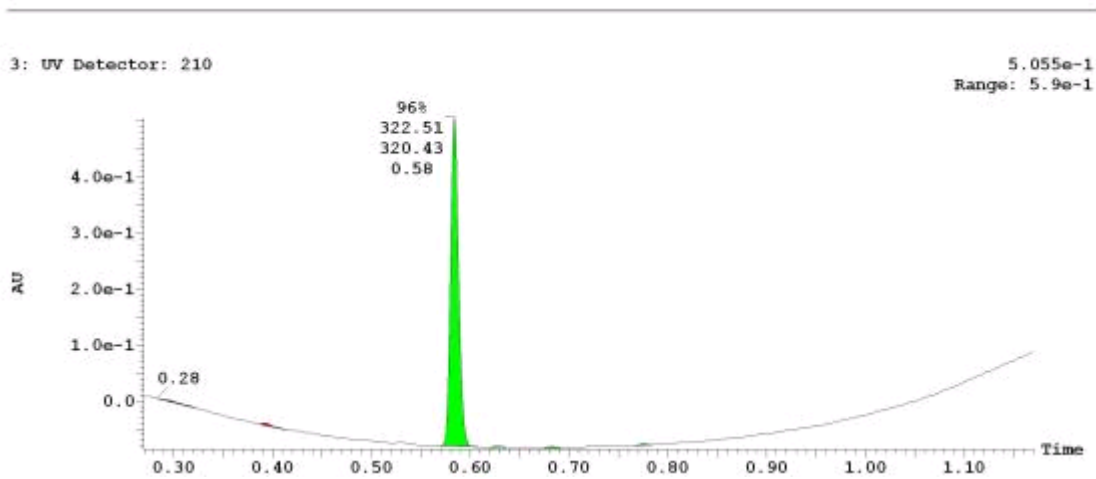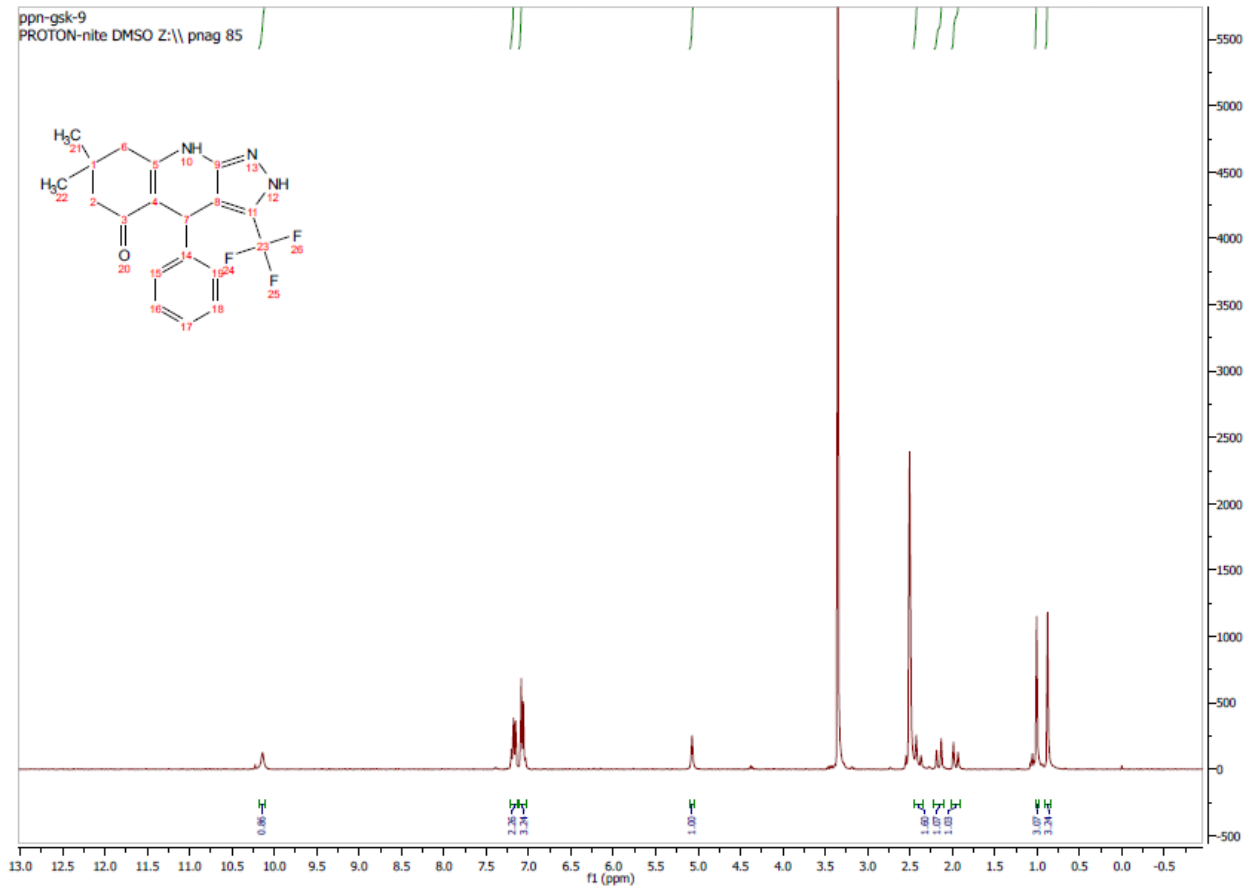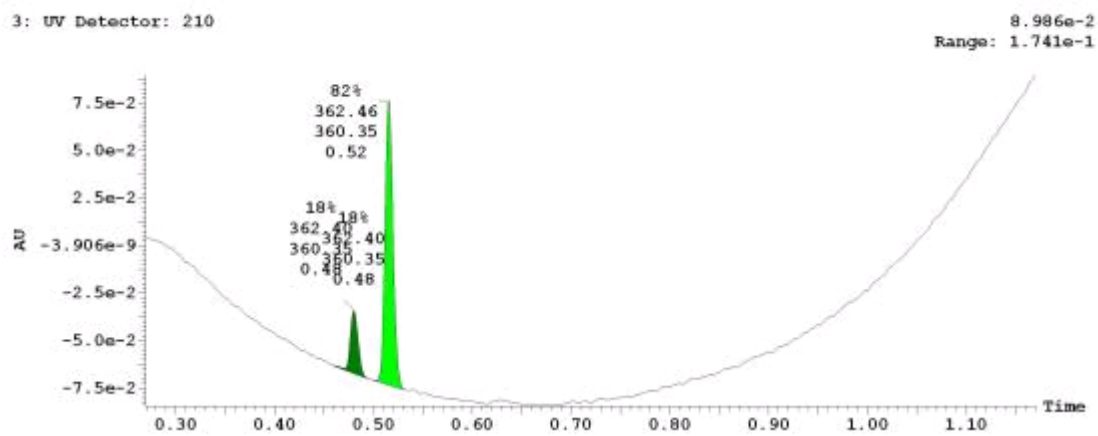**UPLC-MS Chromatogram of CID 56589428**

UPLC-MS Chromatogram of CID 56589405
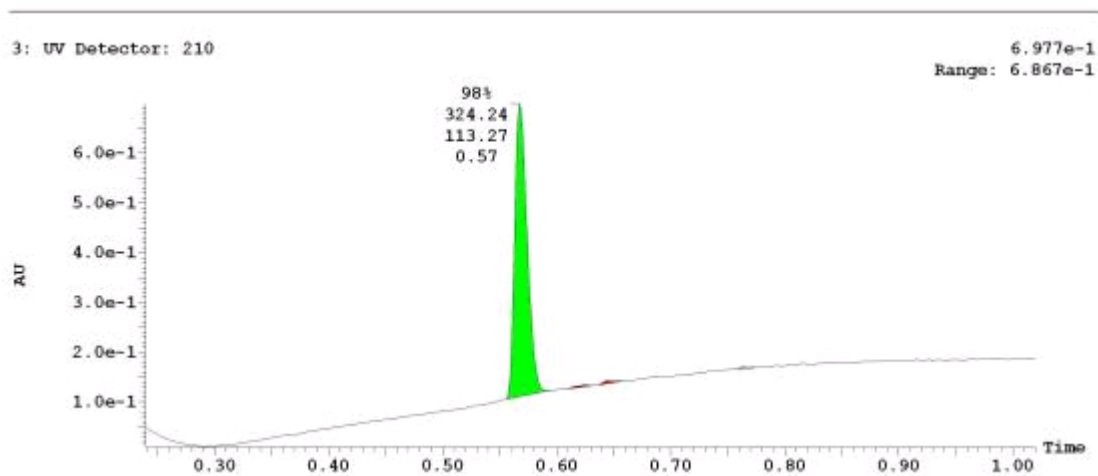
^{1}H NMR Spectrum (300 MHz, CDCl$_3$) of CID 56589411
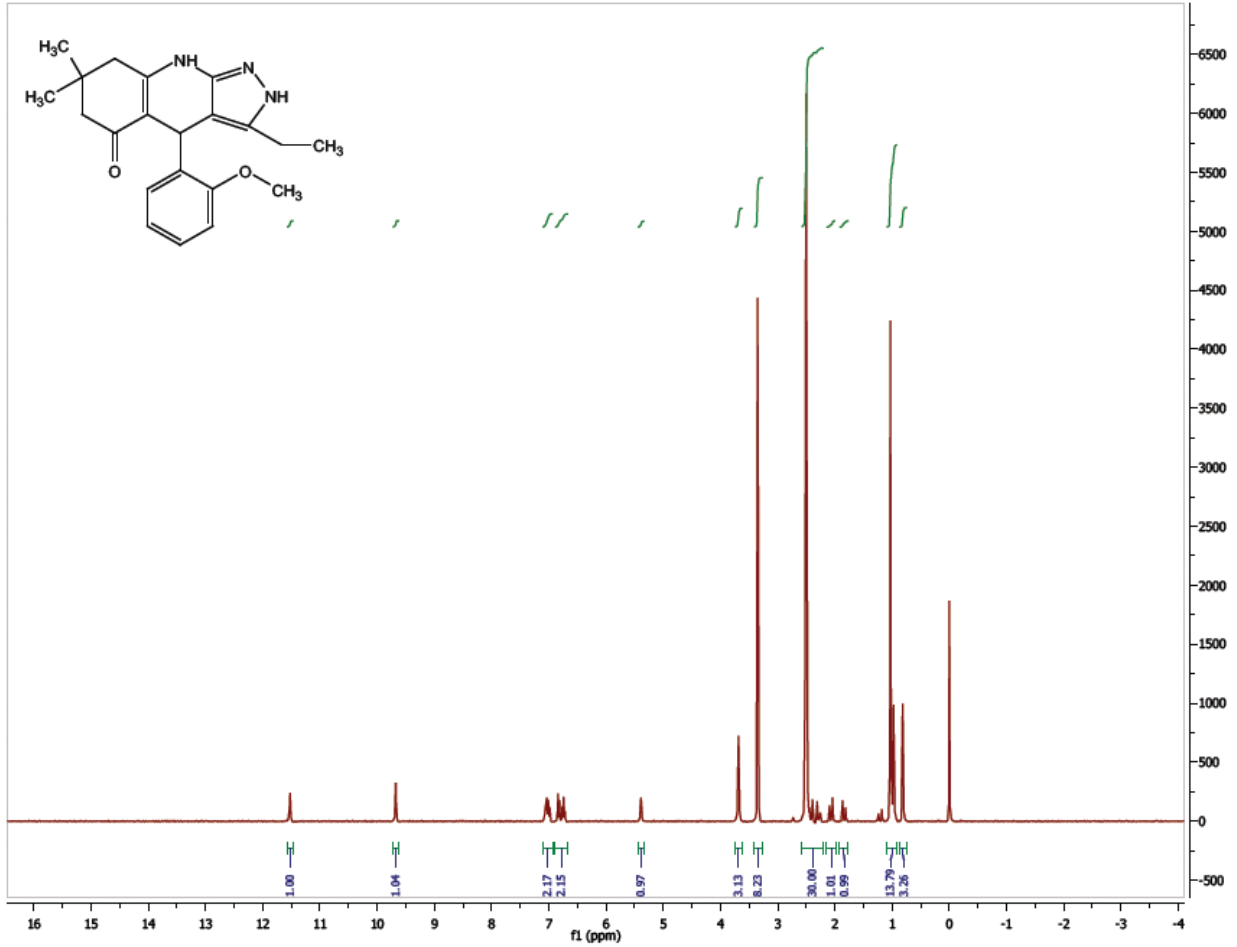
UPLC-MS Chromatogram of CID 56589411
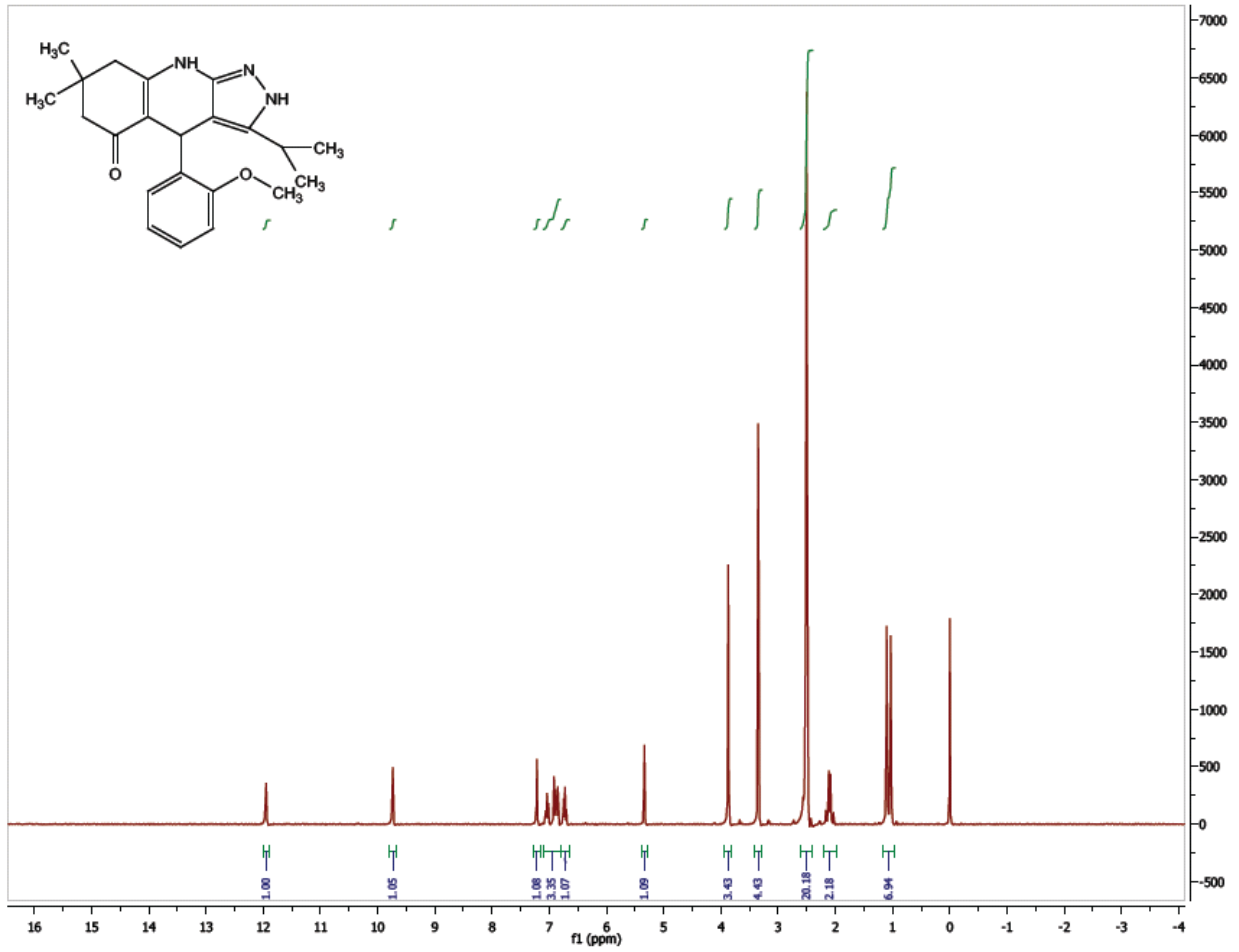
3: UV Detector: 210

6.696e-1
Range: 6.619e-1

93%
352.29
479.15
0.60

5%
350.26
113.28
0.70

UPLC-MS Chromatogram of CID 56589429
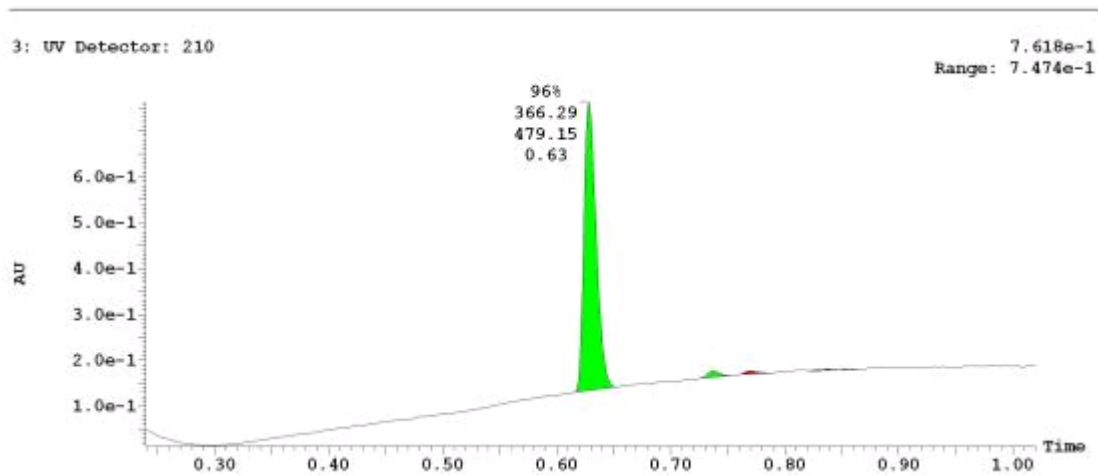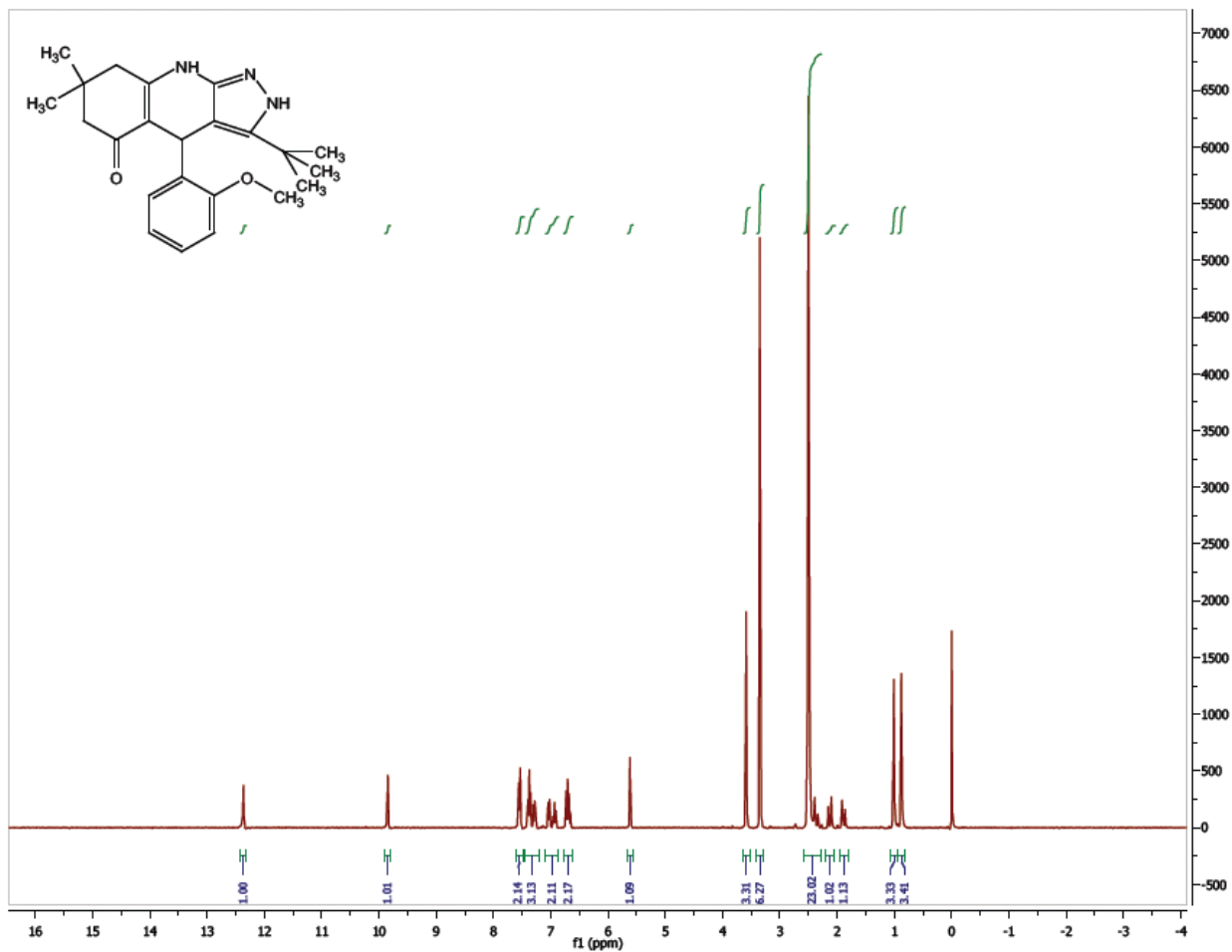
UPLC-MS Chromatogram of CID 56589431
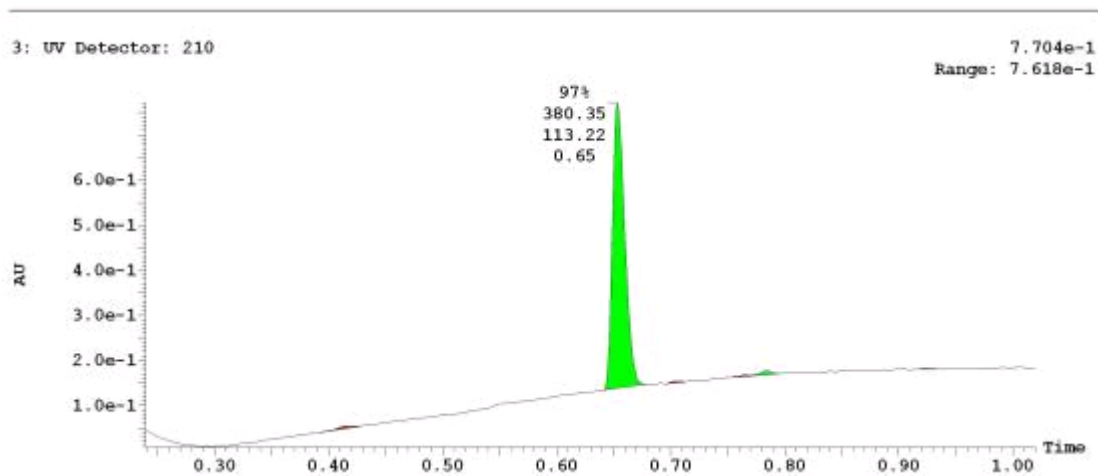
^{1}H NMR Spectrum (300 MHz, CDCl$_3$) of CID 20911996

UPLC-MS Chromatogram of CID 20911996
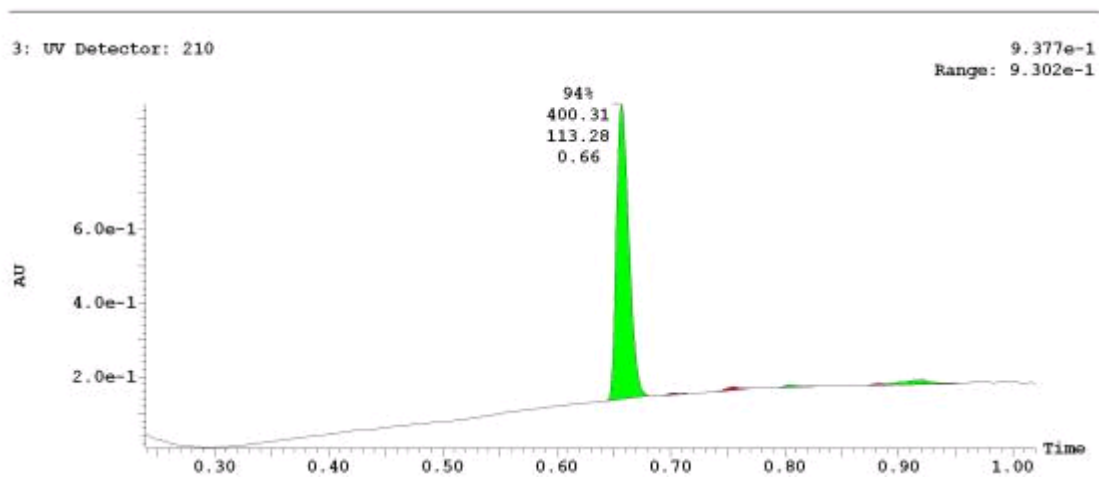
3: UV Detector: 210

9.377e-1
Range: 9.302e-1

94%
400.31
113.28
0.66
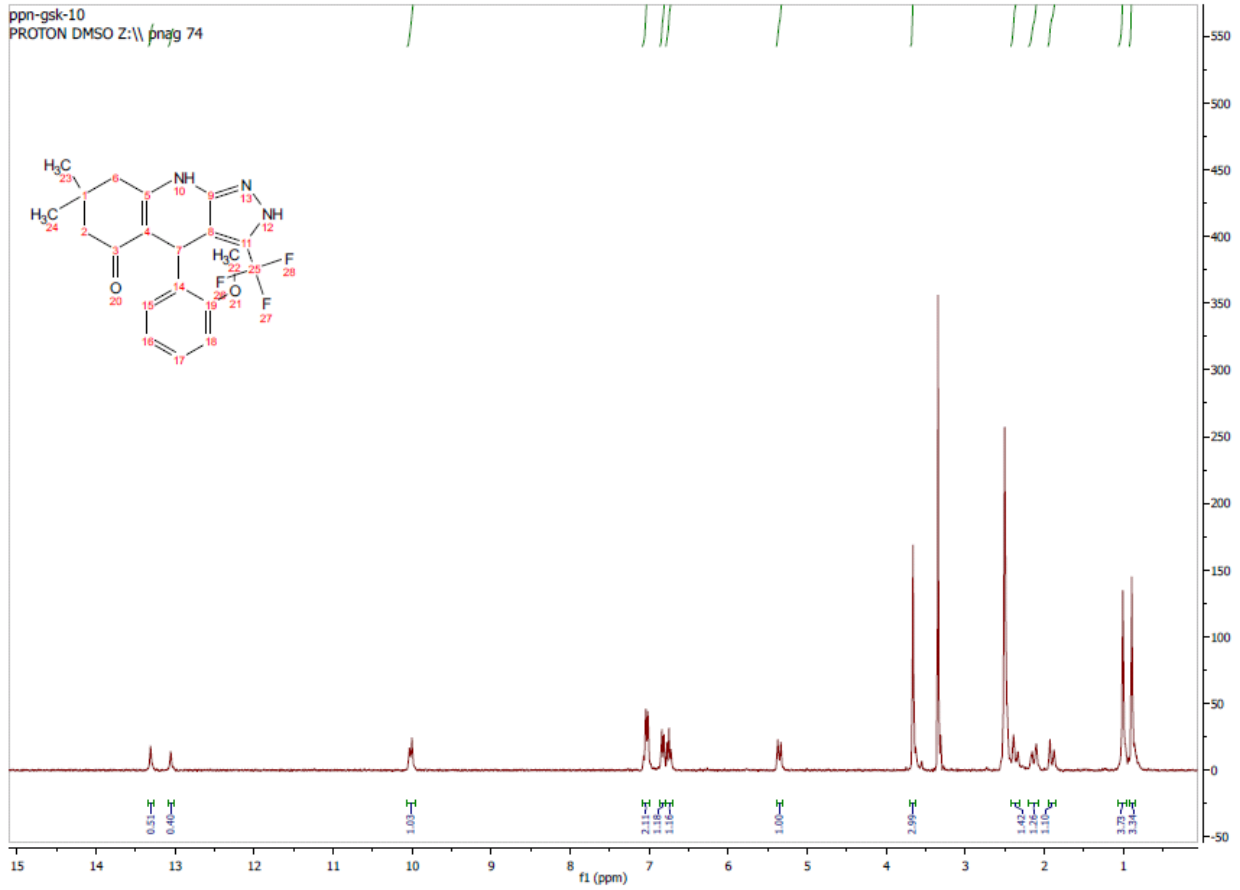
¹H NMR Spectrum (300 MHz, CDCl₃) of CID 17601325

UPLC-MS Chromatogram of CID 17601325
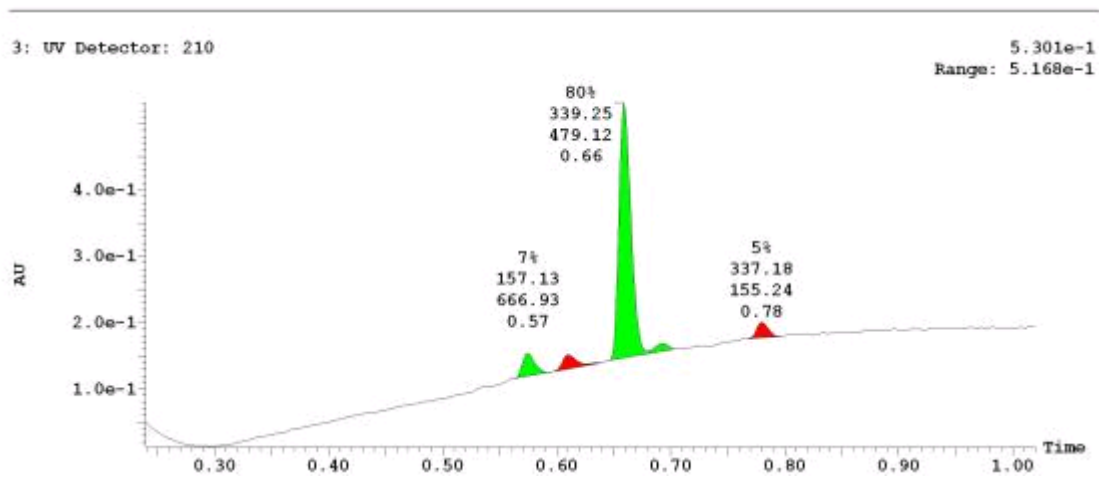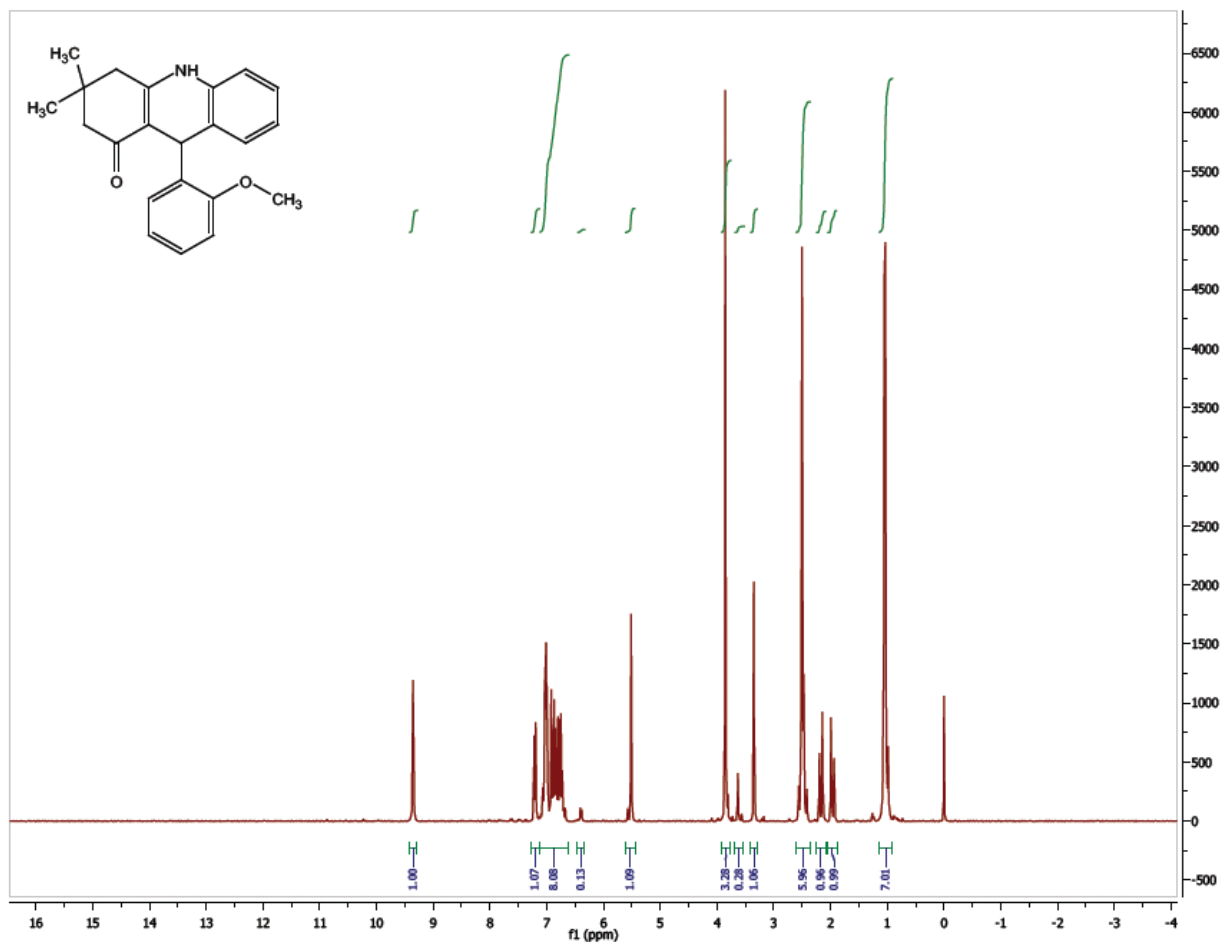
UPLC-MS Chromatogram of CID 56589432
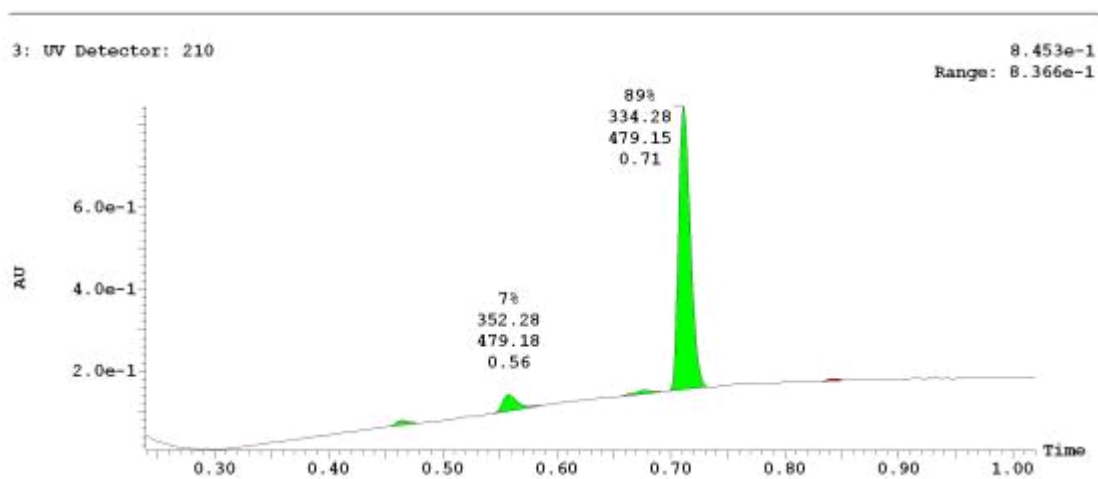
UPLC-MS Chromatogram of CID 56589399

UPLC-MS Chromatogram of CID 56846669

ppn-gsk-9
PROTON-nite DMSO Z:\\ pnag 85

UPLC-MS Chromatogram of CID 56846668

3: UV Detector: 210

8.986e-2
Range: 1.741e-1

82%
362.46
360.35
0.52

18% 18%
362.40 362.40
360.35 360.35
0.48 0.48

¹H NMR Spectrum (300 MHz, CDCl₃) of CID 56846660
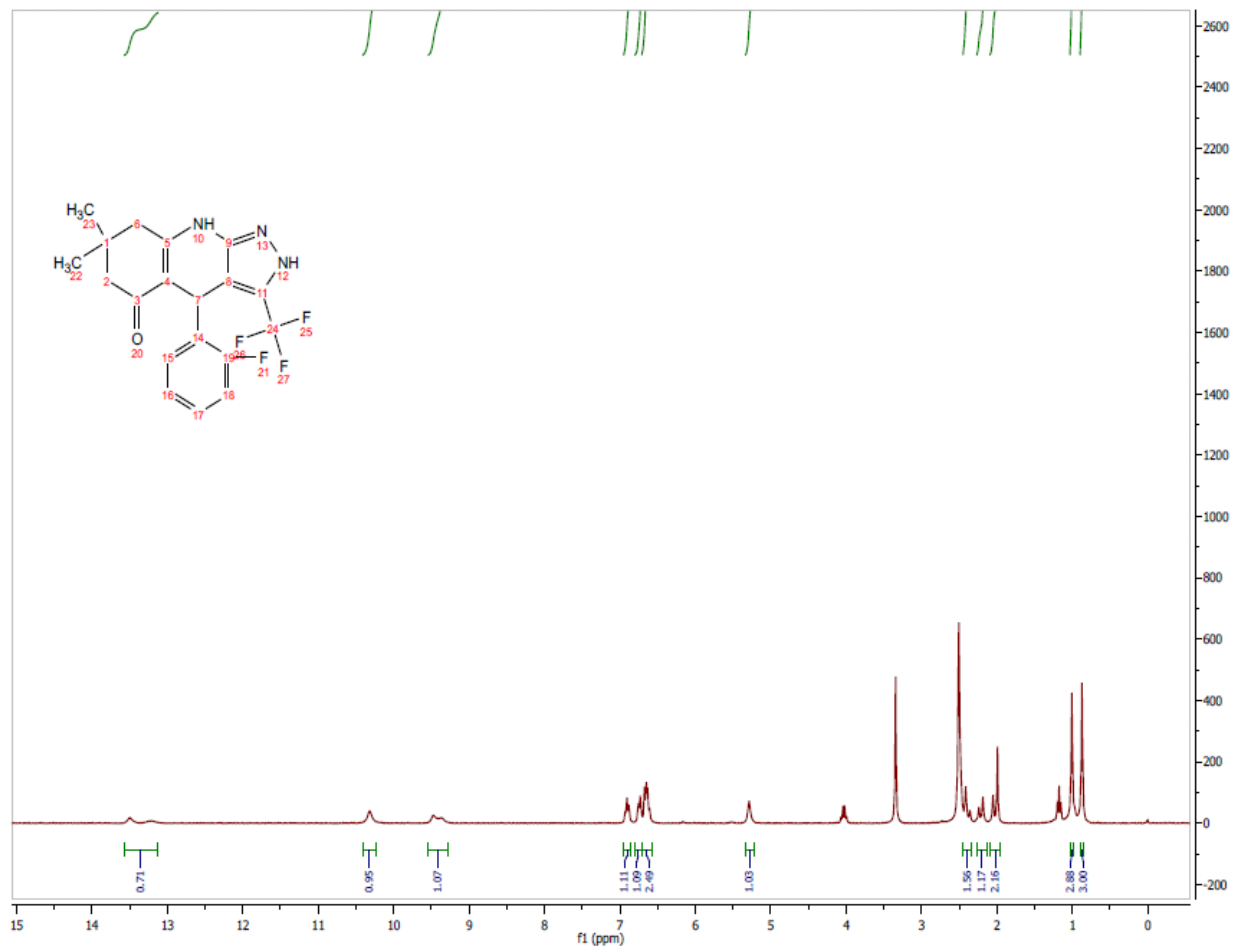
UPLC-MS Chromatogram of CID 56846660
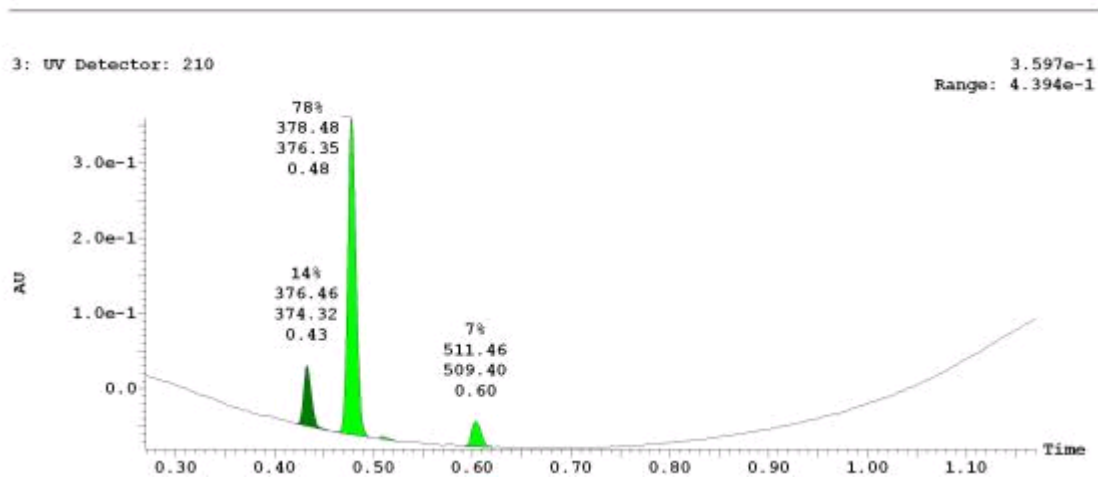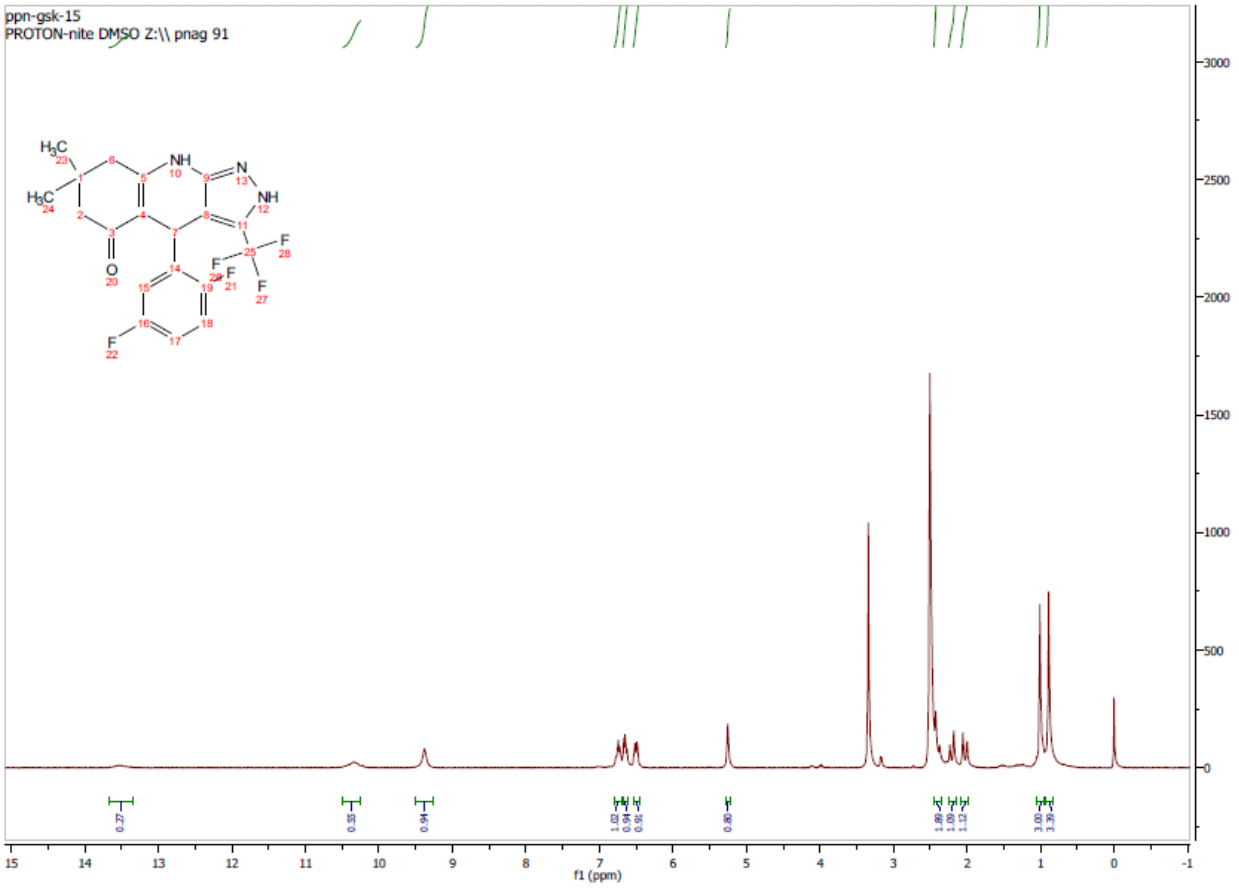
3: UV Detector: 210

3.597e-1
Range: 4.394e-1

78%
378.48
376.35
0.48

14%
376.46
374.32
0.43

7%
511.46
509.40
0.60

¹H NMR Spectrum (300 MHz, CDCl₃) of CID 56846654

ppn-gsk-15
PROTON-nite DMSO Z:\\ pnag 91

UPLC-MS Chromatogram of CID 56846654

3: UV Detector: 210

3.477e-1
Range: 4.281e-1

78%
396.47
394.34
0.48

17%
394.43
392.32
0.44

¹H NMR Spectrum (300 MHz, CDCl₃) of CID 56846657

ppn-gsk-11
PROTON-nite DMSO Z:\\ pnag 87
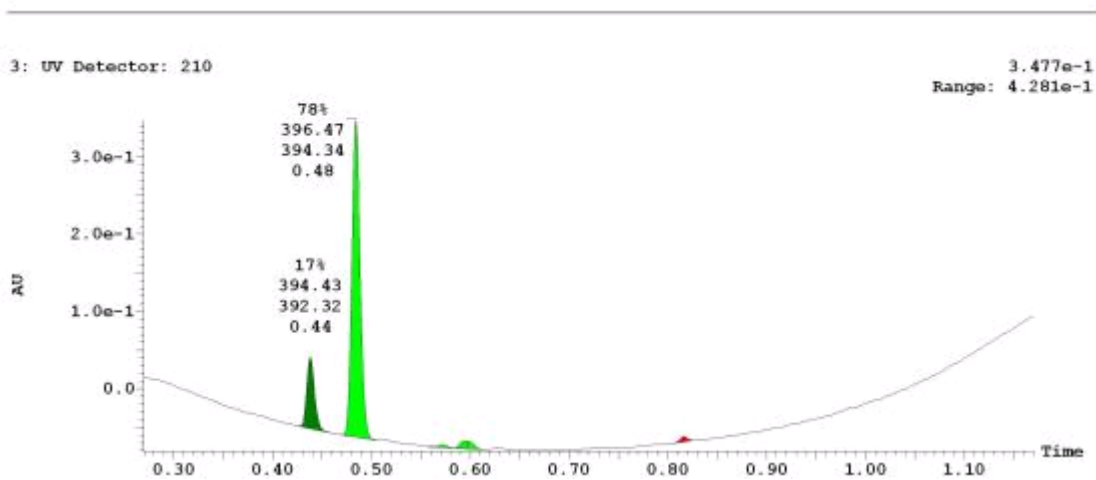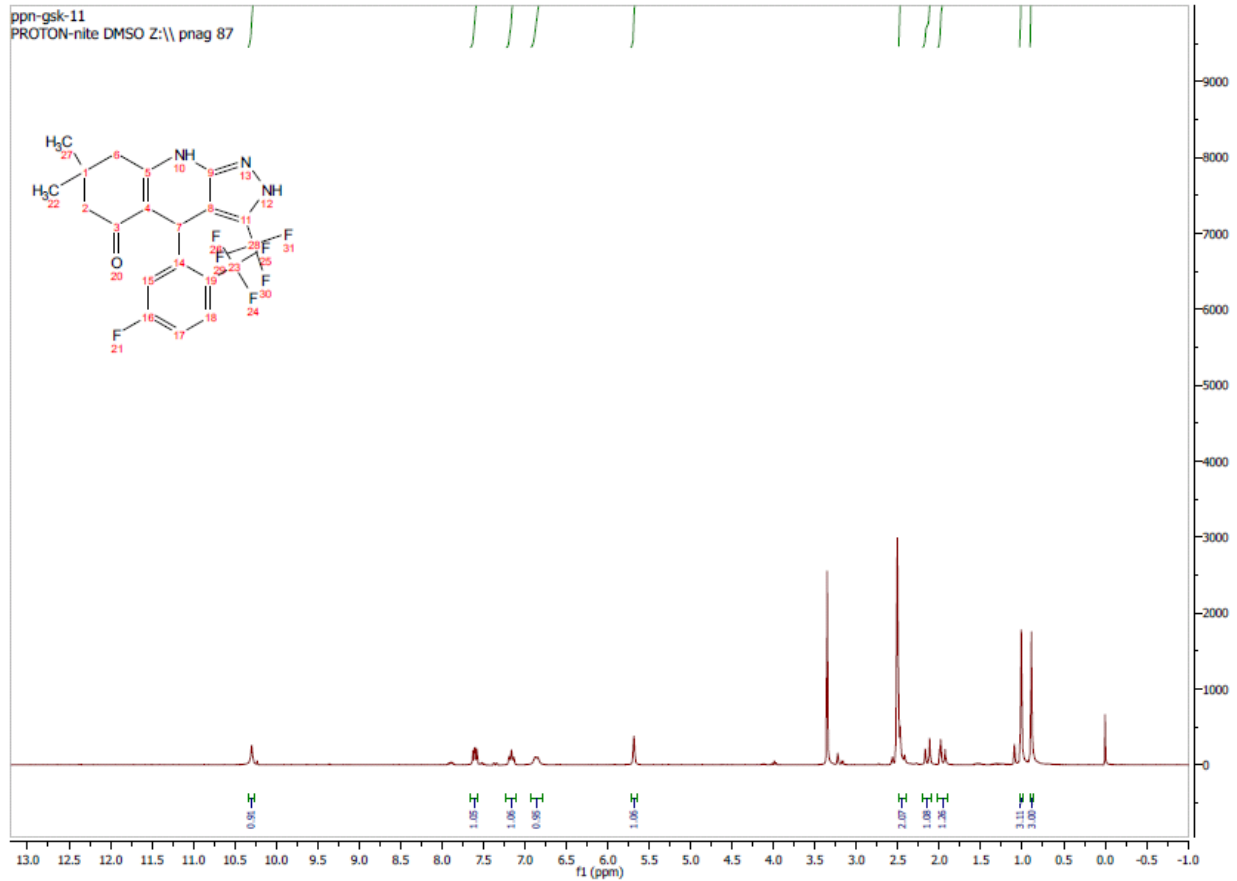
UPLC-MS Chromatogram of CID 56846657
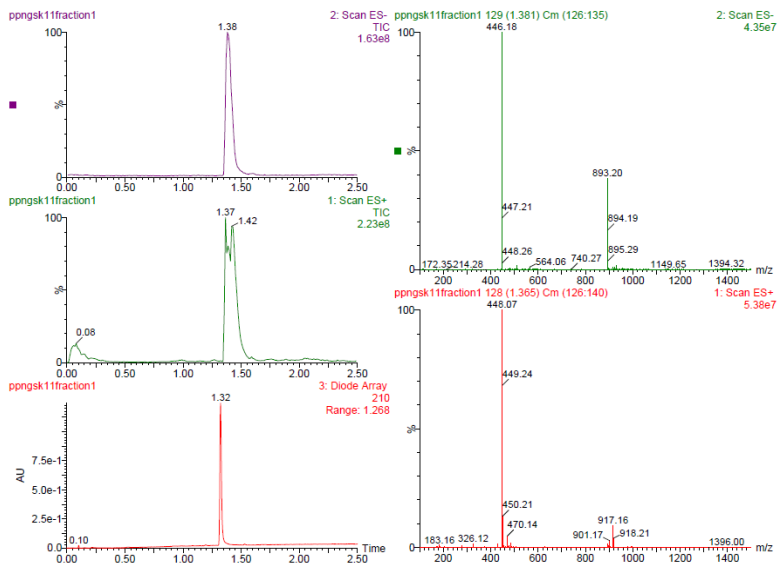
Appendix G: Compounds Provided to Evotec

Table A2. Probe and Analog Information

BRD	SID	CID	P/A	MLSID	ML
BRD-K81491172	134970446	56840716	P	MLS004256802	320
BRD-A18945128	135378259	56846669	A	MLS004256803	NA
BRD-A06244137	134216517	56589435	A	MLS004256800	NA
BRD-A65149943	134216536	56589400	A	MLS004256804	NA
BRD-A72352862	134216539	56589424	A	MLS004256799	NA
BRD-A89407846	134959049	56589437	A	MLS004256801	NA

A = analog; NA= not applicable; P = probe